#4

~~AD- 332~~

SECURITY REMARKING REQUIREMENTS

~~DOD 5200.1-R~~ DEC 78

~~REVIEW~~ ON 28 JUN ~~82~~

Page determined to be Unclassified
Reviewed Chief, RDD, WHS
IAW EO 13526, Section 3.5
Date: 19JUL2013

Office of the Secretary of Defense 5 USC Sec 552 and
Chief, RDD, ESD, WHS
Date: 19JUL2013 Authority: EO 13526
Declassify: X Deny in Full: _____
Declassify in Part: _____
Reason: _____
MDR: 12-M-3147

54-343

12
12-M-3147

~~CONFIDENTIAL~~

AD 332 404

Reproduced
by the

ARMED SERVICES TECHNICAL INFORMATION AGENCY
ARLINGTON HALL STATION
ARLINGTON 12, VIRGINIA

~~CONFIDENTIAL~~

NOTICE: When government or other drawings, specifications or other data are used for any purpose other than in connection with a definitely related government procurement operation, the U. S. Government thereby incurs no responsibility, nor any obligation whatsoever; and the fact that the Government may have formulated, furnished, or in any way supplied the said drawings, specifications, or other data is not to be regarded by implication or otherwise as in any manner licensing the holder or any other person or corporation, or conveying any rights or permission to manufacture, use or sell any patented invention that may in any way be related thereto.

332 404

General Mills

THE GENERAL MILLS ELECTRONICS GROUP

CONFIDENTIAL

NOTICE:

THIS DOCUMENT CONTAINS INFORMATION AFFECTING THE NATIONAL DEFENSE OF THE UNITED STATES WITHIN THE MEANING OF THE ESPIONAGE LAWS, TITLE 18, U.S.C., SECTIONS 793 and 794. THE TRANSMISSION OR THE REVELATION OF ITS CONTENTS IN ANY MANNER TO AN UNAUTHORIZED PERSON IS PROHIBITED BY LAW.

[redacted]

[redacted]

This document consists of 73 pages and is number 7 of 45 copies, series A, and the following - attachments.

SEVENTH QUARTERLY PROGRESS REPORT

ON

DISSEMINATION OF SOLID AND LIQUID BW AGENTS

(Unclassified Title)

[redacted]

For Period December 4, 1961 - March 4, 1962
Contract No. DA-18-064-CML-2745

Prepared for:

U. S. Army Biological Laboratories
Fort Detrick, Maryland

Submitted by: G. R. Whitnah
Project Manager

Report No: 2300
Project No: 82408
Date: June 22, 1962

Approved by: S. P. Jones, Director,
Aerospace Research

Research and Development
2003 East Hennepin Avenue
Minneapolis 13, Minnesota

[redacted]

FOREWORD

Staff Members of the Research and Development Departments who have participated in directing and performing this work include Mr. S. P. Jones, Jr., Mr. G. Whitnah, Mr. M. Sandgren, Mr. A. Anderson, Dr. V. W. Greene, Dr. J. Park, Mr. R. Lindquist, Mr. J. McGillicuddy, Mr. J. Upton, Mr. W. L. Torgeson, Mr. J. Nash, Mr. S. Steinberg, Mr. P. Stroom, Mr. A. McFarland, Mr. G. Morfitt, Mr. L. Graf, Mr. I. Hall, Mr. G. Beck, Mr. J. Walters, Mr. A. T. Bauman, Mr. T. Peterson, Mr. C. Larson, Mr. D. Harrington, Mr. R. Ackroyd, Mr. D. Kedl, Mr. B. Schmidt, Mr. G. Lundy, Mr. R. Dahlberg, Mr. R. Barrett, Mr. O. Durigan, Mr. A. Kydd, Mr. E. Knutson, Mr. G. Leiter, Mr. N. Konopliv, Mr. J. Ungs, and Miss M. Johnson.

[redacted]

[redacted]

[redacted]

ABSTRACT

This Seventh Quarterly Report presents the results of continued work on a large number of technical aspects of BW dissemination.

Progress on the theoretical and experimental studies of powder mechanics is reported. Several new experimental techniques are discussed and more complete analyses of the previously obtained experimental data are given.

The design and fabrication of a new aerosol chamber, equipped with light-scattering instrumentation is described. This chamber will permit studies of aerosol stability. The aerosol generation and sampling apparatus are discussed.

Studies of the viability of Sm and Bg, in the bulk and aerosol forms, are presented. These are investigations of the effects of elevated temperature and additives.

Wind tunnel studies of dissemination and deagglomeration are discussed. The results of further studies of small-scale agglomerates and a description of a new high-flow-rate disseminator model are given.

New experimental work on metering and conveying dry powders is described and data are given on the performance of a full-scale laboratory feeding model.

Progress in completing the wind tunnel and associated apparatus for installation at Fort Detrick is reported.

Design studies covering several features of the dry-agent airborne disseminator are described.

The results of computer studies dealing with the line-source dissemination of the agent UL-2 are given.

The status of work on the design and fabrication of a liquid-agent airborne disseminator is reported, and many detailed aspects of the design are presented.

TABLE OF CONTENTS

Section		Title	Page
1.		INTRODUCTION	1-1
2.		THEORETICAL AND EXPERIMENTAL STUDIES OF THE MECHANICS OF DRY POWDERS	2-1
	2.1	Development of Experimental Apparatus	2-1
	2.1.1	Apparatus for Determining Compaction Characteristics of Dry Powders	2-1
	2.1.2	Triaxial Shear Apparatus	2-2
	2.2	Related Experimental Studies	2-8
	2.2.1	Residual Shear Strength of Compacted Powders	2-8
	2.2.2	Wall Friction Phenomena	2-10
	2.2.3	Compaction Characteristics of Powders	2-11
	2.3	Bulk Tensile Strength of Powders	2-16
	2.3.1	Apparatus and Technique	2-18
	2.3.2	Discussion of Experimental Results	2-22
	2.3.3	Future Work	2-26
	2.4	Mathematical Analysis of the Piston-Cylinder Test	2-27
3.		AEROSOL STUDIES	3-1
	3.1	Main Chamber	3-1
	3.2	Optical Light-Scattering Detection System	3-1
	3.2.1	Monochromatic Light Source	3-1
	3.2.2	Photomultiplier Detection System	3-4
	3.3	Powder Dispersing System	3-7
	3.4	The Aerosol Sampling System	3-10
	3.5	Future Work	3-16
4.		VIABILITY STUDIES	4-1
	4.1	Viability of Dry Aerosols of Bg and Sm	4-1
	4.2	Effect of Cab-O-Sil on Viability	4-7
	4.3	Toxic Effec of Buna Rubber on Sm	4-10

TABLE OF CONTENTS (Continued)

Section	Title	Page
5.	DISSEMINATION AND DEAGGLOMERATION STUDIES	5-1
5.1	General	5-1
5.2	Sm Dissemination - Small-Scale Agglomerate Study	5-1
5.3	Design of High Flow Rate Disseminator Model (GMI-3) and Related Equipment	5-5
6.	EXPERIMENTS WITH THE FULL-SCALE FEEDER FOR COMPACTED DRY AGENT SIMULANT MATERIALS	6-1
6.1	Introduction	6-1
6.2	General Procedure	6-2
6.3	Driving Torque Determinations	6-7
6.4	Motivating Gas and Talc Discharge Rate Measurements	6-11
7.	APPARATUS FOR DISSEMINATION EXPERIMENTS AT FORT DETRICK	7-1
8.	DESIGN STUDIES ON A DRY-AGENT DISSEMINATION SYSTEM	8-1
8.1	The External Configuration of the Store	8-1
8.2	The Rotary Actuator	8-2
8.3	The Power Generator	8-4
8.4	Gas Storage Vessel and Flow Regulating System	8-4
9.	SYSTEMS STUDY	9-1

TABLE OF CONTENTS (Continued)

Section	Title	Page
10.	PROGRESS ON THE LIQUID DISSEMINATING STORE	10-1
10.1	Work on Design and Fabrication	10-1
10.2	Disseminator Description and Information	10-6
10.2.1	Structure	10-6
10.2.2	Generator	10-8
10.2.3	Nose Section Contents	10-9
10.2.4	Plumbing Assembly	10-10
10.2.5	Fluid Handling System Operation	10-10
10.2.6	Boom Assembly	10-13
10.2.7	Actuator Assembly	10-13
10.3	Structural Testing	10-14
11.	SUMMARY AND CONCLUSIONS	11-1
12.	REFERENCES	12-1

LIST OF ILLUSTRATIONS

Figure	Title	Page
2.1	Apparatus for Measurement of Compaction Characteristics of Powders	2-3
2.2	Triaxial Shear Strength Apparatus	2-5
2.3	No Title	2-6
2.4	No Title	2-6
2.5	No Title	2-7
2.6	Shear Characteristics of Talc using Direct Shear Technique	2-9
2.7	Frictional Resistance for Surfaces in Contact with Talc Powder	2-12
2.8	Compaction Stress as a Function of Powder Specific Volume	2-14
2.9	Compaction Energy as a Function of Powder Specific Volume	2-15
2.10	Elastic Modulus E as a Function of Specific Volume for Several Powders	2-17
2.11	Laboratory Setup for Measurement of Bulk Tensile Strength of Compressed Powders	2-19
2.12	Apparatus for Measurement of Bulk Tensile Strength of Compressed Powders	2-20
2.13	Column Segment Cross-Section	2-21
2.14	Bulk Tensile Strength of Zinc Cadmium Sulfide (Curves A and B)	2-23
2.15	Bulk Tensile Strength of Zinc Cadmium Sulfide (Curve C)	2-24
2.16	Compression of a Column of Powder	2-25
2.17	Bulk Tensile Strength "σ" as a Function of Distance "L" from the Compressive Force	2-25

LIST OF ILLUSTRATIONS (Continued)

Figure	Title	Page
2.18	Bulk Tensile Strength "σ_0" Immediately Below Compressive Piston as a Function of Total Plug Length, L'	2-26
2.19	Notation for Piston-Cylinder Analysis	2-28
3.1	Aerophilometer	3-2
3.2	Schematic Drawing of Aerosol Chamber	3-3
3.3	Percent Transmission of #7-60 Filter over a Range of Wavelengths	3-5
3.4	Response of IP21 Phototube over a Range of Wavelengths	3-6
3.5	Overall Response of System	3-8
3.6	Schematic Diagram of Powder Dispersing Apparatus	3-9
3.7	Sketch of Filter and Holder Immersed in an Aerosol	3-11
3.8	Sampling with a Needle Immersed in an Aerosol	3-12
3.9	Schematic Diagram of Aerosol Sampling Apparatus Inside Chamber	3-14
3.10	Schematic Diagram of Aerosol Sampling System Control Manifold and a Sampling Probe	3-15
4.1	Viability of Sm and Bg Aerosols at Elevated Air Stream Temperature	4-2
4.2	Thermal Death Time Parameters of Sm and Bg Aerosols	4-4
4.3	Effect of Cab-O-Sil on Viability of Sm Aerosols	4-8
4.4	Toxic Effect of Rubber	4-11
5.1	Model for Statistical Analysis	5-3
5.2	Percentage of Particles (by number) in Sm Aerosol	5-6

LIST OF ILLUSTRATIONS (Continued)

Figure	Title	Page
5.3	Mechanisms for Preparing Simulated Sm Sample (Fill) for Dissemination	5-8
5.4	High Flow Rate Disseminator Model (GMI-3) for Wind Tunnel Application	5-9
5.5	Disseminator Model and Related Equipment Mounted on Wind Tunnel	5-11
6.1	Schematic Diagram of Test Arrangement used with Experimental Feeder for Compacted Powders	6-3
6.2	Test Arrangement used with Experimental Feeder for Compacted Powders	6-4
6.3	Test Room used for Experimental Work with Dry Powder Materials	6-6
6.4	Thread Cleaner Scheme to Remove Powder from Screw	6-8
6.5	Discharge Rate Curves for Series "A" Tests using Talc in the Experimental Dry Agent Feeder	6-14
6.6	Discharge Rate Curves for Series "B" Tests using Talc in the Experimental Dry Agent Feeder	6-15
9.1	Flow Rate versus Downwind Distance for "Average" Weather Conditions - Agent UL-2	9-2
9.2	Flow Rate versus Downwind Distance for "Good" Weather Conditions - Agent UL-2	9-3
10.1	External View of Liquid BW Agent Disseminator Showing Ram-Air Turbine Installation	10-2
10.2	Fluid Handling System	10-3
10.3	View of Liquid Disseminating Store with Aft Section Removed to Show Installation of Fluid Handling System	10-4
10.4	Boom and Actuator System	10-5
10.5	Plumbing Schematic	10-12

LIST OF TABLES

Table	Title	Page
4.1	Viability of Dry Aerosols of Bg at Various Exposures (Bg from Lot No. X-12, aerosolized with DeVilbiss generator - 51 trials)	4-3
4.2	Viability of Dry Aerosols of Sm at Various Exposures (Sm from Pool #7, aerosolized by explosion - 35 trials)	4-5
4.3	Effect of Cab-O-Sil Coating on Short Term Viability of Sm	4-9
4.4	Influence of 1% Cab-O-Sil on Viability Dry Aerosol of Sm Exposed to Elevated Air Temperatures	4-9
4.5	Effect of Rubber on Sm Suspensions	4-10
6.1	Test Results using Compacted Talc in Experimental Feeder	6-13

SEVENTH QUARTERLY PROGRESS REPORT ON DISSEMINATION OF SOLID AND LIQUID BW AGENTS

1. INTRODUCTION

This is the Seventh Quarterly Progress Report on Contract Number DA-18-064-CML-2745 which is a program of research on the dissemination of solid and liquid BW agents.

During this reporting period, Phase IV of the program was initiated, which provides for a 22-month continuation of the contract. The scope of work under Phase IV includes:

1) Continuation of theoretical analyses and experimental investigations of the parameters which influence the behavior of finely-divided materials.

2) Continuation of studies of methods for uniform metering, conveying, dissemination and deagglomeration of dry finely-divided materials.

3) Continuation of design studies and preparation of a detailed design of a dry-agent dissemination system capable of disseminating dry powders at a practical and effective rate.

4) Fabrication and testing of dry-agent line-source experimental hardware.

5) Preparation of final drawings and specifications of the dry-agent dissemination system.

6) Preparation of an operating and instruction manual for this equipment.

This report covers progress on studies covered by Items (1) through (3) above as well as work which was initiated under Phases II and IIIof the project. Work on Items (4), (5) and (6) above is scheduled for a later part of the program.

2. THEORETICAL AND EXPERIMENTAL STUDIES OF THE MECHANICS OF DRY POWDERS

Studies of the mechanical properties and behavior of dry powders were continued during the period covered by this report. The major effort during this period was devoted to designing and fabricating improved apparatus for measuring significant mechanical properties of dry powders. Recently obtained experimental results relating to powder shear strength and wall friction phenomena are presented. Also included is an analytical study of the stress distribution in a powder subjected to compaction in a piston-cylinder device.

2.1 Development of Experimental Apparatus

Two types of experimental apparatus have been designed and fabricated during the past three-month period: 1) an improved device for measurement of the energy required to compact a powder to a given density state, and 2) a triaxial shear test device. The triaxial apparatus should enable a more precise measurement of the shear strength of a powder than was possible with the direct shear apparatus used in earlier tests. It is hoped that tests carried out with these devices will furnish basic information required for an understanding of the behavior of dry powders. At the same time, such apparatus may prove useful in developing characterization tests for powders.

2.1.1 Apparatus for Determining Compaction Characteristics of Dry Powders

Experimental results reported earlier in the current study program have indicated how the bulk density of a powder depends on the energy invested in compacting the powder[1]. The apparatus used in these experiments was subject to several limitations, however. The most serious problem encountered with this apparatus was a lack of sensitivity in measuring the

deformation of the powder sample. This precluded an accurate measurement of the elastic properties of compacted powders. Also, it was not possible to apply high compaction stresses to the sample because of excessive elastic deformation of the compaction device.

These limitations have been largely eliminated with the apparatus shown in Figure 2.1. This device enables simultaneous measurements of the applied compressive stress and the resulting deformation of the powder sample. Large-scale movement of the piston is measured by means of the dial indicator shown in the photograph. The elastic recovery of the sample, which is observed when the applied load is gradually reduced, is measured electrically by means of a sensitive differential transformer (located directly behind the central column of the device in Figure 2.1). Both the elastic deflection and the applied stress are recorded during the experiment by means of a dual channel Sanborn recorder.

This apparatus is presently undergoing calibration checks with indications that the design objectives have been achieved. Preliminary results for talc agree rather well with previously reported data[1]. It is expected that a detailed account of compaction experiments with our improved apparatus will be included in the next quarterly report.

2.1.2 Triaxial Shear Apparatus

The shear strength characteristics of dry powders appear to be of fundamental importance with respect to the handling characteristics of these materials. However, it has been found to be very difficult to measure the shear strength of a powder in an unequivocal manner.

Shear measurements made to date in the current study have employed a direct shear technique (see Figure 2.6, page 2-9). This technique is fully described in a previous report[1]. While having the advantage of simplicity, the direct shear test cannot be relied upon for absolute shear measurements

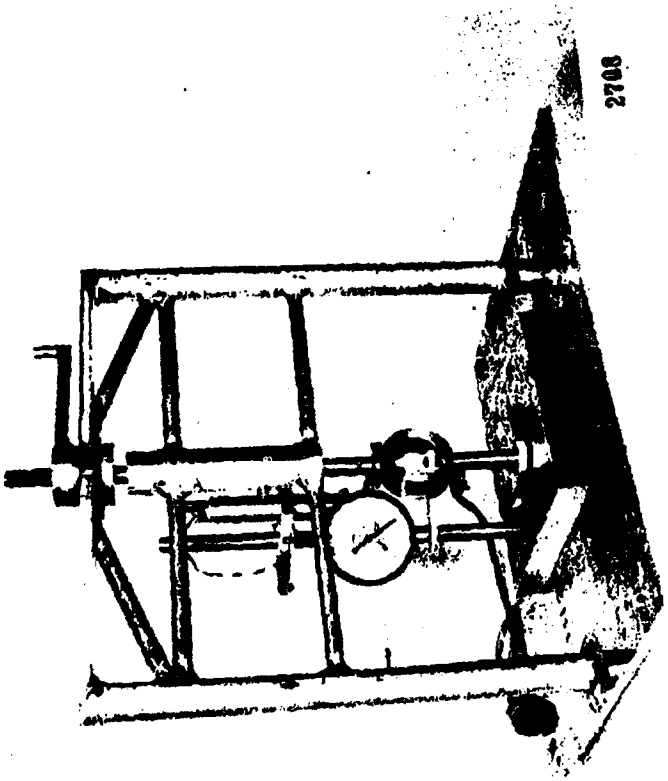

Apparatus for Measurement of Compaction Characteristics of Powders

Figure 2.1

since the material being tested in constrained in an indeterminate manner by the apparatus. This constraint is likely to be evidenced as an apparent increase in shear strength of the material.

The triaxial test method, which has also been described in an earlier report[2], is based upon controlling the stresses applied to the sample during the shear test. The shear resistance of the powder can then be found from the known applied stresses as described subsequently.

A prototype triaxial test device has been developed in order to apply this test technique in dry powder research. The device, shown in Figure 2.2, will be used in the following way:

The sample is compacted in a thin rubber membrane which is used to seal the sample during the test. As can be seen from Figure 2.3, the test sample has the form of a right circular cylinder, with a cylindrical fitting placed at each end. The end fittings insure that the axial stresses applied to the sample are properly distributed and also facilitate sealing of the sample. A vent is provided in the top fitting to avoid entrapment of air due to compression of the sample (Figure 2.4). The sample is placed in the test device as shown in Figure 2.2, and the chamber is pressurized. An axial load is then gradually applied to the sample until shearing occurs. The axial force is measured by means of strain gages mounted inside the chamber. Failure is detected by means of a sensitive linear potentiometer which indicates the motion of the loading piston By feeding both the potentiometer and strain gage outputs to a dual channel recorder, a simultaneous recording of data is possible.

The shear characteristics are found by conducting triaxial tests at several chamber pressures and constructing a Mohr stress circle at each load condition. Two stress circles, corresponding to the chamber pressures p_2 and p_2^1, are shown in Figure 2.5. The points σ_2 and σ_2^1 on the diagram represent lateral stresses applied to the sample; thus, we have $\sigma_2 = p_2$ and $\sigma_2^1 = p_2^1$. The points σ_1 and σ_1^1 are the axial stresses

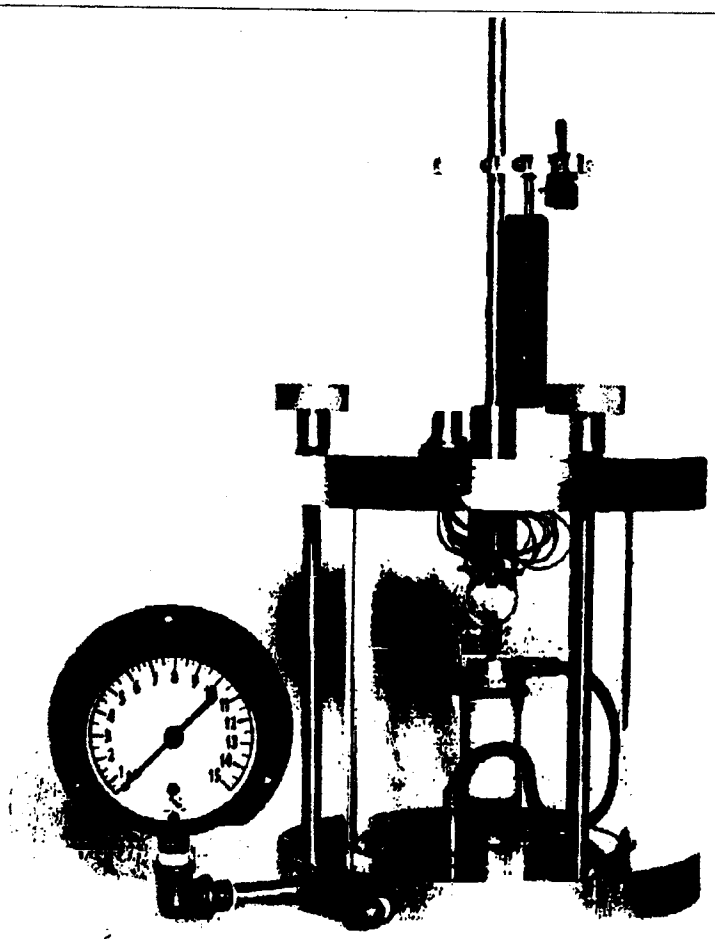

2709

Figure 2.2 Triaxial Shear Strength Apparatus

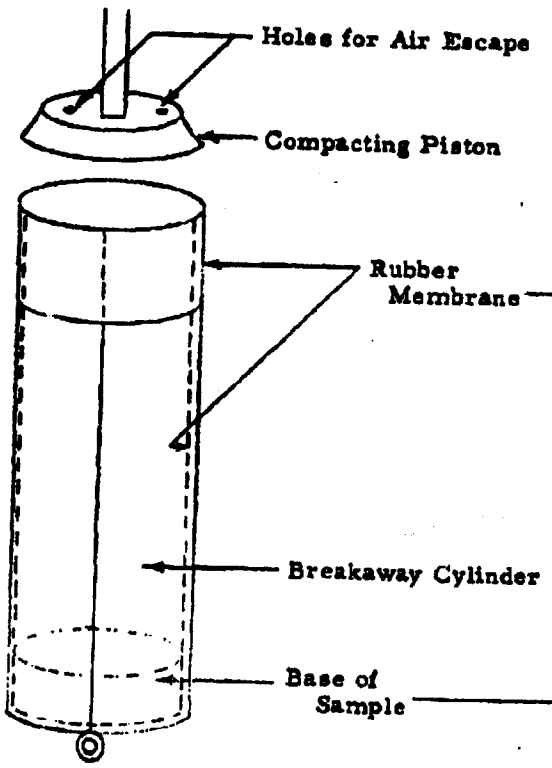

Figure 2.3

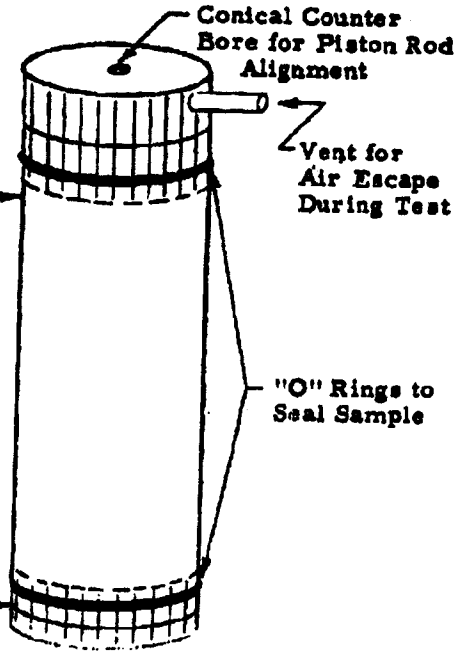

Figure 2.4

applied to the sample. If the applied load is F, the axial stress is $p_2 + F/A$, where A is the cross-sectional area of the sample.

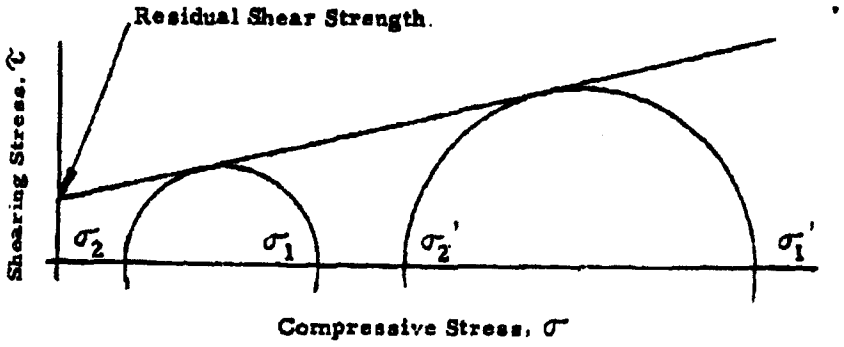

Figure 2.5

In the general case, the shear strength characteristic is defined by the envelope of a series of stress circles. The intercept of the shear strength characteristic curve at $\sigma = 0$ is of particular interest since this yields the residual shear strength of the compacted power sample, i.e., the strength of the powder under zero load.

Preliminary tests with this apparatus have revealed several problems connected with sealing the sample to prevent infiltration of high-pressure air from the pressure chamber. At the present time, this problem and several other minor difficulties have been cleared up and it is expected that routine shear tests with the triaxial shear apparatus can now be undertaken.

Experimental results obtained with the triaxial apparatus will be compared with shear characteristics obtained from direct shear tests. If, as expected, these methods yield different results, a critical evaluation of both

test methods will be necessary. As mentioned earlier, it appears likely that the direct shear test will yield a higher shear resistance than the triaxial test because of constraints applied to the powder sample in the direct shear test. Another point of difference between these test methods is in the compaction process, or more specifically, in the way stresses are applied to produce sample compaction in each case. A general discussion of these matters will be deferred until experimental data are available from tests of identical powder samples by both techniques.

2.2 Related Experimental Studies

A number of experiments were carried out during the past quarterly period for the purpose of providing insight into the static behavior of dry powders. The results of these tests are presented below. Also, previously reported results of compaction studies[1] have been reviewed and are presented herein in a different and more meaningful form.

2.2.1 Residual Shear Strength of Compacted Powders

The residual shear strength of talc powder was investigated by using the direct shear apparatus described in an earlier report[1]. These tests were conducted in the usual manner, with one important change. Prior to application of a tangential shearing force to the upper shear disk (see Figure 2.6), the sample was compacted by application of a compressive stress σ_c. This stress was then reduced to the value σ_r and the shearing stress, τ_c required to shear the sample was determined. A series of tests of this type were carried out over a range of compaction stresses σ_c while keeping σ_r fixed. The results of these tests are shown in Figure 2.6 for $\sigma_r = 4.2 \times 10^3$ dynes/cm^2 and $\sigma_r = 8.2 \times 10^3$ dynes/cm^2. Each data point shown in the figure is the average of 5 or more runs. The maximum deviation from the mean values was within ± 5 percent.

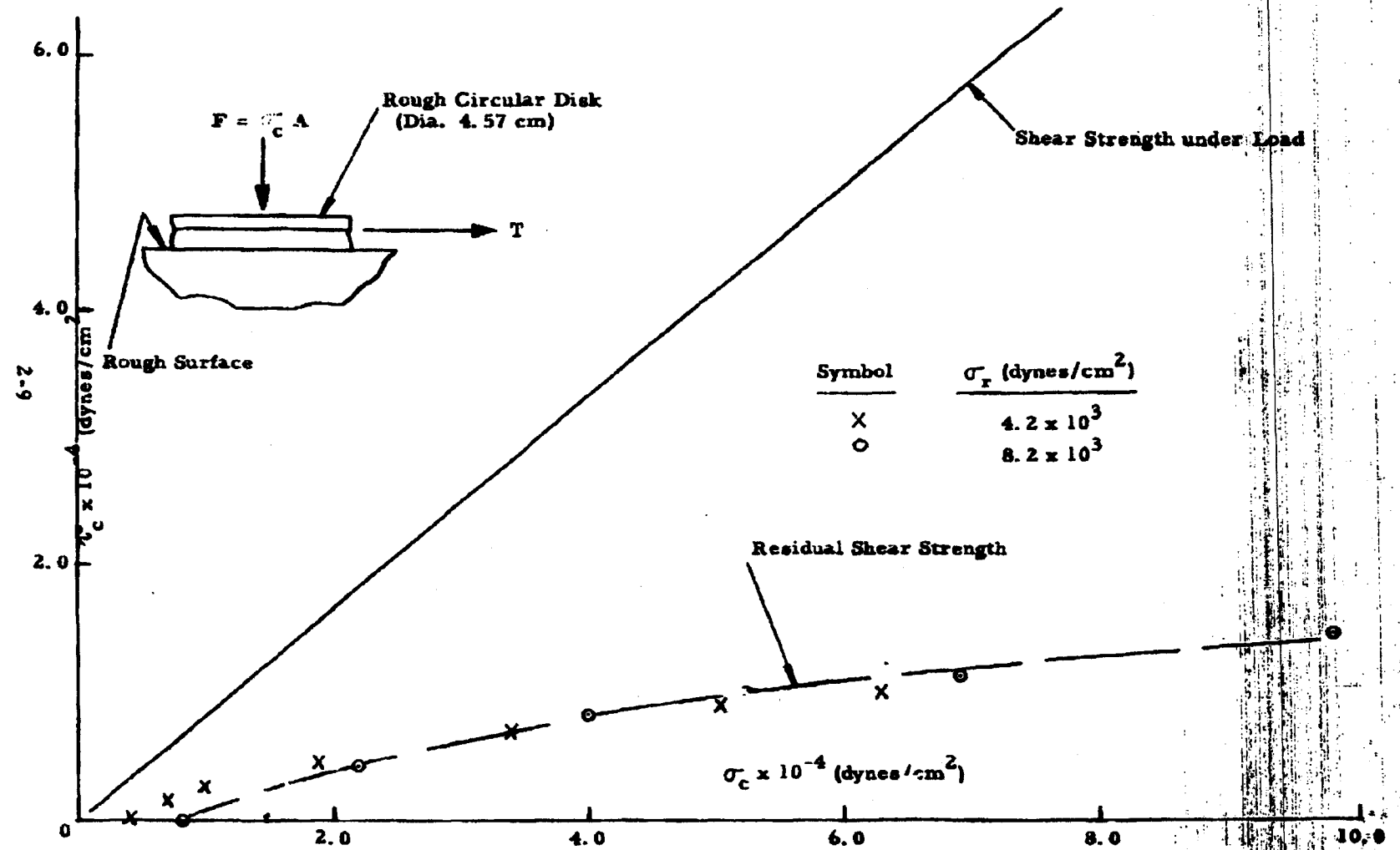

Figure 2.6 Shear Characteristics of Talc using Direct Shear Technique

The shear strength of the powder was found to increase with the compaction stress σ_c in accordance with the power relationship: τ_c = constant x $\sigma_c^{0.44}$ for $\sigma_c \geq 10^4$. The residual shear strength of the compacted powder can be estimated by subtracting the shear stress corresponding to the compressive stress σ_r from the measured values. The resulting shear strength characteristics shown in Figure 2.6 were determined in this manner. It is apparent that the residual shear strength of the powder is dependent to some extent on the compressive stress σ_r maintained during shearing of the sample. Although these experiments and the interpretation given above may not be conclusive, the trend exhibited in Figure 2.6 is of considerable interest.

Comparing the shear strength of talc under load with the residual shear strength of the compacted powder, it is apparent that the relative effect of compaction on shear strength decreases with increasing compressive stresses.

A decisive test of this conclusion will be possible by using the triaxial test apparatus described in the preceding section of this report. It will of course be necessary to test a number of powders in this manner in order to draw general conclusions as to the behavior of dry powders.

2.2.2 Wall Friction Phenomena

In many practical situations, it is necessary to understand the nature of the mechanical interaction between a powder and a solid surface. In particular, the friction angle or coefficient of friction for a surface exposed to a powder is of importance in the compaction of a powder in piston-cylinder devices.

Accordingly, an experimental investigation of wall friction has been undertaken, using essentially the same apparatus employed for direct shear measurements. In these tests, the rough disk usually employed in the shear tests is replaced by a geometrically similar disk, one face of which

has been prepared for the friction test. This face is placed in contact with the powder and, from this point on, the test is carried out in exactly the same manner as the direct shear test.

Friction tests of this type have been performed for several materials of varying surface roughness in contact with talc powder. Results of these experiments are plotted in Figure 2.7. Three types of surfaces were investigated: stainless steel, aluminum alloy and aluminum covered with an epoxy resin yielding a smooth, glossy surface. From Figure 2.7 it can be seen that the frictional resistance is essentially proportional to normal stress for each surface tested. Furthermore, a substantial variation in friction angle was observed for the different surfaces, ranging from $\theta = 35.5°$ for an unpolished stainless steel surface (10 to 12 microinches nominal surface roughness) to a minimum of $\theta = 30°$ for a polished aluminum surface (6 to 8 microinches s. r.). These friction angles are substantially below the shear angle for talc powder ($\phi = 40°$).

Further tests of this type are planned for the immediate future. It is of particular interest and importance for theoretical as well as practical reasons to determine the influence of surface roughness on the friction angle. Means for minimizing wall friction are also of practical importance.

2.2.3 Compaction Characteristics of Powders

Data from compaction experiments reported in a previous report[1] have been re-examined during the current report period and subjected to further analysis. These results are presented in Figures 2.8, 2.9 and 2.10 showing respectively the compaction stress, compaction energy and equivalent elastic moduli as a function of density for talc and Sm powders.

Figure 2.7 Frictional Resistance for Surfaces in Contact with Talc Powder

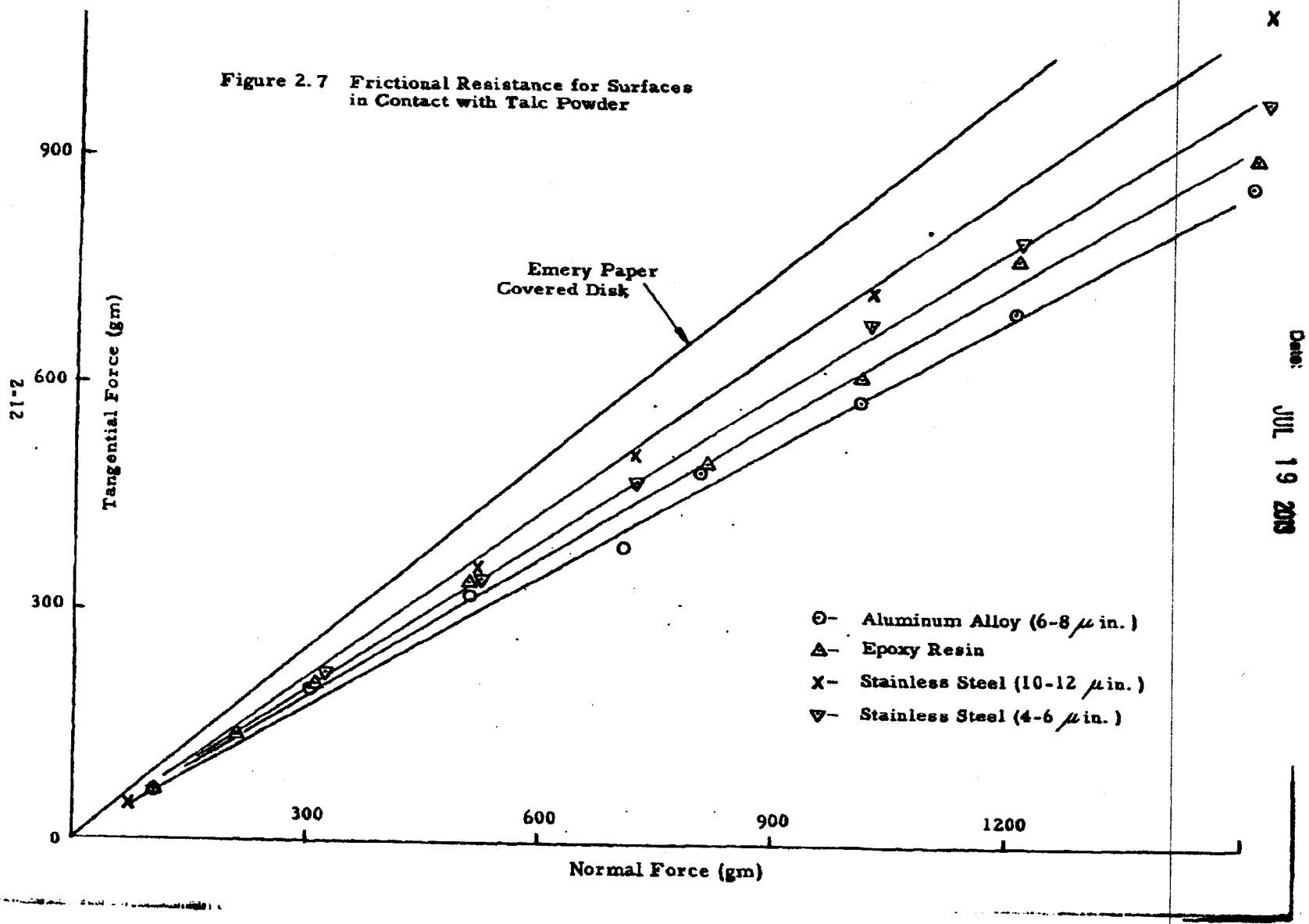

2.2.3.1 Stress Required for Compaction of a Dry Powder

The compressive stress required to achieve a given powder density in a piston-cylinder compaction device (see Reference 1) is plotted as a function of the specific volume in Figure 2.8. Two curves are shown for each material: 1) the compressive stress required to obtain the density under loaded conditions, and 2) the stress required to obtain the density after removal of the load; i.e., after allowance is made for elastic recovery of the powder.

2.2.3.2 Energy Required for Compaction

The energy per gram required for compaction of a powder to a given density is shown in Figure 2.9. When allowance is made for elastic recovery of the powder a shift in the energy and density of the sample occurs as indicated in the figure. It is of interest to observe that Figure 2.9 indicates that the elastic energy stored in the powder is proportional to the total energy at a given density for the conditions of these experiments.

2.2.3.3 Effective Elastic Moduli for Dry Powders

In order to describe the elastic properties of a powder, we may define an equivalent elastic modulus of the form:

$$\overline{E} = \frac{\sigma h_e}{\Delta_x} \qquad (2\text{-}1)$$

where:

σ = the applied stress

h_e = the compressed depth of the powder sample

Δ_x = the measured elastic recovery after removal of the load

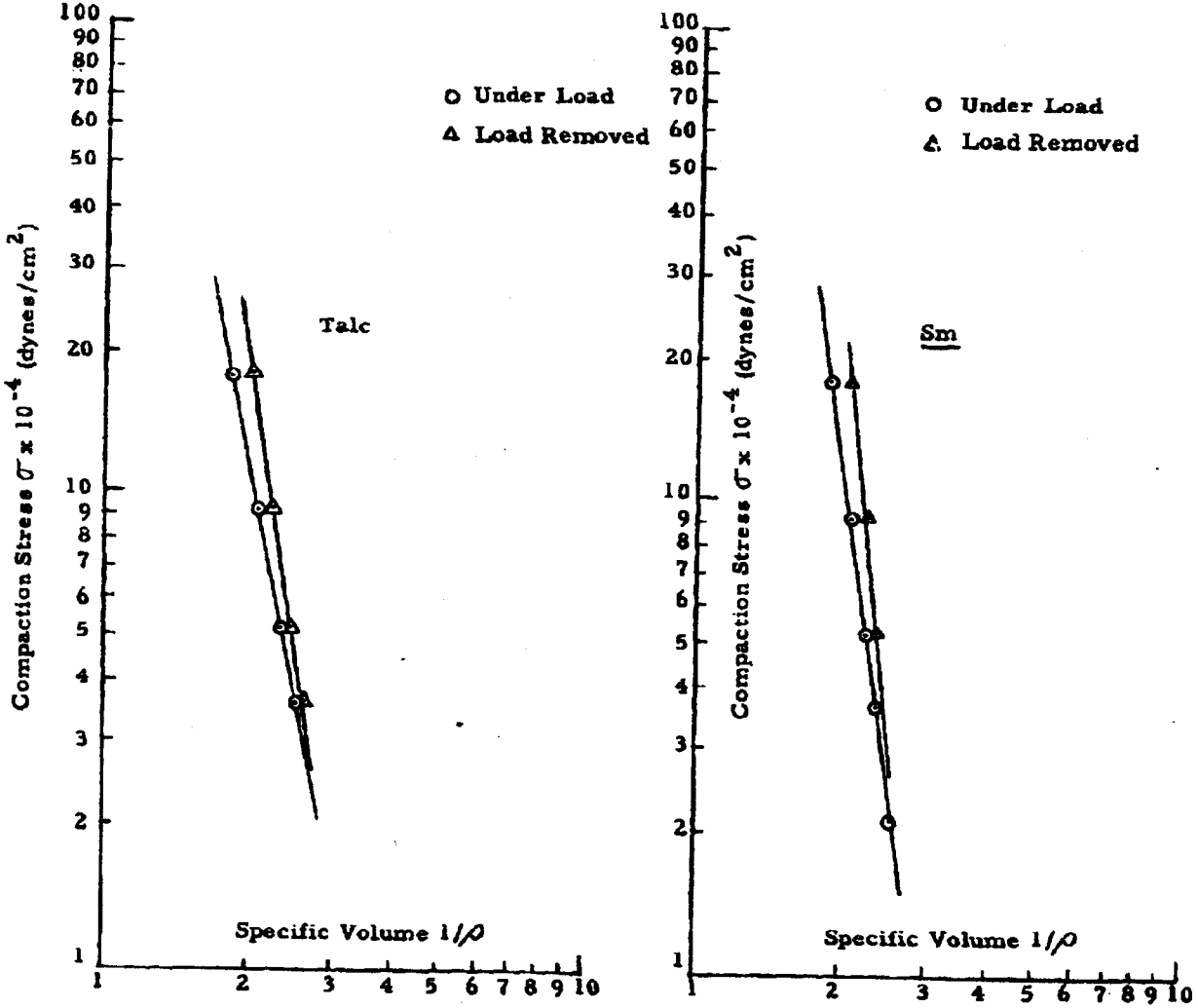

Figure 2.8 Compaction Stress as a Function of Powder Specific Volume

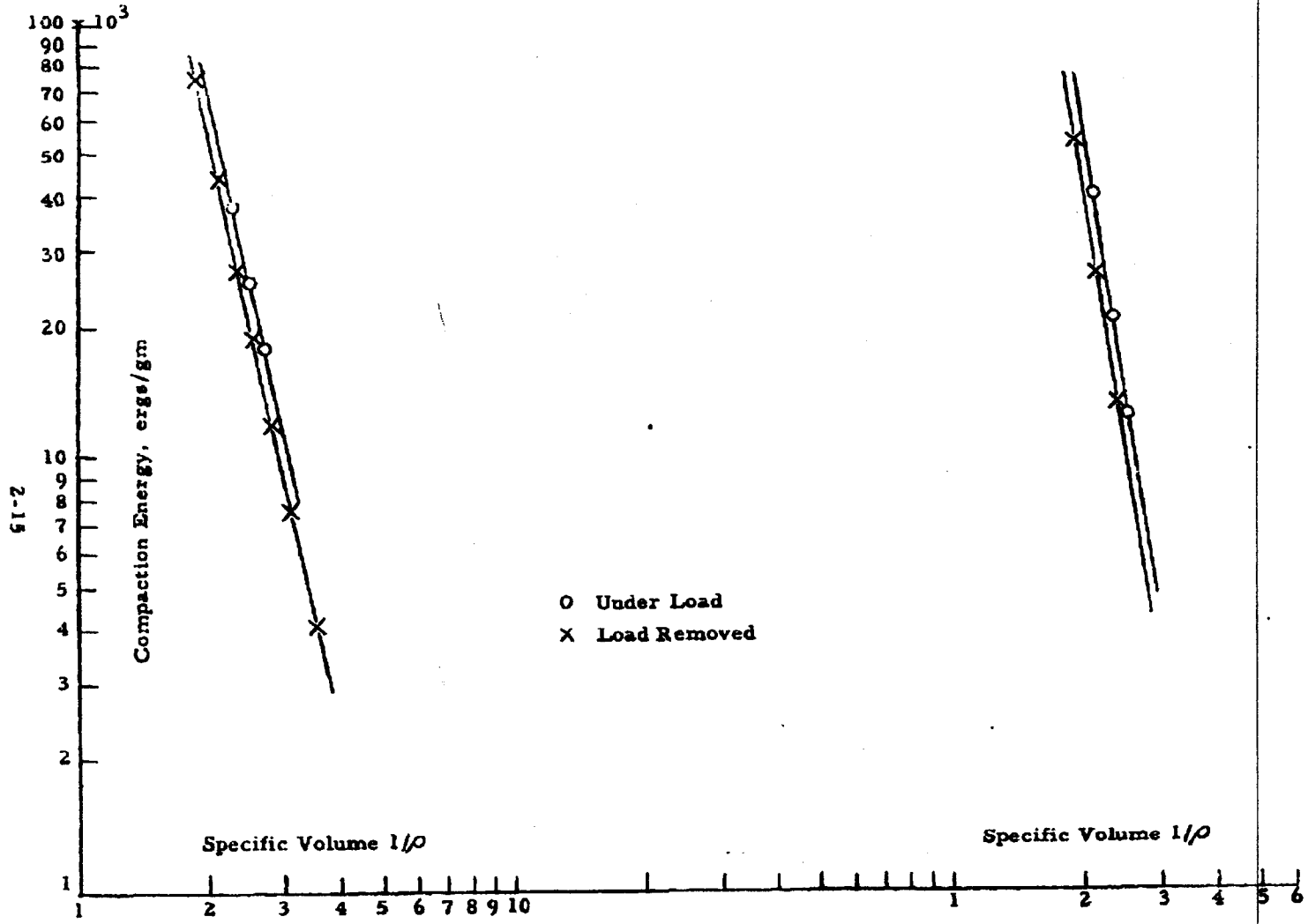

Figure 2.9 Compaction Energy as a Function of Powder Specific Volume

The equivalent elastic modulus is plotted as a function of specific volume in Figure 2.10 for talc, Sm and saccharin. It is apparent from the figure that the elastic properties of the three powders are remarkably similar, at least under the conditions of these tests.

Further studies of the elastic properties of powders will be carried out with the more sensitive compaction apparatus discussed in Section 2.1.1.

2.3 Bulk Tensile Strength of Powders

A versatile new apparatus for the determination of the bulk tensile strength of a column of compressed powder has been designed and perfected. The apparatus permits the bulk tensile strength measurement to be made as a function of 1) bulk density, 2) distance from compressive force application to fracture plane, and 3) total column length. In addition to this, we should by proper extrapolation of data from 2) and 3) be able to obtain a value for the bulk tensile strength of a compressed powder which is dependent only upon the physical properties of the compressed powder and on the magnitude of the compressive force applied and therefore independent of the geometry of the apparatus. This should provide an absolute method for the comparison of the bulk tensile strength of various compressed powders.

Theoretically the bulk tensile strength of a compressed powder is an exponential function of the distance from the compressive piston to the fracture plane[3].

$$\sigma = \sigma_o e^{-kL} \qquad (2\text{-}2)$$

where:

σ = bulk tensile strength of a column of compressed powder at distance L from the piston

σ_o = bulk tensile strength of compressed powder immediately below the piston

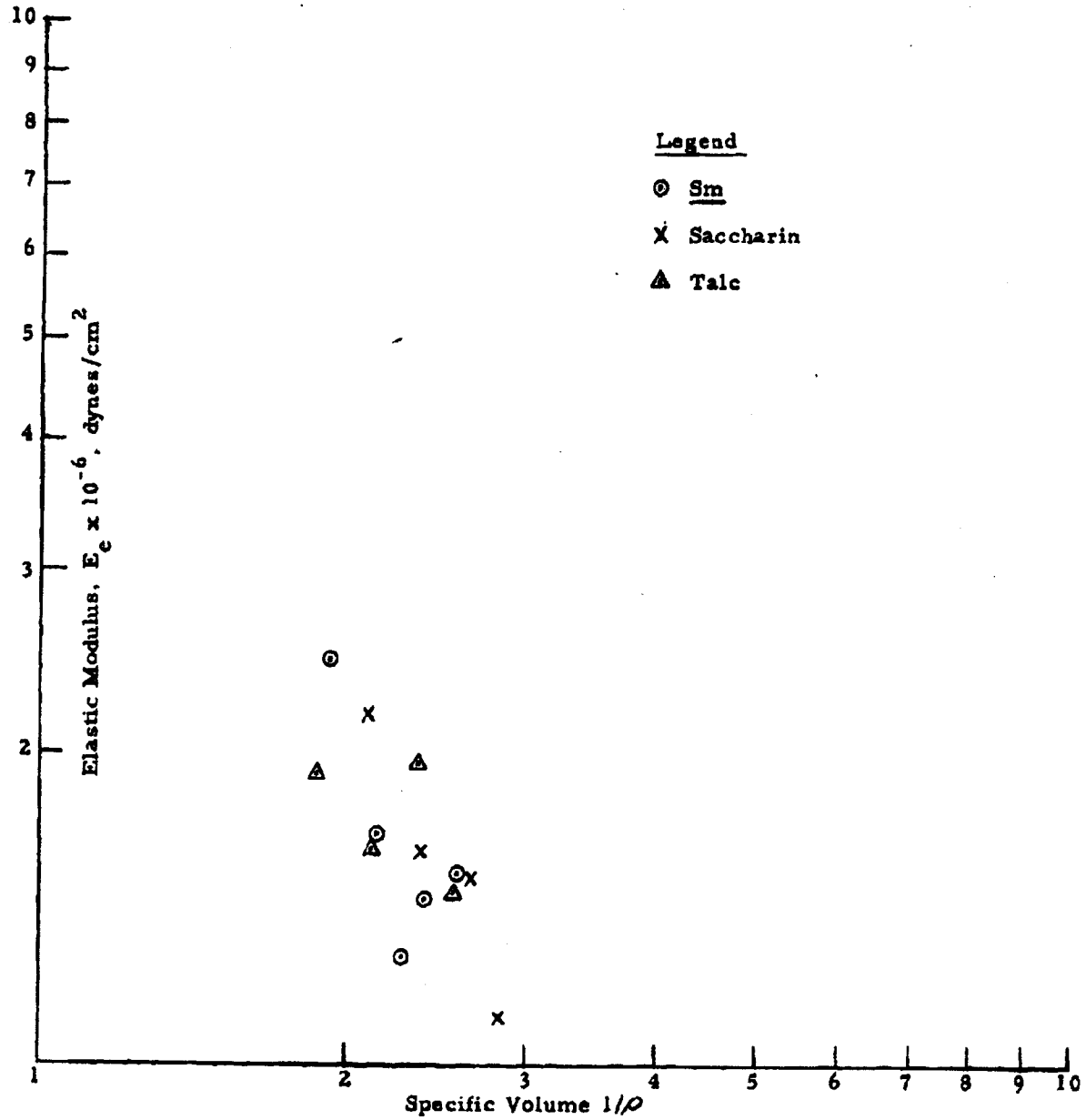

Figure 2.10 Elastic Modulus E as a Function of Specific Volume for Several Powders

k = constant

L = distance from piston to fracture plane

An experimental apparatus must therefore be capable of fracturing the column of compressed powder at several different distances from the piston applying the compressive force. An apparatus has been designed and perfected to accomplish this.

2.3.1 Apparatus and Technique

The column to be packed with powder is fabricated of aluminum and has an I.D. of 3/4-inch (see Figures 2.11 and 2.12). The bottom half of the column is divided into six 1/2-inch segments (Figure 2.13) whose construction eliminates horizontal motion but allows a vertical force to break the powder column at the boundary of each segment without a significant error being contributed by frictional forces between the metal segments. Prior to fracture of the column, the column segments are held in place by metal spring clips. A vertical compressive force is applied to the powder by the piston assembly shown (Figure 2.12). The platform at the top of the piston assembly is recessed to accommodate the special set of weights which have uniform diameters and varying heights. This technique aids the operator in applying the force vertically above the powder column. After the column of powder is compressed the individual segments are caused to fracture by a vertical force exerted by a lever arm and pulley assembly containing a strain gauge system to measure this applied force. The signal from the strain gauge system is electronically recorded by Sanborn equipment for a permanent record of the experiment. The entire apparatus with the exception of the electronic equipment is housed in an isolator lab maintained at constant humidity by a synthetic mixture of dry and moist air. The humidity within the isolator lab is constantly monitored by an infrared hygrometer.

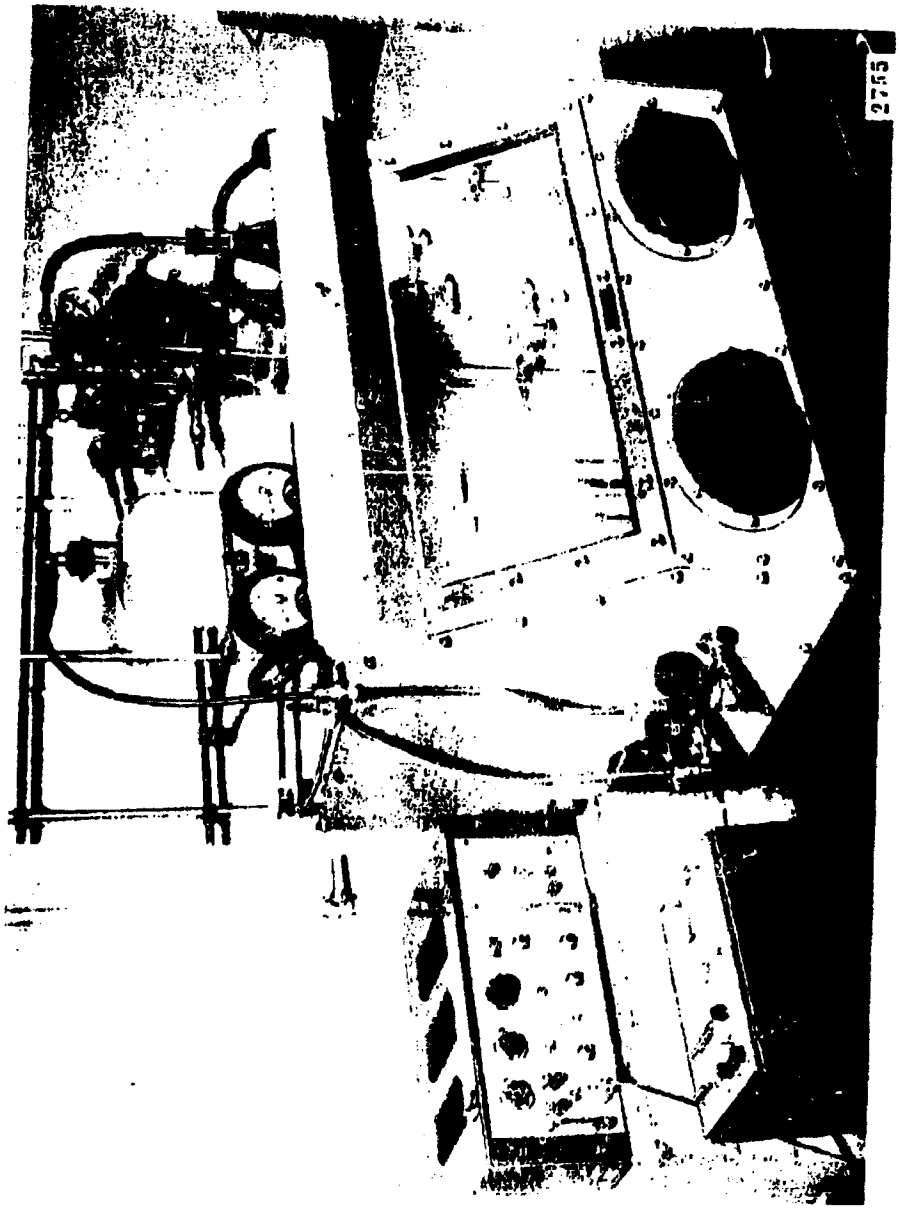

Laboratory Setup for Measurement of Bulk Tensile Strength of Compressed Powders

Figure 2.11

Apparatus for Measurement of Bulk Tensile Strength of Compressed Powders

Figure 2.12

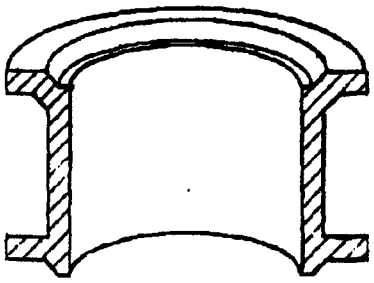

Figure 2.13 Column Segment Cross-Section

In experiments conducted so far zinc cadmium sulfide has been used as a test powder. Although its tensile strength is comparatively low it is known to give reproducible results for this type of physical measurement[3].

In a typical experiment the powder is preconditioned in the isolator lab at the desired humidity (15% in this case) for at least 48 hours. The column is then filled by sifting the powder through a glass powder funnel fitted with a fine mesh screen to assure uniform packing of the powder. The piston assembly is then clamped into position and the vertical force is applied. During early experimentation it was found necessary to clamp the entire column rigidly prior to application of the compressive force since the individual segment clamps were not strong enough to prevent bending of the column and thus cause partial fracture of the compacted powder prior to measurement of the tensile strength. After compression, the piston assembly and upper filling tube are carefully removed. A "lift cap" assembly designed to clamp firmly to the top of each segment is fitted into place and

connected to the lift assembly. By turning a crank in the lift assembly the column is fractured at the bottom of each segment after it is unclamped. The tensile force is recorded by the strain gauge assembly.

2.3.2 Discussion of Experimental Results

The primary purpose in this preliminary set of experiments was to check the reliability of the equipment and apparatus. As shown in Figures 2.14 and 2.15, the tensile strength data follow the exponential relationship quite well. It is believed that the scatter of points at large values of L can be diminished by refinement of technique. It should be noted that the data indicate a dependence of tensile strength upon length of time of comparison. When the weights were allowed to compress the powder overnight (16 hours) a significant change in σ_o occurred. This phenomenon will have to be explored further, but for the purpose of comparing one powder with another it may be found expedient to agree upon a standard time of compression.

As each segment of powder is broken, its weight can also be recorded so that we can also follow the change in bulk tensile strength with bulk density.

In our measurements we are actually measuring the tensile strength at the fracture point at a distance "L" from the piston (Figure 2.16). We then plot the tensile strength "σ" versus L as shown in Figure 2.17.

By extrapolation to L = 0 we obtain σ_o, the bulk tensile strength of the powder at the surface of the piston. This assumes that σ_o is independent of "L", the total plug length. Recent experiments indicate that this is probably not the case. The design of this apparatus is such that we can also vary the value of L' (total plug length). Thus by plotting L' versus σ_o and extrapolating to L' = 0, as shown in Figure 2.18, we would obtain a value σ_o' for the bulk tensile strength of the powder which is dependent only upon the physical properties of the powder and the magnitude of the compressive force applied but independent of the geometry of the apparatus. This should provide an

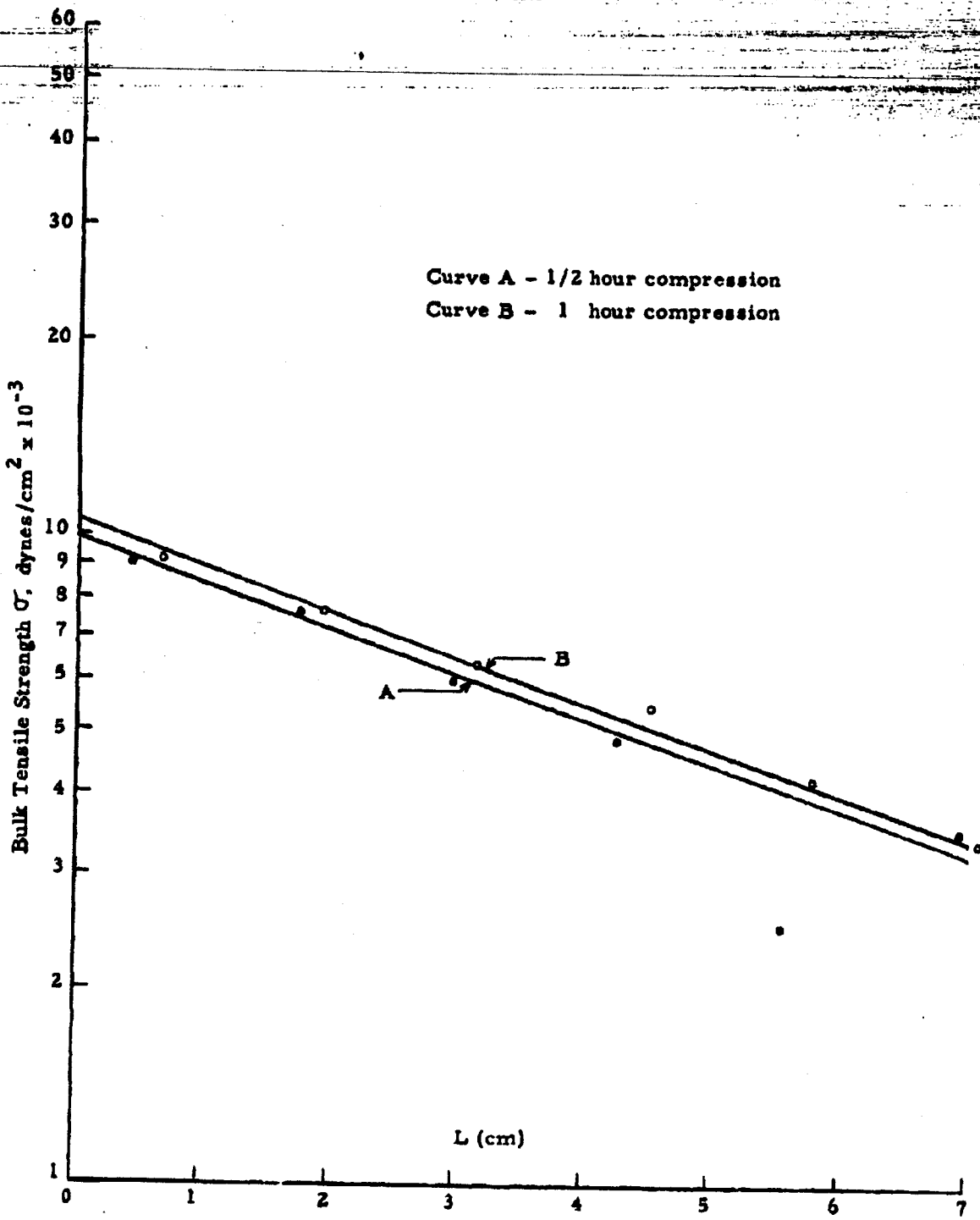

Figure 2.14 Bulk Tensile Strength of Zinc Cadmium Sulfide (Curves A and B)

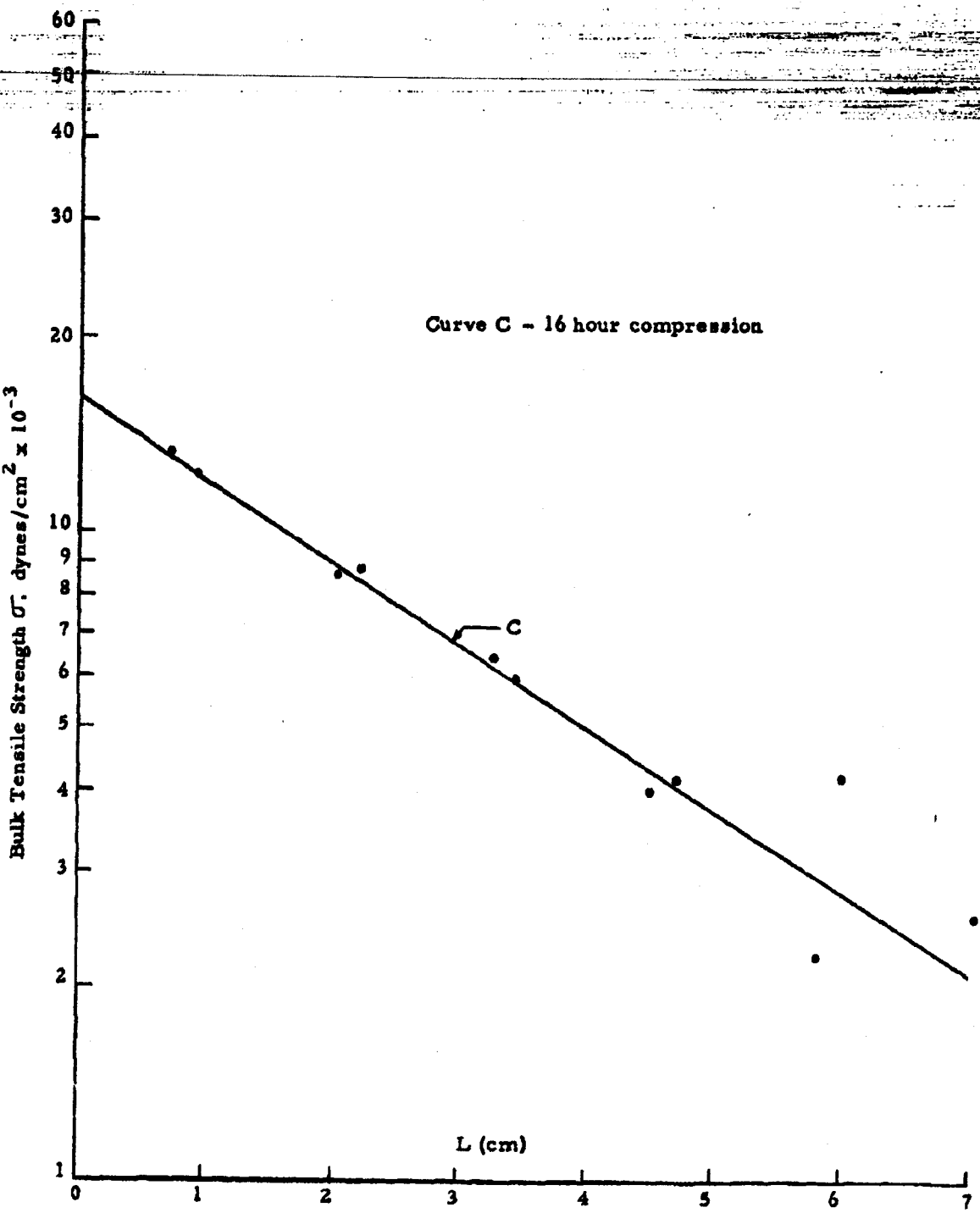

Figure 2.15 Bulk Tensile Strength of Zinc Cadmium Sulfide (Curve C)

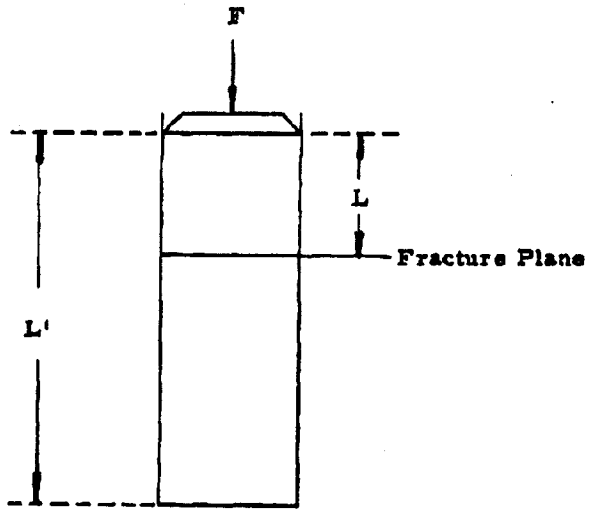

Figure 2.16 Compression of a Column of Powder

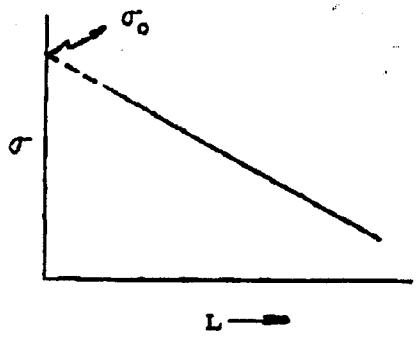

Figure 2.17 Bulk Tensile Strength "σ" as a Function of Distance "L" from the Compressive Force

absolute method for comparison of the bulk tensile strength of a compressed powder. The determination of σ_o' would of course involve a considerable amount of laboratory time per powder and for practical purposes simpler comparisons of tensile strength can be made by further defining the method by which the measurement is made.

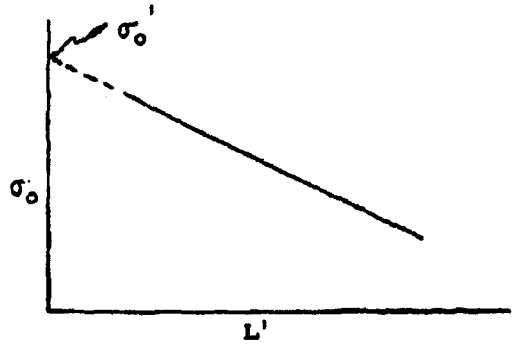

Figure 2.18 Bulk Tensile Strength "σ_o" Immediately Below Compressive Piston as a Function of Total Plug Length, L'

2.3.3 Future Work

The apparatus as designed is capable of giving a wealth of information concerning the variation of bulk tensile strength throughout a system of compressed powders. Reliable results do, however, depend upon very careful work. The effect of time of compression upon bulk tensile strength must be studied further to determine what time factor should be considered for most satisfactory results. When this is done measurements of bulk tensile strength will be made on other powders.

2.4 Mathematical Analysis of the Piston-Cylinder Test

The piston-cylinder test has been described in previous reports from both the experimental and theoretical points of view[1,4]. Experimentally it has been found that the ratio of applied force F_A to resistive force F_R at the point of slippage can be expressed by means of the empirical equation:

$$\frac{F_A}{F_R} = e^{\frac{4KL}{D}} \qquad (2\text{-}3)$$

where:

L = the length of the powder plug

D = the cylinder diameter

The factor K was found to be independent of the load for tests conducted with a given powder in a given cylinder. This result is of considerable importance since it implies that the stress distribution in the powder is independent of the degree of compaction produced by the applied loads. From this it may be inferred that a powder element undergoing compaction tends to maintain a fixed ratio of minor to major principal stresses. If we assume this to be true of the compaction process, it is possible to determine the stress distribution in the powder. This analysis may be carried out as follows. For statical equilibrium, the stress distribution must satisfy the following equilibrium conditions (see Figure 2.19 for notation):

$$\frac{\partial \sigma_r}{\partial r} + \frac{\partial \tau}{\partial z} + \frac{\sigma_r - \sigma_o}{r} = 0 \qquad (2\text{-}4a)$$

$$\frac{\partial \tau}{\partial r} + \frac{\partial \sigma_z}{\partial z} + \frac{\tau}{r} = 0 \qquad (2\text{-}4b)$$

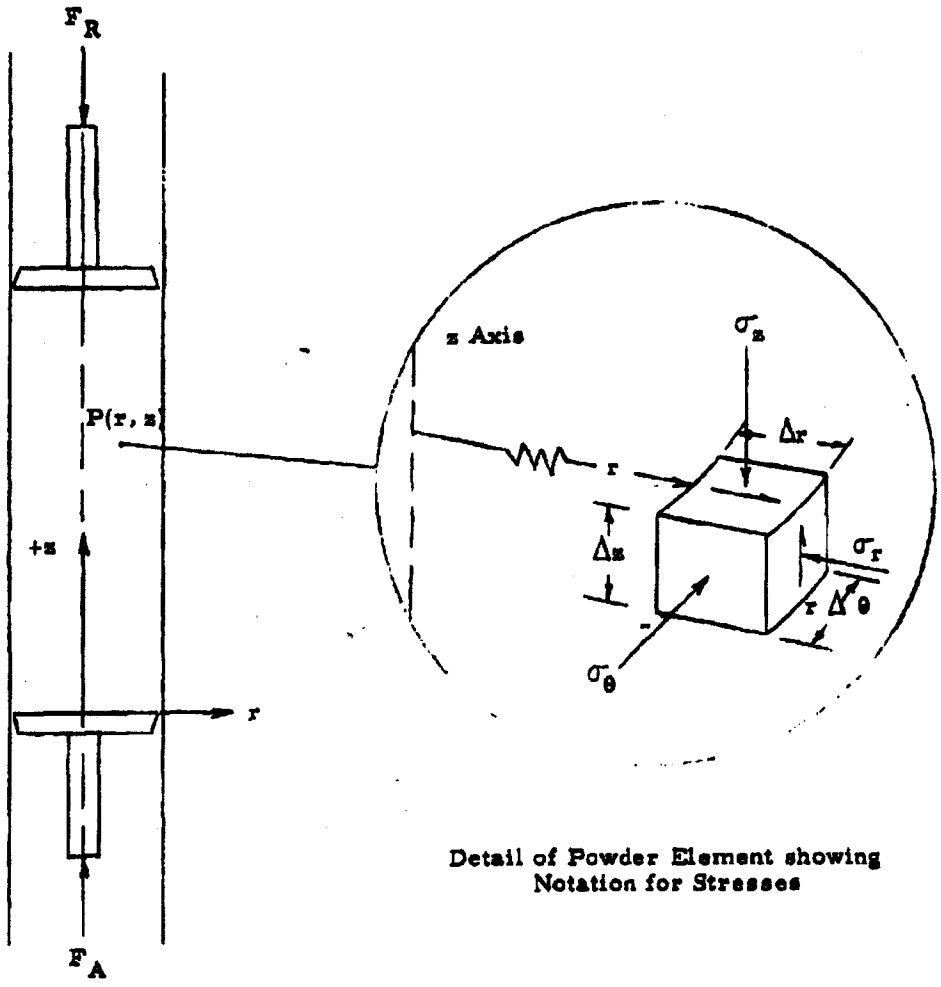

Detail of Powder Element showing Notation for Stresses

Figure 2.19 Notation for Piston-Cylinder Analysis

If the shear stress is small, we may assume that:

$$\frac{\sigma_r}{\sigma_z} = \frac{1 - \sin \phi}{1 + \sin \phi} = C \qquad (2\text{-}5)$$

where ϕ is the shear angle of the powder. The meaning of this assumption can be seen by referring to Figure 2.19. In the stress plane, if we impose the condition that τ is small relative to the difference in principal stresses $\sigma_1 - \sigma_2$, it is apparent that $\sigma_r = \sigma_\theta \doteq \sigma_2$ and $\sigma_z \doteq \sigma_1$. Furthermore, if shearing is imminent, we must have $\sigma_2/\sigma_1 = C$ or $\sigma_r/\sigma_z \doteq C$.

With these assumptions, the above equations become:

$$\sigma_r = C\,\sigma_z \qquad (2\text{-}6a)$$

$$\frac{\partial \sigma_r}{\partial r} + \frac{\partial \tau}{\partial z} = 0 \qquad (2\text{-}6b)$$

$$\frac{\partial (r\tau)}{\partial r} + r\,\frac{\partial \sigma_z}{\partial z} = 0 \qquad (2\text{-}6c)$$

This system of equations can be solved in a straightforward manner, yielding the following expressions for the stresses:

$$\sigma_z = \frac{F_R\, e^{K\bar{z}}}{2\pi R^2 f(\alpha)} \left\{ 1 + \sum_1^\infty \frac{\alpha^{2n}\, \bar{r}^{2n}}{2^{2n}\,(n!)^2} \right\} \qquad (2\text{-}7a)$$

$$= F_R\, \frac{e^{K\bar{z}} K}{2\pi R^2} \left(\frac{R}{L}\right) \left\{ \frac{\bar{r}}{2} + \sum_1^\infty \frac{\alpha^{2n}\, \bar{r}^{2n+1}}{(2n+2)2^{2n}\,(n!)^2} \right\} \qquad (2\text{-}7b)$$

where:

$$K = 2\frac{\mu CL}{R}$$

$$\alpha^2 = 4\mu^2 C$$

$$f(\alpha) = \frac{1}{2} + \sum_{1}^{\infty} \frac{\alpha^{2n}}{(2n+2)\,2^{2n}\,(n!)^2}$$

$$\bar{z} = \frac{z}{L} \qquad \bar{r} = \frac{r}{R}$$

This solution applies at the point of slippage of the powder plug, the wall friction coefficient being μ. By integration of Equation (2-7a), the applied force F_A is found to be:

$$F_A = 2\pi \int_0^R r\,\sigma_z\,dr = F_R\,e^{\frac{2\mu CL}{R}} \tag{2-8}$$

which agrees formally with Equation (2-3) if we take $K = \mu C$.

Since by hypothesis the friction angle $\theta = \tan^{-1}\mu$ is small compared with the shear angle ϕ, we have $\alpha^2 \ll 1$. Consequently, it is permissible to ignore higher order terms in the series expressions for the stresses, yielding the following approximate equations:

$$\sigma_z \doteq \frac{F_R\,e^{K\bar{z}}}{2\pi R^2 f(\alpha)}\left(1 + \frac{\alpha^2\,\bar{r}^2}{4}\right) \tag{2-9a}$$

$$\tau \doteq \frac{F_R\,e^{K\bar{z}}}{4\pi R^2} K\left(\frac{R}{L}\right)\bar{r} \tag{2-9b}$$

As an example, if $\mu = 0.25$ and $\phi = 40°$, we obtain $C = 0.216$ and $\alpha^2 = 0.054$. The variation of σ_z over a cross-section of the powder slug is given by the term:

$$1 + \frac{\alpha^2 r^{-2^n}}{4} = 1 + 0.014\,\bar{r}^2 .$$

Thus, the axial stress has a maximum variation of about 1.4 pescent over the cross-section. On the other hand the shearing stress increases linearly from zero on the axis to the value:

$$\tau_w = \frac{\mu C_0 K\bar{z}}{2\pi R^2} \qquad (2\text{-}10)$$

at the wall.

The above analysis leads to conclusions which is no way conflict with experimental results for the piston-cylinder configuration. This lends a degree of support to the principal assumption on which the analysis was based: that compaction of a dry powder occurs under conditions of imminent shear.

3. AEROSOL STUDIES

The design and fabrication of an aerophilometer, a light-scattering instrumented aerosol chamber, for use in studying the settling properties of aerosols is almost complete. A photograph and schematic drawing of this device in its present state are presented in Figures 3.1 and 3.2 respectively. The aerophilometer consists of: 1) a main chamber, 2) an optical light-scattering detection system, 3) a powder dispersing system, and 4) an aerosol sampling system.

3.1 Main Chamber

The main chamber, constructed of sheet aluminum, has an internal dimension of one cubic meter. The sides of the chamber are joined by rivets and sealed with epoxy resin. The door (one entire side of the chamber) is connected on one edge by means of a hinge to the chamber. The door closes against a Dor-tite gasket and is locked by link-lock fasteners.

At the right lower corner of the chamber is a 4-inch fan blade. The motor for the fan blade is located outside the chamber and has its shaft projecting into the chamber through a Teflon seal.

3.2 Optical Light-Scattering Detection System

The optical light-scattering detection system is shown as part of the aerosol chamber (aerophilometer) as depicted in Figure 3.2. This system consists of a monochromatic light source and two sensitive photomultiplier detection systems.

3.2.1 Monochromatic Light Source

The lamp is a General Electric projection lamp. In order to avoid fluctuations in the light, power is supplied from a Sorenson regulator and the lamp voltage is controlled by an autotransformer. In addition, the lamp circuitry is such that the lamp cannot be turned on unless its cooling blower is operating.

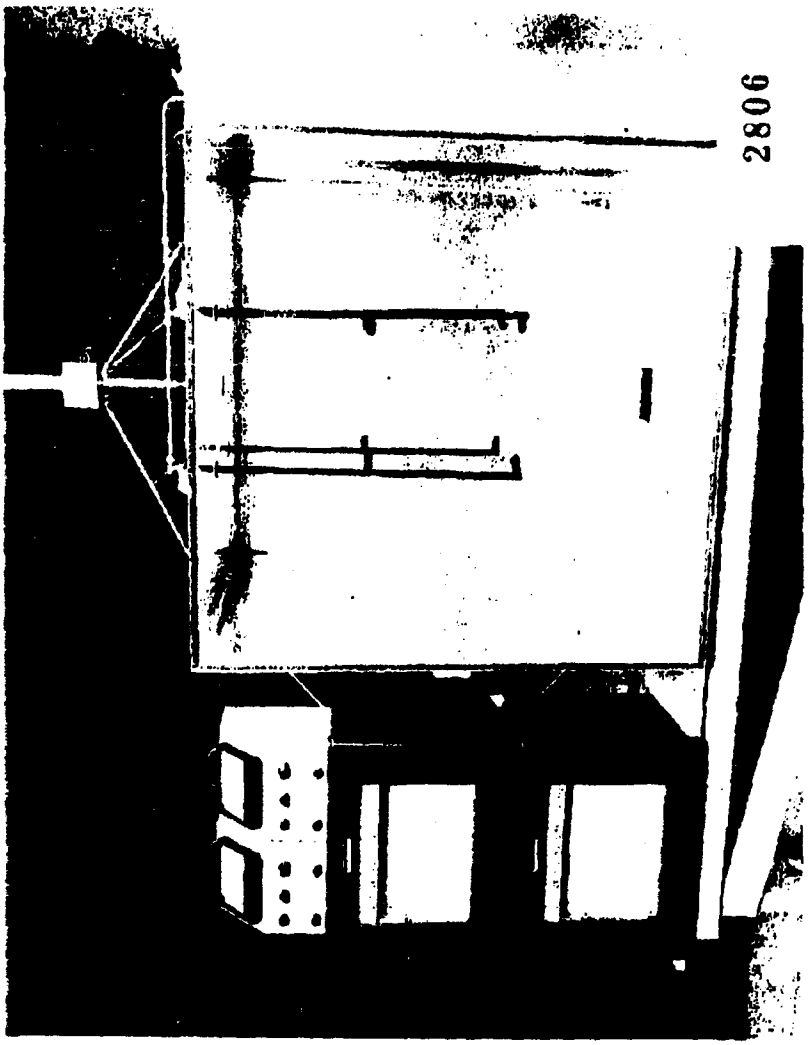

Figure 3.1 Aerophilometer

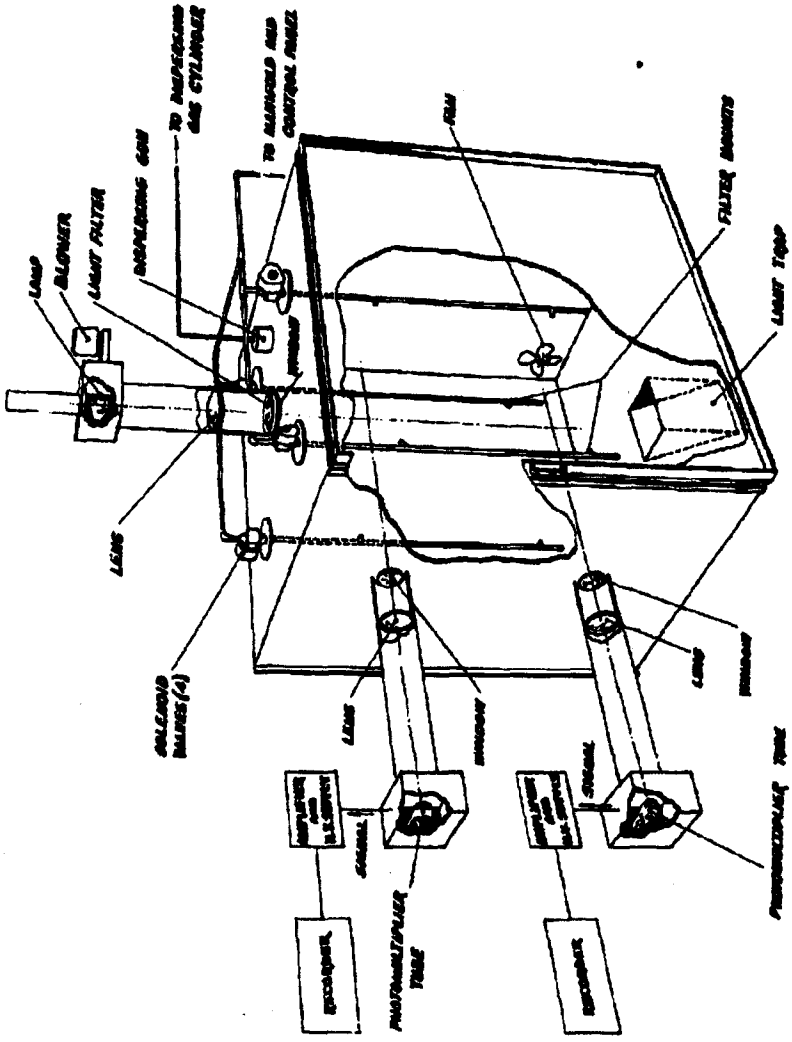

Schematic Drawing of Aerosol Chamber

Figure 3.2

A cone of light from the lamp is admitted into the lens housing through a 0.5-inch aperture. Midway between this aperture and the lens is a baffle with a 1.25-inch aperture. These two baffles limit the amount of light reaching the lens. To reduce the amount of undesirable light the lens housing is black anodized.

A 5 cm diameter lens with a focal length of about 19 cm is placed such that the image of the lamp filaments is at the floor of the main chamber of the aerophilometer in a light trap. The light trap is an open-end polyhedron made of sheet aluminum. The angles of the polyhedron are chosen such that the specularly reflected light undergoes many reflections before re-entering the chamber. The inside of the trap is painted black to insure a large amount of absorption at each reflection of the light.

Positioned between the lens and the main chamber is a Corning glass light filter #7-60. This filter transmits only light within narrow bands of wavelengths. Figure 3.3 gives the percent transmission over a range of wavelengths for this filter. An optical flat glass window seals the main chamber from the lens housing.

3.2.2 Photomultiplier Detection System

There are two complete identical photomultiplier detection systems. Both are placed in the center of one side of the chamber perpendicular to the light beam. One is 1/3 of the distance down the side from the top of the chamber and the other is 2/3 of the distance down.

The photomultiplier tubes used in this apparatus are RCA type IP21. These tubes have a projected sensitive area of 5/16" x 15/16". In order to make a well-defined aperture for the sensitive area and attempt to reduce the possibility of extraneous light reaching this area, the tubes except for the sensitive area have been completely masked with black tape. The response of phototube IP21 is given in Figure 3.4 over a range of wavelengths.

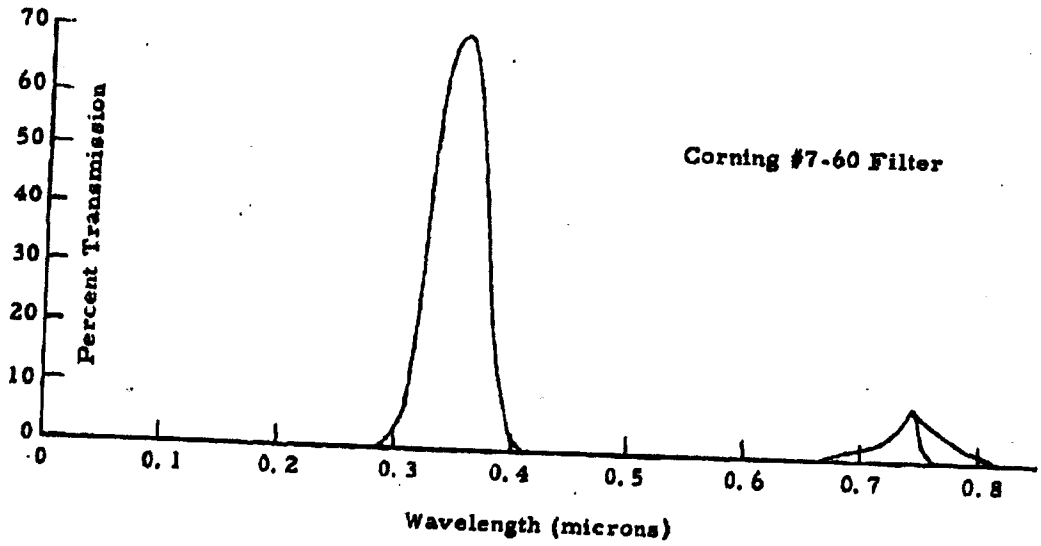

Figure 3.3 Percent Transmission of #7-60 Filter over a Range of Wavelengths

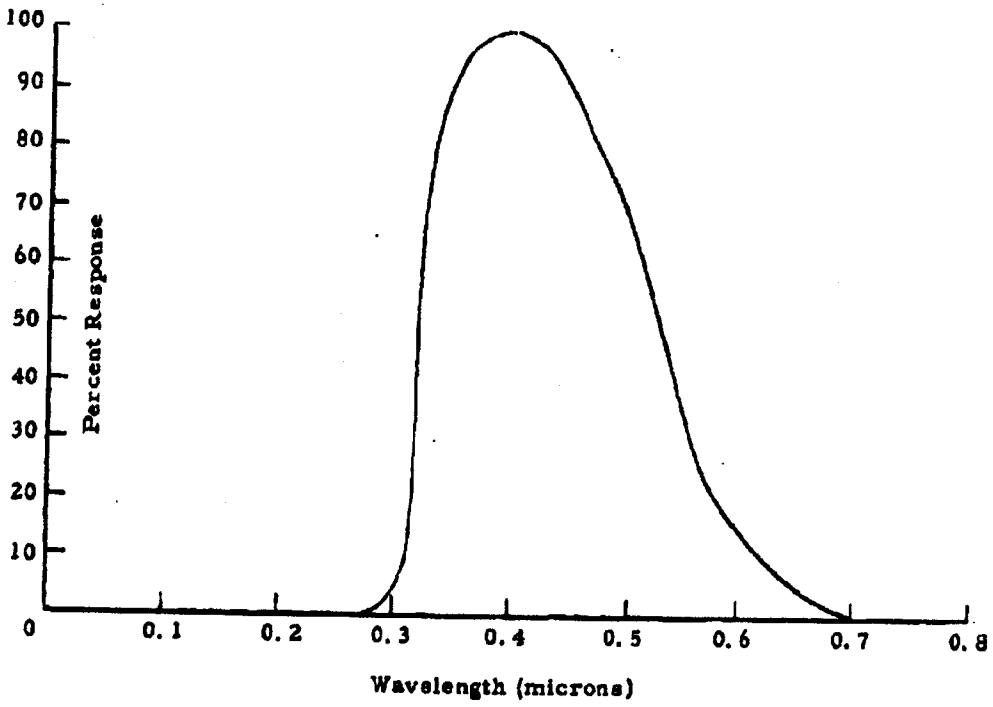

Figure 3.4 Response of IP21 Phototube over a Range of Wavelengths

In order to reduce extraneous light sources, the photomultiplier tube housings and photomultiplier lens housings are black in color. As in the case of the light source lens housing, the chamber is sealed from the phototube lens housing by an optical flat glass window.

The phototube lenses, which are similar to the light source lens, are positioned such that the image plane of the phototube aperture is in the center of the light beam. This image dimension is 4-1/2 cm x 1-1/2 cm. Thus, only particles within a rectangularly shaped volume (whose width is determined by the light beam and height is 1-1/2 cm) are capable of scattering light into the phototube. Each of the two phototubes receives equal amounts of light flux. Therefore, if each volume contains the same number and size of particles, each will scatter the same amount of light into the phototubes.

Each photomultiplier tube is connected to an Aminco photomultiplier microphotometer which in turn is connected to a Brown recorder. The microphotometer is a power supply for the tube, a controller, a signal amplifier, and a meter, while the Brown recorder gives a continuous record of the output signals from the microphotometer.

In order to relate output signals to the concentration and size of particles of the aerosol by means of electromagnetic wave scattering theory, the light flux received should be monochromatic. By the choice of light filter and phototube used in this apparatus, a nearly monochromatic light beam has been achieved. Its wavelength is 0.365 $\pm$ 0.02 microns and is illustrated in Figure 3.5 which gives the overall response of the system over a range of wavelengths.

3.3 Powder Dispersing System

The powder dispersing system, shown in Figure 3.6, is located on top of the chamber and is of the bursting diaphragm variety.

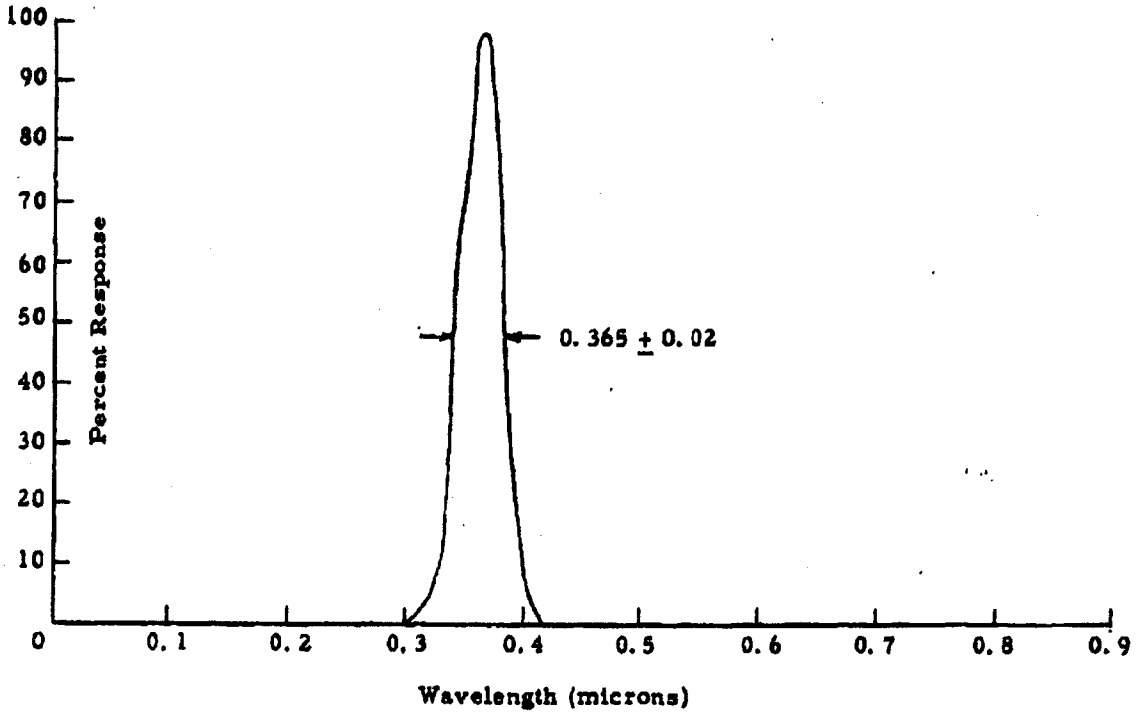

Figure 3.5 Overall response of System

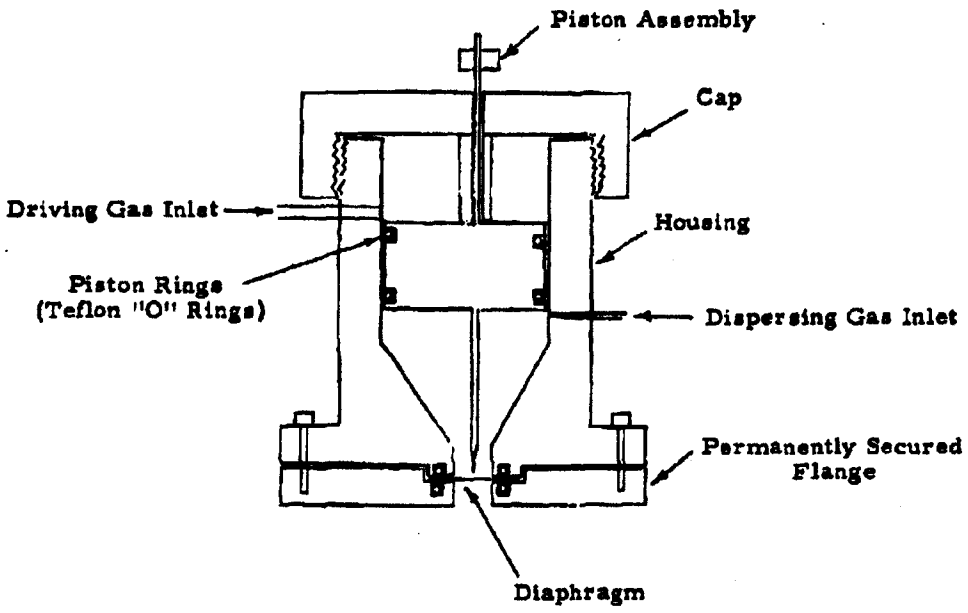

Figure 3.6 Schematic Diagram of Powder Dispersing Apparatus

The cycle of operation of the dispersing unit is as follows: First, the housing is removed from the mounting flange which is permanently sealed to the top of the chamber and a diaphragm is installed. Next the housing is resecured and the cap, which also carries the piston assembly, is removed. This permits loading of the powder. The cap is then replaced. Dry nitrogen, the dispersing gas, is metered in through a needle valve and the gas pressure is monitored by a gauge. When the dispersing gas has reached the desired pressure, dry nitrogen is then diverted to the driving gas inlet by means of a toggle valve. The driving gas pushes the piston downward, simultaneously closing the dispersing gas inlet and puncturing the diaphragm.

With a proper combination of dispersing gas pressure and diaphragm material, it is believed that the diaphragm will rupture cleanly and the powder will be efficiently dispersed. Bench testing of the unit, however, is in its early stages; further experimentation will be necessary to find the suitable combination.

3.4 The Aerosol Sampling System

An aerosol sampling system has been installed in the chamber. This will enable "spot checks" of the aerosol by direct sampling. This data may then be correlated to the data from the light scattering system, which continuously monitors the aerosol condition.

The direct sampling of the aerosol is accomplished by drawing an aerosol specimen through a filter. The filter used is the Millipore 13 mm diameter Type AA, which has an 0.8-micron pore size. Design considerations for the sampling system center around the filter. These considerations will be discussed prior to presenting the sampling system as a whole.

Figure 3.7 shows a filter and its holder immersed in an aerosol. When the appropriate valve is opened, for a period of time the pump draws the air contained in the volume roughly indicated by the dashed line through the filter. It has been estimated that for typical aerosol densities it will be

necessary to draw from 10 to 100 cc through the filter to provide a conveniently countable sample. A second requirement concerns the sampling speed. If the sample is withdrawn too slowly, aerodynamic forces will be incapable of overcoming gravitational forces for the larger particles. The sample will thus be biased in favor of the smaller particles. In order to avoid such biasing, it was stipulated that the velocity of all air elements which eventually pass through the filter must at all times be large compared to the Stokes' fall velocity of a 10-micron particle. This insures unbiased sampling for particles of diameter less than 10 microns.

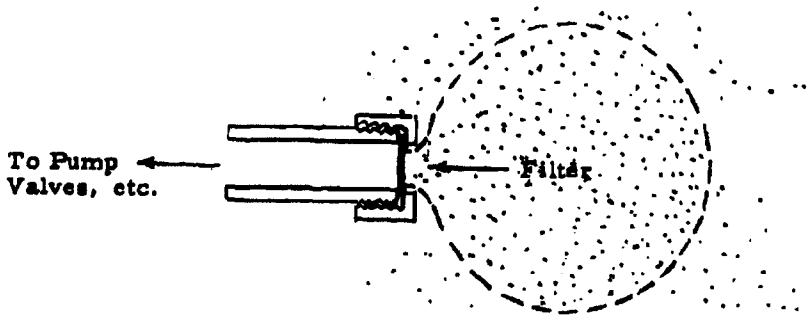

Figure 3.7 Sketch of Filter and Holder Immersed in an Aerosol

The restriction concerning sampling time may be applied by considering a comparable, but simpler, situation. Suppose that the air is withdrawn through a very small orifice, say that of a hypodermic needle (see Figure 3.8). The volume withdrawin in this case will be spherical, so that the following relation holds:

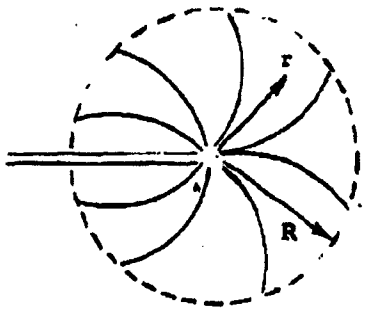

Figure 3.8 Sampling with a Needle Immersed in an Aerosol

$$v(r) = \frac{f}{4\pi r^2}$$

where:

f = the flow rate through the orifice

v(r) = the velocity of an element of air located a distance r from the orifice.

Further, the sampled volume V is given by

$$V = ft = \frac{4\pi}{3} R^3$$

where:

t = the sampling time

R = the radius of the region sampled.

Now, since we need consider $r \leq R$, it may be noted that

$$v(r) = \frac{f}{4\pi r^2} \qquad \frac{f}{4\pi R^2} = v(R)$$

Imposing the condition

$$v(R) \gg 0.35 \text{ cm/sec} \quad ,$$

which is the Stokes' fall velocity of 10-micron particle, it is seen that

$$f = 4\pi R^2 \cdot v(R) \gg 0.35 \text{ cm/sec} \cdot 4\pi R^2$$

but

$$R^2 = \left(\frac{3V}{4\pi}\right)^{2/3}$$

so that the condition is

$$f \gg 0.35 \text{ cm/sec} \times 4\pi \times \left(\frac{3V}{4\pi}\right)^{2/3} .$$

Since also $V/f = t$ there is the condition

$$t \ll \frac{V}{0.35 \text{ cm/sec} \times 4\pi \times \left(\frac{3V}{4\pi}\right)^{2/3}}$$

on t. For $V = 10 \text{ cm}^3$ these conditions imply $f \gg 8 \text{ cm}^3/\text{sec}$ and $t \ll 1.3$ sec while for $V = 100 \text{ cm}^3$, there results $f \gg 37 \text{ cm}^3/\text{sec}$ $t \ll 2.7$ sec.

It should be noted that increasing the sampled volume V increases both the lower limit on f and the upper limit on t.

The actual sampling situation, of course, is more nearly that depicted in Figure 3.7. Further study will probably show that the relation between v and f, though more complicated than the one analysed for Figure 3.6 will result in less stringent conditions on f and t.

The filter system installed in the aerophilometer utilizes a 3/8-inch diameter portion of the filter disk. The Millipore Co. published curves show that the pressure differential required to produce a flow of 8 cm^3/sec is about 3 cm Hg, while for 37 cm^3/sec the requirement is about 18 cm Hg. Both conditions are easily attainable.

The aerosol sampling system comprises eight filter holders suspended in the aerosol chamber by four probes. These probes are located in the chamber as shown in Figure 3.9. The filter holders form the eight corners of a cube of edge length 33 cm. This cube is centrally located within the chamber.

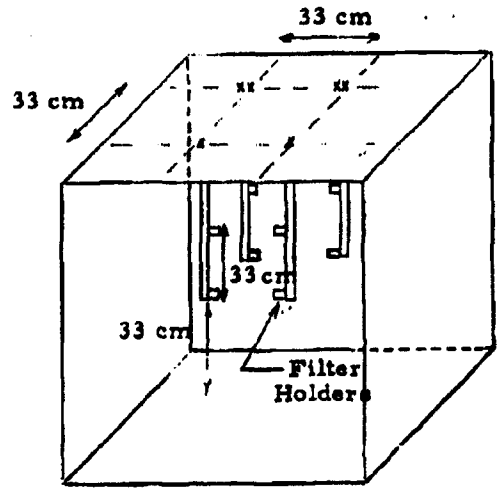

Figure 3.9 Schematic Diagram of Aerosol Sampling Apparatus Inside Chamber

Each of the four probes is separately controlled, which enables samples to be drawn at four different times in the history of a given aerosol.

The control manifold for the sampling system is shown schematically (only one of the probes is shown) in Figure 3.10.

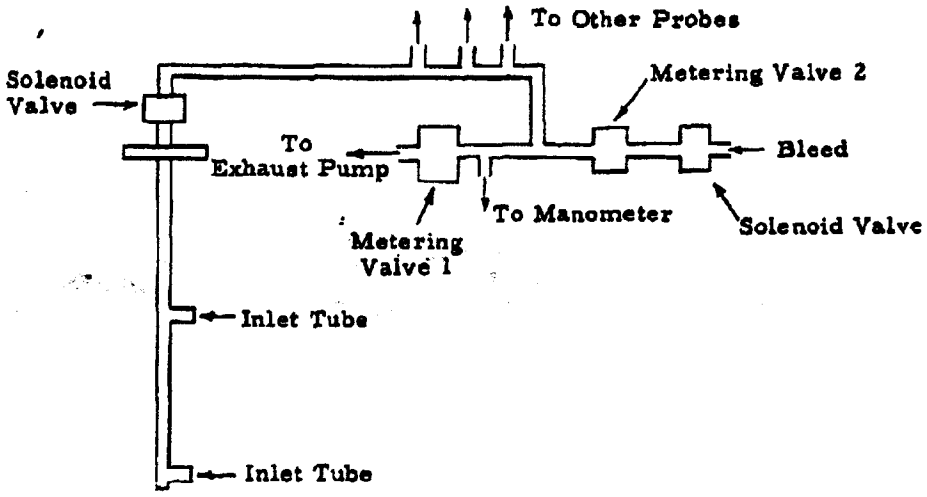

Figure 3.10 Schematic Diagram of Aerosol Sampling System Control Manifold and a Sampling Probe

This system operates as follows: The four solenoid valves on the probes are normally closed, while that on the bleed is normally open; the wiring is such that actuating any one of the four probe solenoids actuates the bleed solenoid. With one of the probe solenoids open, Metering Valve 1 is

adjusted to give the desired flow as indicated by the manometer. After the probe solenoid is closed (which action also re-opens the bleed solenoid) Metering Valve 2 is adjusted to reproduce the pressure drop on the manometer. Thus, the manifold is continuously run at the negative pressure (with respect to atmospheric) which corresponds to the desired flow rate. This, together with the fact that the manifold piping makes up the bulk of the sampling system volume, insures minimum response time of the system.

The filter holders are so constructed that they may be easily removed from the probe inlet tubes. This enables carrying of the filter holder – filter unit to a microscope for examination without disturbing the filter.

3.5 Future Work

As previously stated, the fabrication of the aerosol chamber described above is nearly complete. Preliminary tests, though few in number to date, have indicated that design estimates are sufficiently close to reality as to require no major modifications of the various systems.

The work of the first few weeks of the next reporting period will be concerned with determining optimum operating conditions necessary to produce a well dispersed aerosol. The variables primarily under study will be dispersing gas pressure, diaphragm material, and amount of initial fan stirring.

The main objective after details of operation are worked out is investigation of factors affecting the settling rate of aerosols. This essentially is a study of agglomeration rates of particles in the aerosol. Factors to be studied will include, but necessarily be limited to:

1) Concentration of aerosol
2) Particle size and type
3) Charge characteristics of particles and environment
4) Water vapor content of particle

5) Relative humidity of environment

6) Turbulent and tranquil settling

Aerosol turbulence may be an important factor in agglomeration of aerosol particles. In view of the low Stokes' fall velocity of a typical particle (0.7 mm/sec for a 5-micron diameter particle), a truly tranquil settling condition is difficult to achieve in practice. Because of this fact, the use of two separate phototube scanning units is highly advantageous. While details of individual light-scattering curves are related to aerosol conditions in a complicated way, the relative behavior of two such curves is more easily understood.

4. VIABILITY STUDIES

In previous reports data were presented on the viability of wet and dry aerosols of S. marcescens and B. globigii after exposure to a series of temperatures ranging from 75°C to 130°C for periods up to 1.68 seconds. During the present reporting period, the same apparatus and techniques were employed to extend this study over a wider temperature range (up to 200°C). The data were then used to calculate the thermal-death-time parameters which are characteristic for these systems.

Preliminary studies were undertaken to evaluate the effect which coating Sm with Cab-O-Sil (an amorphous silica composed of 15 to 20 millimicron particles) had on the viability of the system, its culturing properties and its susceptibility to elevated air streams.

The apparent toxic influence of the buna rubber liquid-store liner on proliferating and resting cells was investigated and was found to be a bacteriostatic rather than a bactericidal effect.

4.1 Viability of Dry Aerosols of Bg and Sm

Until the present reporting period, no effect of heat on the viability of Bg aerosols could be observed. At the higher temperatures studied during this period, however, a significant diminution in viability was demonstrated. These observations are summarized in Table 4.1 and are plotted in Figure 4.1. Exposure at temperatures up to 150 degrees for 1.68 seconds and 175 degrees for 0.5 seconds manifested no observable effect. More severe treatments, either at increased temperatures or for more extended periods markedly affected viability. Since the apparatus used in these studies was not designed to study exposures greater than 200°C for 1.68 seconds, it was impossible to extend these observations further. However, examination of the few reliable points obtained indicates that the characteristic of thermal death for Bg spores after dry aerosolization would not differ markedly from

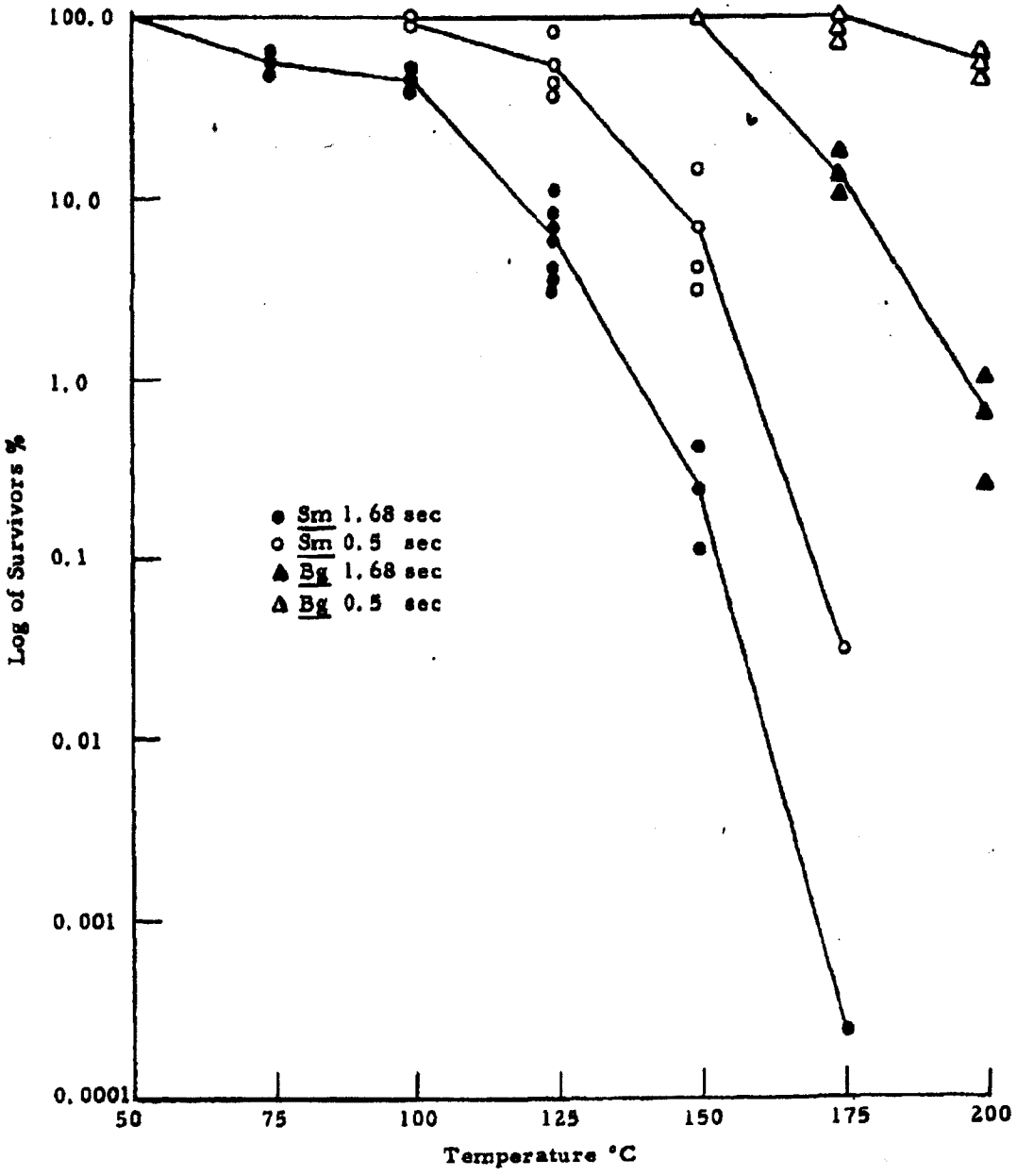

Figure 4.1 Viability of Sm and Bg Aerosols at Elevated Air Stream Temperature

those of Sm aerosols. In each case, apparently, the destruction is retarded in the initial phase, then becomes accelerated until logarithmic death occurs. The major difference between Bg and Sm is the critical exposure at which thermal effect becomes apparent.

Table 4.1 Viability of Dry Aerosols of Bg at Various Exposures (Bg from Lot No. X-12, aerosolized with DeVilbiss generator - 51 trials)

Temperature (°C)	Exposure Time (sec) (Calculated at Room Temperature)	Average Viability (%) (Experimental)	Corrected Viability* (%) (Calculated)
Room Temp.	1.68	100	100
125	1.68	100	100
150	1.68	100	100
175	1.68	14.2	16.5
200	1.68	0.63	0.77
175	0.5	94.0	100
200	0.5	54.5	67.0

* Values corrected for differences in sample volumes from heated and control legs due to variation in flow rates at different temperatures.

During this study period it was possible to observe the logarithmic thermal death of aerosolized Sm through several orders of magnitude. Previous reports, which included data only up to 130°C for 1.68 seconds did not illustrate the true shape of the destruction curve. The results reported in Table 4.2 and Figure 4.2, on the other hand, are high significant. It is evident that at the less severe exposures, the death rates resemble those obtained for multicellular organisms. This type of curve is always obtained with clumped cells where all members of the clump must be killed before it fails to form a colony[5]. Since the aerosolized Bg and Sm suspensions probably exist in the form of multicellular clumps, these experimental

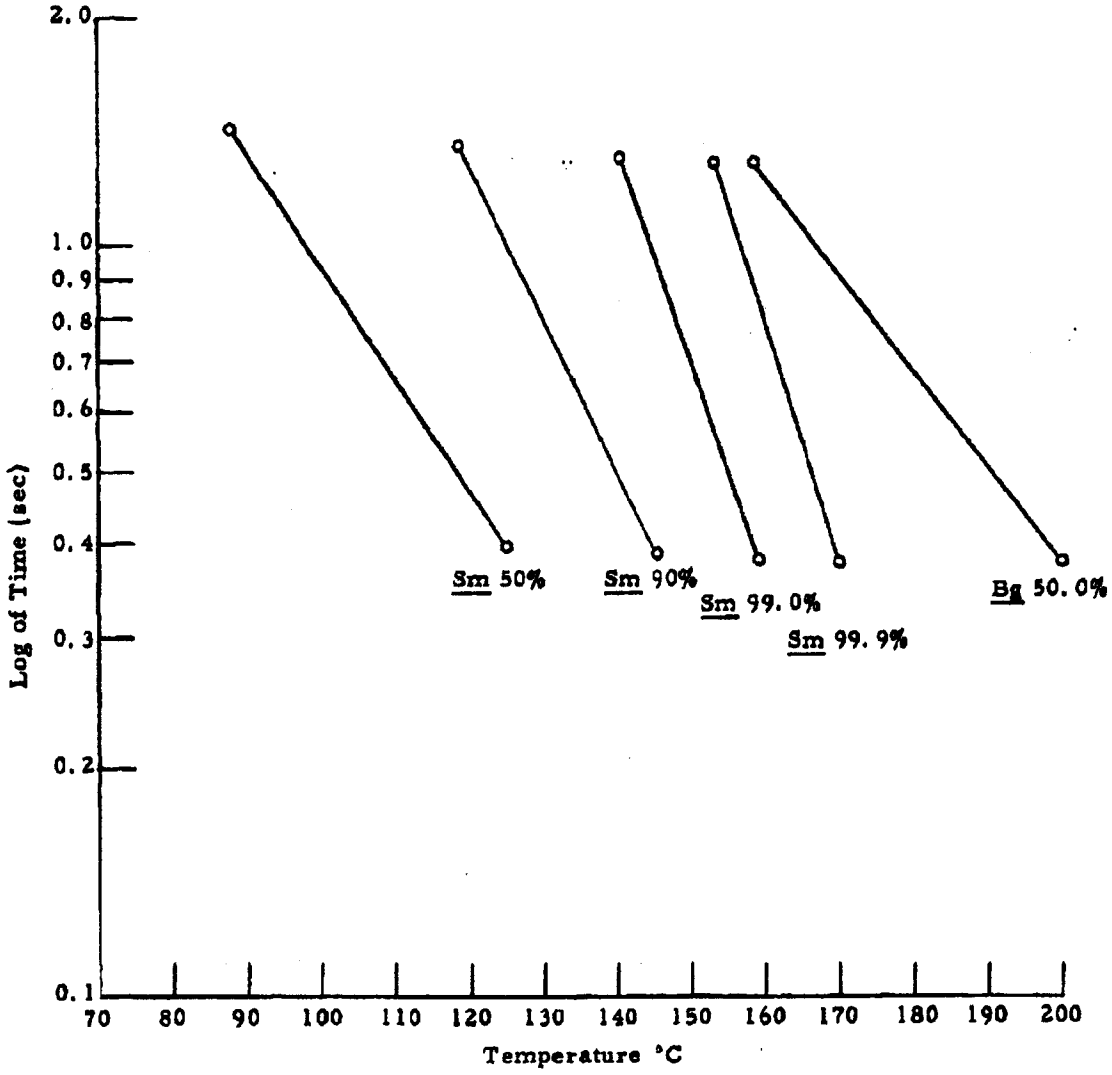

Figure 4.2 Thermal Death Time Parameters of Sm and Bg Aerosols

curves agree well with the theory. This phenomenon, however, could not be observed (and was not previously observed) unless the observations were extended over a wide range of lethal exposures such as performed in this study.

Table 4.2 Viability of Dry Aerosols of Sm at Various Exposures (Sm from Pool #7, aerosolized by explosion - 35 trials)

Temperature (°C)	Exposure Time (sec)	Average Viability, % (Experimental)	Corrected Viability, %* (Calculated)
75	1.12	71.0	71.0
	1.68	55.0	55.0
100	0.5	99.0	100.0
	1.12	61.2	64.0
	1.68	43.6	46.0
125	0.5	54.7	59.0
	1.12	33.3	36.0
	1.68	6.1	6.4
150	0.5	7.2	7.9
	1.68	0.25	0.275
175	0.5	0.032	0.035
	1.68	0.00024	0.00026

* Values corrected for differences in sample volume from heated and control legs due to variation in flow rates at different temperatures.

Figure 4.1 also illustrates the variation that may be expected in results for any given exposure, and the need for multifold replication of trials in order to gain valid points for the plot of thermal destruction curves. It appears that significance should be ascribed only to differences which vary by an order of magnitude or more.

During this phase of the study several possible sources of error associated with our techniques were considered. Aside from the normal experimental error which could occur, it was recognized that the two following corrections might have to be applied because of the variation in flow rate through the heated leg of the apparatus at elevated temperatures:

1) correction for sample volume difference from heated and unheated leg during simultaneous sampling for identical time period

2) correction for actual exposure time which would differ from the theoretical one calculated for room temperature

The first correction was made on the basis of observed flow rate measurements for each individual run and is included in the tabulated data. The second correction can be calculated as follows:

$$t_{actual} = \frac{T_{room}}{T_{observed}} \cdot \frac{F_{room\ temp}}{F_{observed}} \cdot t_{calculated}$$

where:

t_{actual} = the time exposure time in seconds

T_{room} = absolute temp in control leg

$T_{observed}$ = absolute temp in heated leg

$F_{room\ temp}$ = flow rate through control leg = 0.43 cfm

$F_{observed}$ = flow rate through heated leg

$t_{calculated}$ = exposure time calculated for control leg between origin and sampler

These corrections were included in the data plotted in Figure 4.2 which represent the thermal death time parameters for the system under study.

The values in Figure 4.2 are calculated from the experimental values obtained and are characteristic "Z" value curves from which interpolations can be confidently made for the times and temperatures shown. Essentially this chart permits the prediction of the level of destruction which would be expected at any exposure within the range shown.

4.2 Effect of Cab-O-Sil on Viability

Preliminary experiments were performed to determine the effect of Cab-O-Sil on the viability of Bg and Sm powders, under storage and elevated air stream conditions.

To determine any inhibitory effects, Cab-O-Sil was incorporated into nutrient agar in concentrations ranging from 0.1 to 5.0 percent. Both Bg and Sm grew on these media with no sign of inherent inhibition. Cab-O-Sil was then mixed with Sm powder in concentrations of 0.1 and 1.0 percent. The dry mixtures were refrigerated and samples were taken at intervals for culturing. The test results are shown in Table 4.3 and indicate that no demonstrable bactericidal effects occur during short term storage periods under these conditions.

Mixtures of Cab-O-Sil and Sm were aerosolized into the elevated temperature air stream apparatus and viability was measured by previously described techniques at 125, 150 and 175 degrees. The results of these trials are tabulated in Table 4.4 and plotted in Figure 4.3 together with the averaged data for pure powders of Sm at the same exposures. There appears to be a very slight protective effect exerted by Cab-O-Sil; however, too few trials have been performed at this date to lend any significance to the observed deflections. It can be concluded, nevertheless, that Cab-O-Sil does not exert any deleterious influence on the viability of Sm during growth, short term storage, and upon aerosolization.

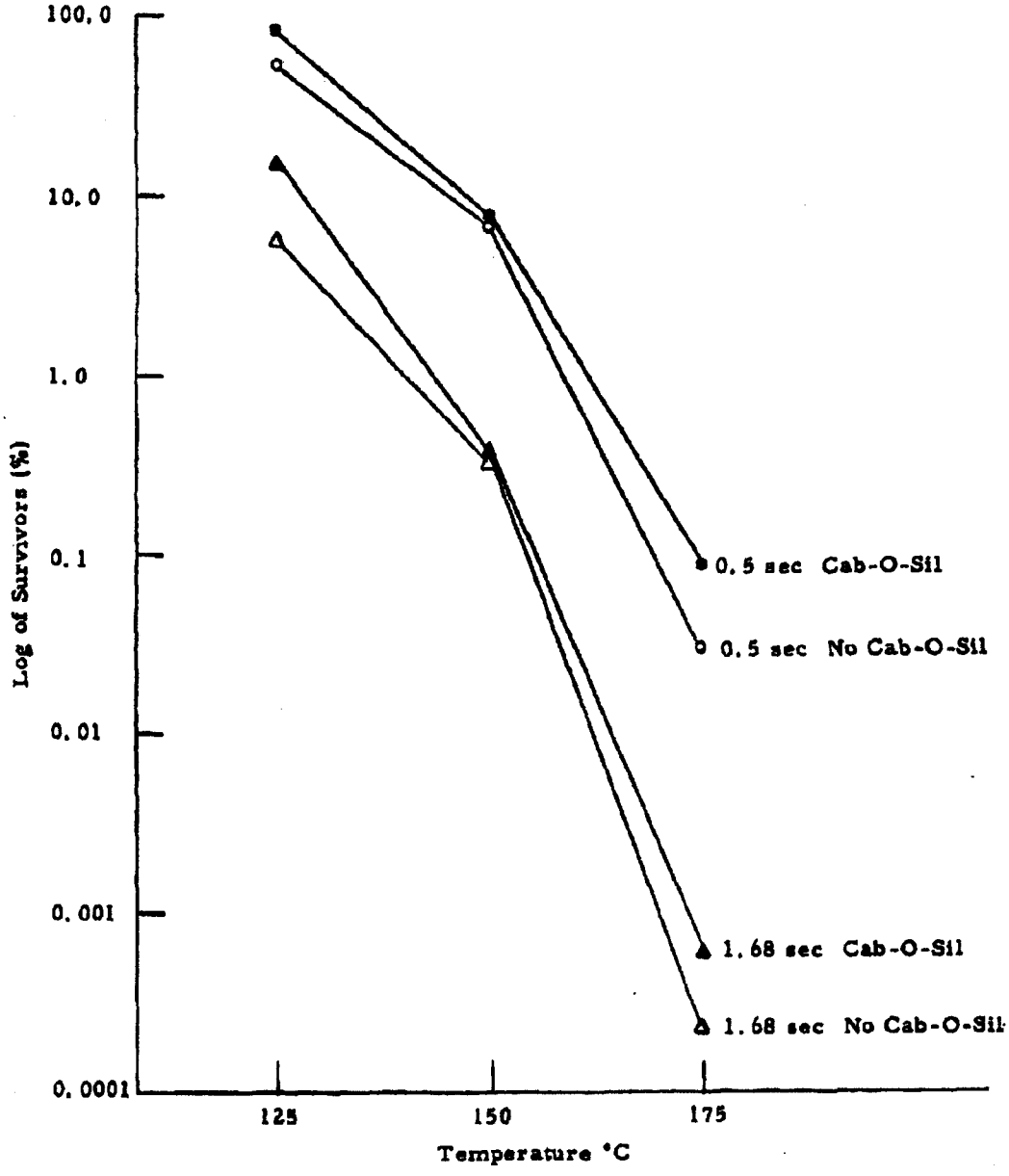

Figure 4.3 Effect of Cab-O-Sil on Viability of Sm Aerosols

Table 4.3 Effect of Cab-O-Sil Coating on Short Term Viability of Sm

Storage Period (Days)	% Cab-O-Sil	Diluent	Viable Count per gm x 10^{-10}
0	-	Tryptose phosphate	8.0
0	1.0	"	5.0
	0.1	"	4.0
3	1.0	"	4.8
	0.1	"	3.6
5	1.0	"	3.4
	0.1	"	6.7
	1.0	Tween 20 (0.1%)	4.8
	0.1	Tween 20 (0.1%)	3.7

Table 4.4 Influence of 1% Cab-O-Sil on Viability of Dry Aerosol of Sm Exposed to Elevated Air Temperatures

Temperature (°C)	Time (sec)	Average Viability, % Control	Cab-O-Sil
125	0.5	54.7	84.0
	1.68	6.1	16.6
150	0.5	7.2	7.3
	1.68	0.25	0.25
175	0.5	0.032	0.090
	1.68	0.00024	0.0006

4.3 Toxic Effect of Buna Rubber on Sm

Several strips of cured, sterile buna rubber (Stoner Rubber Co.) were embedded into nutrient agar plates, and overlaid with a thin layer of clear agar. Streak inoculations were made on the overlay of Sm, Bg, a mold suspension and an actinomycete. The results are diagrammed in Figure 4.4. In each case, growth was markedly inhibited in the vicinity of the rubber, indicating the presence of some soluble, diffusible toxic agent.

Triplicate suspensions of Sm in tryptose phosphate buffer were prepared and refrigerated. Square sections of sterile rubber were placed in two of the flasks, and the third flask was retained as a control. Aliquots were taken at 24-hour intervals and viability of the Sm was determined by plating. The results, shown in Table 4.5, indicated that the rubber did not exert a bactericidal effect and that its toxic principle was essentially bacteriostatic.

Table 4.5 Effect of Rubber on Sm Suspensions

Storage Period (hours)	Viable Count per $cm^3 \times 10^{-4}$		
	No Rubber	Rubber (25 cm^2)	Rubber (1 cm^2)
0	2.9	0.9	1.5
24	2.3	1.2	1.1
48	2.3	1.3	1.6
96	2.0	0.6	0.5
120	1.3	1.5	1.2
144	1.6	0.9	1.3
168	0.8	0.7	0.7

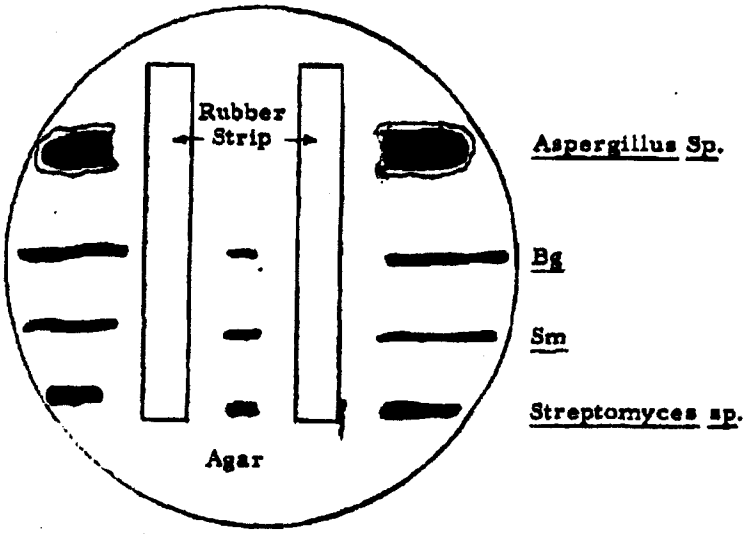

Figure 4.4 Toxic Effect of Rubber

5. DISSEMINATION AND DEAGGLOMERATION STUDIES

5.1 General

The degree of deagglomeration during dissemination of Sm in the wind tunnel was further studied during this period by making an analytical estimation of the effect of filtration on determinations of small-scale agglomeration in the 1 to 20-micron range. In the previous report it was stated our data represented the upper limit on the degree of deagglomeration, since all apparent agglomerates, viewed under a light microscope, were counted even though some of them resulted from filtration process employed in sampling the aerosol. This study shows that a significant percentage of the apparent agglomeration may be due to filtration.

Considerable effort during this period was devoted to the design, fabrication and development of a new dissemination model capable of a 30 lb/min powder flow rate, similar to the full-scale disseminator currently being designed. Apparatus used for preparation of the powder samples were also constructed. These included a compaction device and a mechanical deagglomerator for reducing the resulting slugs of material to small agglomerates and basic particles. The equipment will be utilized in wind tunnel tests both in our laboratory and in forthcoming experiments in the Fort Detrick large aerosol sphere.

5.2 Sm Dissemination – Small-Scale Agglomerate Study

In our previous work, apparent agglomerates present in the aerosol in the small-scale range, 1 to 20 microns, were collected on Millipore filters and counted under a light microscope. The statistical analysis which follows was conducted to estimate the quantity of agglomerates formed by filtration.

Due to the complexity of the problem, it is necessary to assume that the particles are uniform in size. By definition, an agglomerate is formed

during filtration if one or more particles fall within one diameter of the center of a particle which already rests upon the filter. Figure 5.1 depicts this situation where:

A_t = total filter area observed under the microscope

$A_s = \pi D_p^2$ = projected filter area

D_p = particle diameter

The filtration effect is dependent on the projected area of the particles in the aerosol. Therefore, the particle dimension used in the calculation is the mean diameter with respect to the surface, defined from the particle size distribution by:

$$D_p^2 = \frac{\sum_1^\infty D_{p_i}^2 \, n_i}{N}$$

where:

n = number of particles in any interval (i)

N = total particles in distribution

The value of this term was obtained for the Sm sample disseminated in the tests.

Poisson's law can be used to predict the probability of two or more separate particles falling on the filter within the area A_s. The law is valid for cases with a large number of variables and a small probability, both of which are satisfied in this analysis.

In general, Poisson's law states that the probability of finding any number (x) of basic partices in the area A_s is

$$P(x) = \frac{e^{-m} m^x}{x!} \qquad (5-1)$$

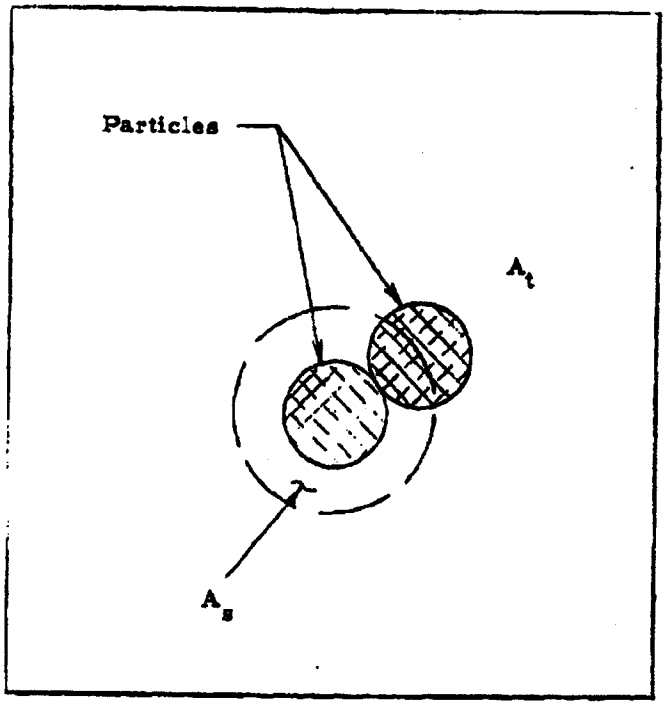

Figure 5.1 Model for Statistical Analysis

where m is the mean number of particles in all areas (A_s)

$$m = \frac{n}{A_t} A_s \tag{5-2}$$

where n = total number of particles observed.

Since the sum of the probabilities of all possible values (x) must equal one, the probability of finding two or more particles in A_s is

$$P\ (2 \text{ or more}) = 1 - P(o) - P(1) \tag{5-3}$$

Thus,

$$P\ (2 \text{ or more}) = 1 - e^{-m} - e^{-m}\ m \quad . \tag{5-4}$$

or

$$P\ (2 \text{ or more}) = 1 - e^{-m}\ (1 + m) \tag{5-5}$$

The expected number of agglomerates (a) on the observed area of the filter due to filtration is simply:

$$E(a) = \left[\frac{A_t}{A_s}\right] P\ (2 \text{ or more}) \tag{5-6}$$

In analysing the experimental data presented in the previous report, the surface mean diameter of the aerosol particle distribution was calculated and the following results were obtained[6].

$$D_p = 2.5\mu$$

$$A_s = 1.96 \times 10^{-7} \text{ cm}^2$$

$$m = 0.075 \text{ particles/area } (A_s)$$

Thus:

$$P \text{ (2 or more)} = 26.7 \times 10^{-4}$$

and

$$E(a) = 40 \text{ agglomerates}$$

The percentages of particulate material in the aerosol which formed apparent agglomerates and those estimated to be formed during filtration are shown in Figure 5.2. The computation shows that filtration does have a significant effect on our data analysis: at low bulk density (0.33 gm/cc) about 57 percent of the apparent agglomerates present may be attributed to filtration, whereas at bulk density (0.65 gm/cc) this value is 31 percent.

It should be noted that the expected agglomeration due to filtration is directly proportional to the particle size. Therefore, data presented in the last report in the 5 to 20-micron range are influenced more by filtration than those in the 1 to 5-micron range.

5.3 Design of High Flow Rate Disseminator Model (GMI-3) and Related Equipment

Experimental work on the dissemination of Sm in the wind tunnel up to the present time has provided a basic understanding of the aerodynamic break-up process and characteristics of both mechanical and pneumatic disseminators. At this time, it is desirable to investigate more specifically, parameters that are being considered in the design and development of the prototype unit. Therefore, a new model disseminator has been designed and fabricated to accomplish this objective.

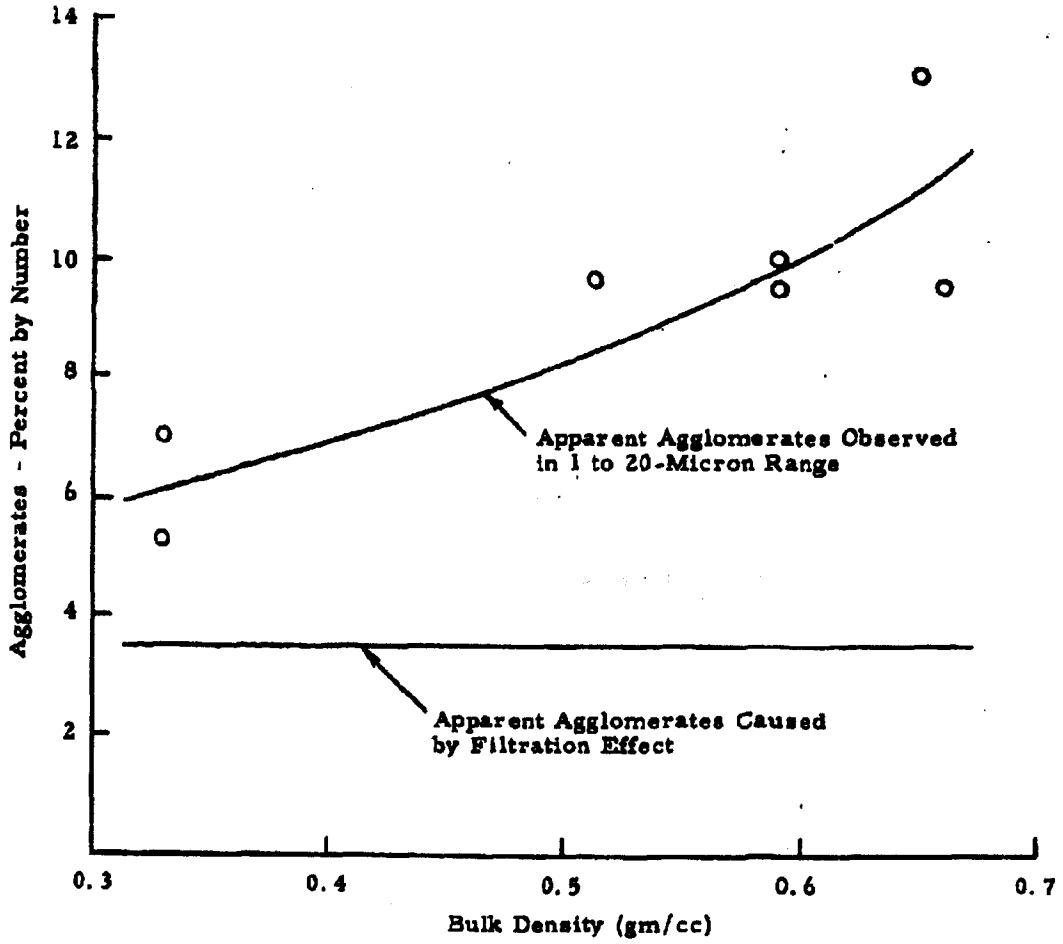

Figure 5.2 Percentage of Particles (by number) in Sm Aerosol (which consist of apparent agglomerates in the 1 to 20-micron range as compared to apparent agglomerates caused by filtration effect (wind tunnel Mach number 0.5)

The prototype unit will utilize a mechanical mechanism to partially break up the large compacted slugs of material into small agglomerates and basic particles. The material will form a bed in the disseminator which will be transported from the unit into the atmosphere by a gas.

To simulate the complete process, equipment has been constructed for compacting the powder in the density range 0.40 to 0.65 gm/cc and shearing the slugs. Figure 5.3 shows the devices. Compaction is accomplished by using a low friction piston and dead weights. Mechanical break-up is achieved by rotating and advancing the compacted slugs into a single blade with a cutting depth of 0.050 inch.

Models using a purely pneumatic mechanism for transporting material into the wind tunnel were investigated for this new system. However, it was found difficult to disseminate one gram of material in 0.004 second, required for a 30 lb/min flow rate. Thus, a mechanical piston concept was employed as shown in Figure 5.4. The transport mechanism in this case does not tend to break up the material prior to its entry into the tunnel, whereas in the case of gas transport, there is partial reduction of agglomerates. Therefore, deagglomeration data obtained with the model should be on the conservative side – performance of the prototype should be slightly better.

The system utilizes compressed gas to actuate the piston. In comparison with the previously used spring system, this method provides greater flexibility for varying the ejection velocity and simplifies the loading operation. For this high speed ejection process it is necessary to apply the actuating force to the piston rapidly. This is achieved by retaining the piston with an electromagnet and pressurizing the air chamber to 12 psig. The piston is released when the circuit to the coil is opened.

For a 30 lb/min flow rate the orifice diameter is 0.394 inches and the ejection velocity is 33.5 ft/sec.

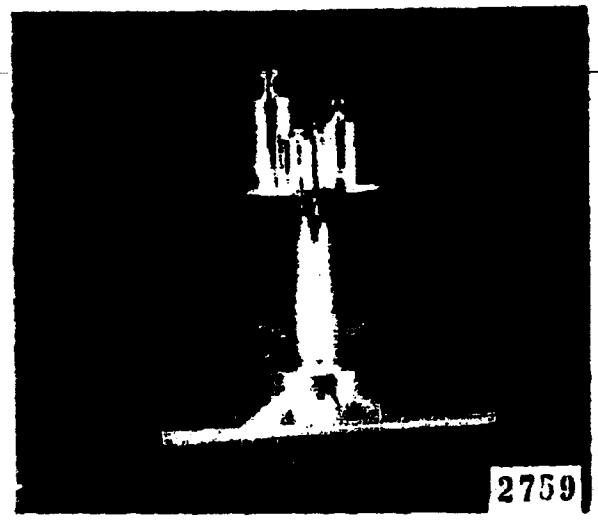

(a) Compactor

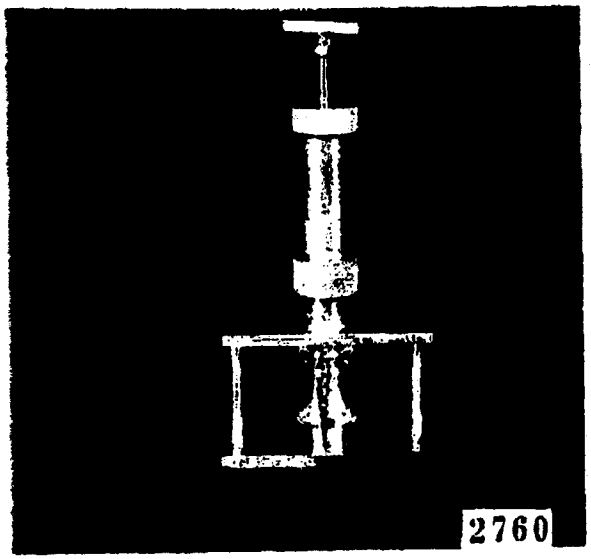

(b) Cutter

Mechanisms for Preparing Simulated Sm Sample (Fill) for Dissemination

Figure 5.3

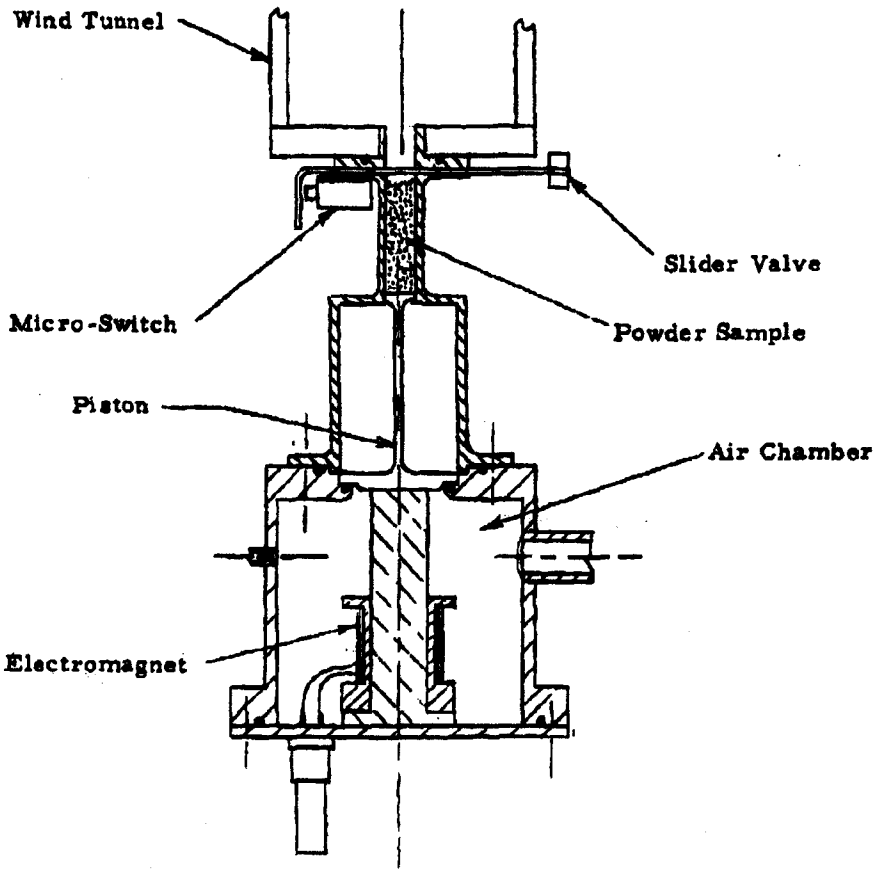

Figure 5.4 High Flow Rate Disseminator Model (GMI-3) for Wind Tunnel Application

The sample is enclosed at the wind tunnel end of the system of a slider valve which is connected to a micro-switch in such a way that the coil circuit is opened when the slider is pulled open.

The complete apparatus set-up is shown in Figure 5.5 where the model is mounted to the wind tunnel. Related equipment includes a power supply consisting of two, 6-volt dry cells and a regulator and pressure gauge.

At the present time the apparatus has been tested for operational characteristics. In the immediate future, experiments will be conducted to determine the degree of deagglomeration during dissemination of Sm. The same analysis techniques as were discussed in our previous report will be used in this work. Also, during this next period the unit will be used in viability recovery tests at Fort Detrick in the 40-foot test sphere.

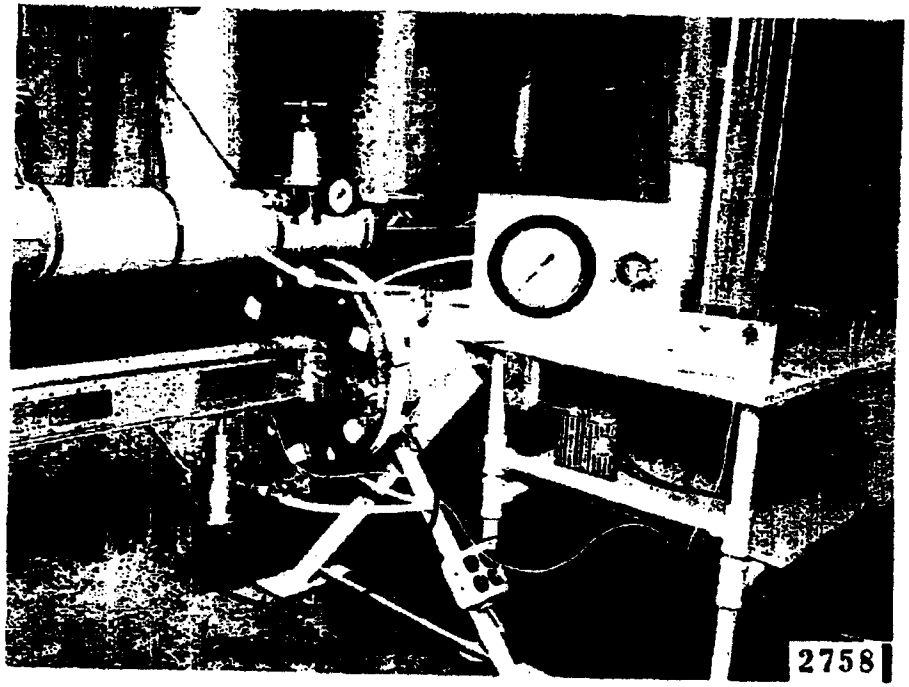

Disseminator Model and Related Equipment Mounted on Wind Tunnel

Figure 5.5

6. EXPERIMENTS WITH THE FULL-SCALE FEEDER FOR COMPACTED DRY AGENT SIMULANT MATERIALS

6.1 Introduction

A full-scale device for disaggregating and feeding compacted powder materials was described in the sixth quarterly progress report[7]. This device embodies the essential design features proposed for use in an airborne store capable of disseminating dry BW agent materials which are carried aboard the store in a compacted state. The main objectives of the experiments with the full-scale feeder are to demonstrate the feasibility of the proposed design concept[8] and to obtain data required for the design and fabrication of a disseminator suitable for flight testing.

Perhaps the two most important questions relative to the proposed design concept have been:

1) Will the force required to translate the compacted powder down the cylinder be low enough to allow a practical drive system?

2) Will the amount of gas required to motivate the disaggregated powder be low enough to permit storing sufficient gas aboard the store?

The desired objective is to have a driving torque which does not exceed 2500-inch-pounds and a gas consumption which does not exceed approximately 3 percent by weight of the agent material.

During the reporting period covered by this document, it was demonstrated that both the torque and gas requirements are low enough to consider the design feasible in these regards.

The experiments which are being reported have also served to provide qualitative information relative to items such as: the size of discharge opening required, the effectiveness of the cutters in shaving off and breaking up the compacted powder, gas pressures required for proper operation of the feeder, uniformity of powder flow rate, and other behavior characteristics of the feeder and the compacted dry talc. In general, the

performance of the experimental feeder has been very encouraging and indications are that the proposed concept for disseminating compacted dry agent materials is quite feasible. Even though the results obtained thus far are somewhat preliminary in nature, it is believed that the following discussions will prove to be of value to those following the progress of work on the dissemination of dry agent materials.

6.2 General Procedure

The procedure employed in the experimental work is to load and compact the powder material into the feeder and then to mount the unit in a test stand where the powder can be collected and weighed as the feeder is driven by a variable speed drive. As the feeder is operated, several operational characteristics such as driving speed, driving torque, time to discharge a given quantity of powder, gas flow rate, gas pressure inside feeder, and gas pressure at the supply regulator are observed and recorded.

A schematic diagram of the arrangement used in the experiments is presented in Figure 6. 1. A photograph of the actual equipment is shown in Figure 6. 2. In this picture the feeder is shown in the test stand and connected to the drive unit. The gas manometers and flow meter are mounted on the cart so that they can be readily disconnected and moved out of the way during the loading operation.

The torque required to drive the feeder is measured two ways. When the drive screw is rotated manually a torque wrench is used. When the power drive is used, torque is determined by measuring the reaction torque on the drive unit. The drive unit is mounted on two bearings in line with the axis of the feeder and restrained by a dynamometer. The force registered on the dynamometer is multiplied by the lever arm to obtain the torque.

Since relatively low pressures are employed in the gas system beyond the regulator, simple manometer tubes are used to measure pressures.

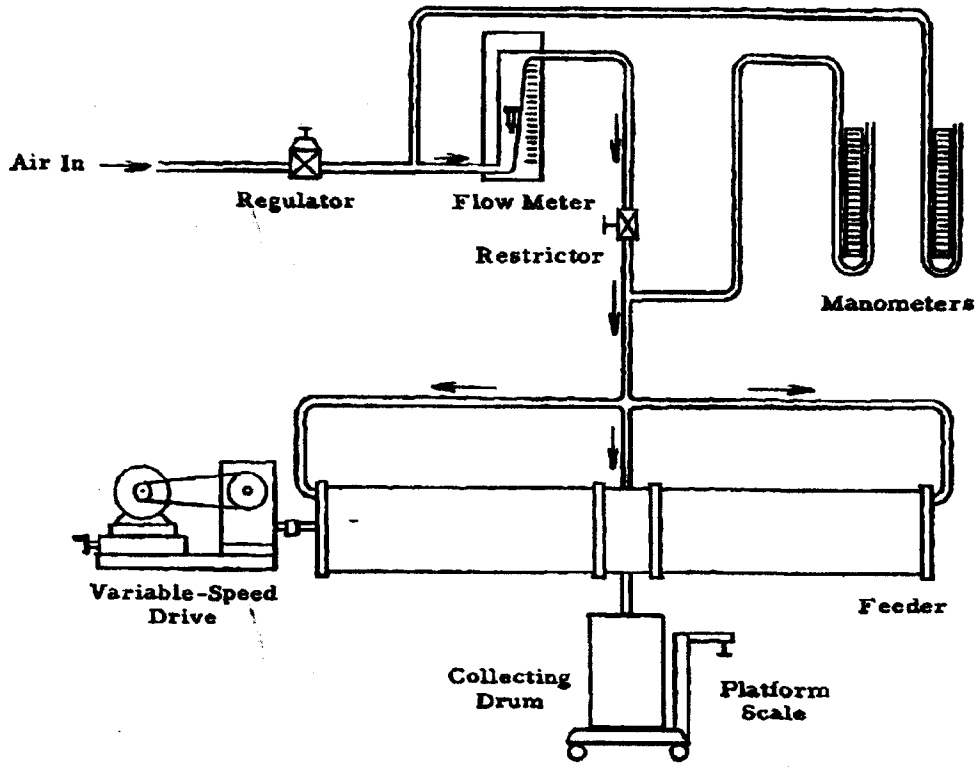

Figure 6.1 Schematic Diagram of Test Arrangement used with Experimental Feeder for Compacted Powders

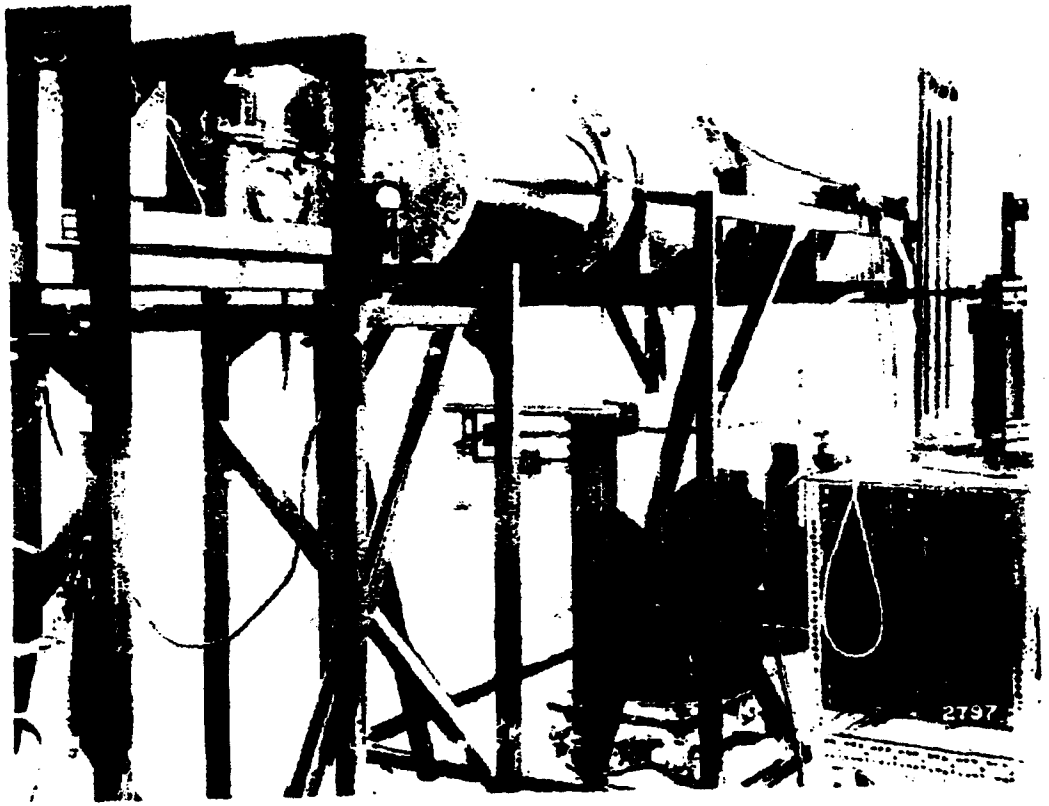

Figure 6.2 Test Arrangement used with Experimental Feeder for Compacted Powders

The amount of gas being used is measured with a variable-area type flow meter placed in the supply line between the pressure regulator and the feeder. The restrictor is used to control the amount of air flowing into the feeder.

"Mistron Vapor" talc produced by the Sierra Talc & Clay Co., has been used in all of the experiments thus far. This material has a maximum particle size of 8 microns, a mean diameter of 1.03 microns, and a specific gravity of 2.75. The particles have a plate-like shape. Talc is being used in the preliminary work because with talc it is not necessary to operate with low humidity conditions in the test area and there is no explosion hazard. However, it is important that face masks be worn by personnel to prevent inhalation of the material.

The talc is loaded into the feeder by separating the cylinder at the center section and standing each half on end. The piston is moved to the fully retracted position at bottom of the cylinder. Talc is loaded into the cylinder and compacted in increments to obtain a uniform density throughout.

Density is calculated from the weight of talc required to fill the known volume within the feeder. The density obtained was 0.44 grams per cc in the first loading and 0.46 grams per cc in the second loading. The feeder was loaded with 438 lbs of talc in the first loading and 443 lbs in the second.

The experimental work is being conducted in a special test room fabricated for the purposes of confining powder materials to a specific area and of subsequently providing a means of operating under controlled humidity conditions. The room is shown in Figure 6.3. It has a floor 9 by 15 feet and is 11 feet 8 inches high. The test room is fabricated from rigid plastic-fibre glass sheets secured to a structural aluminum framework with epoxy resin to obtain an air-tight enclosure. There is an air lock to minimize influx of unconditioned air as personnel pass through the doorway. The current work has been conducted with the door open and using a blower to pull air through the room and out through a filter before discharging it to

Figure 6.3 Test Room used for Experimental Work with Dry Powder Materials

the outside. When the room is to be operated under low humidity conditions, the room air will be circulated through a dryer to remove water vapor. The dryer has not been installed.

All electrical equipment installed in the test room is explosion proof.

6.3 Driving Torque Determinations

While operating the feeder to discharge the first load of talc, a considerable portion of the operating time was devoted to studying the driving torque problem. Before proceeding with power-driven operation of the loaded feeder, the drive screw was turned manually with a torque wrench. Two important observations were made. First, the pistons moved approximately six inches along the cylinder before the other end of the powder slug started moving into the disaggregator cutters. Second, as the feed screw was rotated the required torque gradually increased until a value of 250 ft-lbs was exceeded. Since the desired torque objective of 200 ft-lbs had been exceeded, steps were taken to reduce the torque before proceeding with the power operation.

The cylinder was opened at the ends and the pistons were removed without disturbing the powder. It was observed that the talc being forced out of the threads of the drive screw was highly compacted and appeared to be locking the piston nut to the drive screw. In addition, the oil was coming out of the bronze Oilite material of the nut and mixing with the talc to form a hard gummy residue in the threads.

The thread friction was reduced by changing to a free-machining brass material for the piston nuts and by incorporating a thread cleanout feature in the nut, as shown in Figure 6.4. This nut is constructed so that powder material in the screw thread is removed at the front face of the nut and directed through a radial passageway to the rear face of the piston where it falls into the cylinder behind the piston.

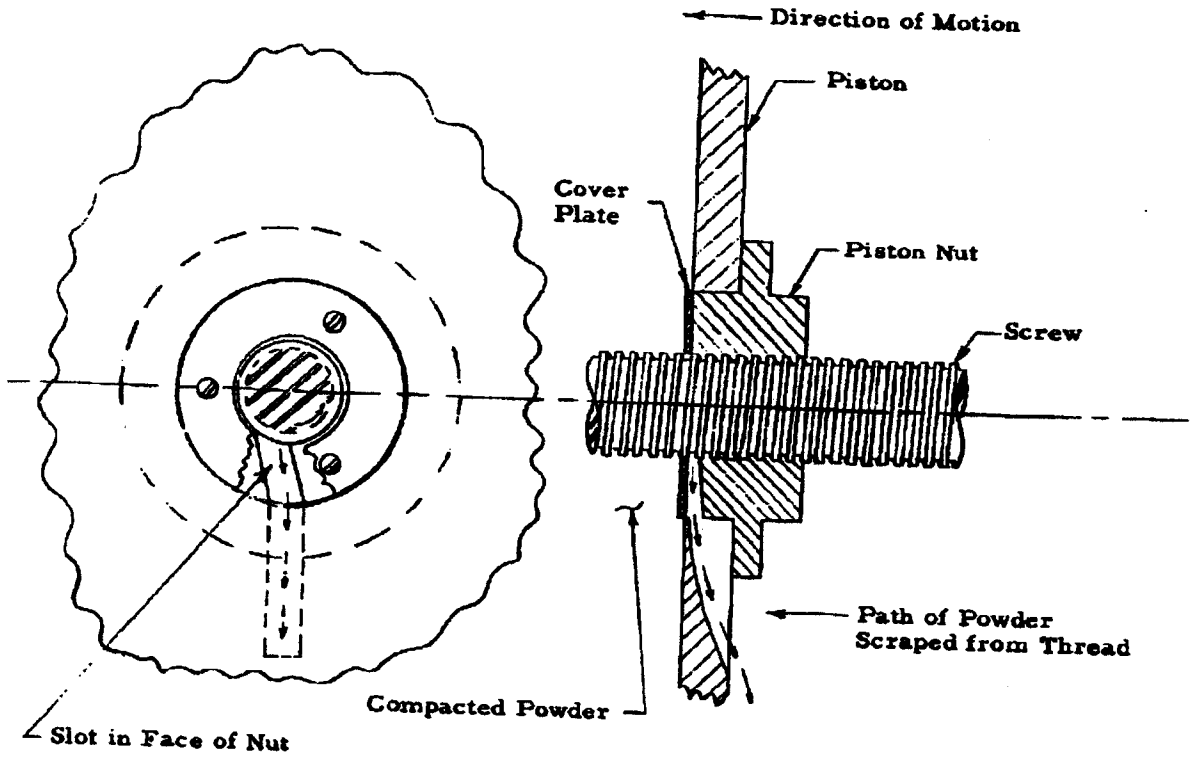

Figure 6.4 Thread Cleaner Scheme to Remove Powder from Screw

After modifying the piston nuts the torque required to drive the feeder was approximately 200 ft-lbs indicating that the modification reduced the thread friction by a little more than 50 ft-lbs. No attempt was made to obtain a torque reading for thread friction independent of other forces contributing to the overall driving torque requirement.

Having achieved a sufficiently low driving torque value it was possible to proceed with power-driven operation of the feeder. In operating the feeder, the material was discharged in a series of short runs of one to two minutes duration. It was observed that the torque required to start the feeder after each shut-down was excessive because the talc was bearing against the disaggregator discs at the center of the cylinder. By rotating the disaggregator back and forth manually, it was possible to clear the powder back to the cutting plane (approximately 3/32 inches from the disc in the first test series). When this was done the torque reduced to an acceptably low value of 200 ft-lbs or less. It was noted that something was causing the compacted powder to expand when the feeder was stopped at the end of a run.

As a consequence of the series of runs with the first load of talc it was learned that the following factors can contribute to the torque load which must be overcome by the drive unit:

1) force required to translate the powder slug down the cylinder - approximately 180 ft-lbs.

2) torque required to rotate the disaggregator discs if the powder bears against the discs - variable depending upon bearing pressure; calculated to be 86 ft-lbs for a pressure of 0.5 psi.

3) torque required to stir powder in the center section after it has been shaved off by the cutters - calculated to be approximately 2 ft-lbs.

4) torque to rotate the feeder when empty (friction from bearings, screw-threads, piston rubbing on cylinder, disaggregator rubbing on cylinder) - approximately 15 ft-lbs.

5) torque from powder being forced out of feed screw and resisting travel of the nut - approximately 50 ft-lbs.

With the above knowledge of factors contributing to torque it was easy to see why the total torque initially exceeded the desired 200 ft-lbs objective and why it was necessary to take action directed at reducing torque where possible. The thread clean-out feature incorporated in the piston nut which eliminated torque Item (5) has already been described. Corrective action taken to lower other torque items is discussed below.

The force required to translate the powder slug down the cylinder, Item (1) above, was reduced by allowing the compacted powder to expand radially after compaction thus eliminating sidewall forces of powder against the cylinder. This was accomplished by lining the cylinder with strips of 1/8-inch thick aluminum before loading and compacting the powder in the cylinder. These strips were then removed to form a radial clearance space all around the slug of powder. When the cylinder was positioned horizontally it was observed that the space created in this manner was more than adequate to relieve compaction stresses and that the powder was not contacting the cylinder wall on the upper side.

An attempt was made to reduce the torque resulting from powder bearing against the disaggregator discs by mounting the cutters on the outer surfaces (toward compacted powder) of the discs. This placed the cutting plane approximately 13/32 inches away from the disc. This arrangement provided additional space for the powder to expand and contributed to a reduction in the required driving torque. However, subsequent tests demonstrated that this was not the complete solution to the powder expansion problem and that further torque reductions should be possible if the powder expansion can be minimized.

The torque required to rotate the disaggregator was reduced by mounting rollers on the perimeter of the discs which support the cutters.

The success of these measures in reducing torque was demonstrated in the series of tests made with the second loading. The torque was only 35 ft-lbs during the first test of this series when the feeder was full of powder. By the end of the second test run the torque had increased to 150 ft-lbs. During the rest of the runs the torque ranged from 100 to 160 ft-lbs.

The loading procedure employing removable strips to create a radial expansion space for the powder also eliminated the initial delay in powder feeding. In the preceding discussions of the results without using removable strips during loading, it was pointed out that the piston moved approximately six inches before the central end of the slug of material started feeding into the cutters. When the powder was allowed to expand radially after compaction, the piston pushed the powder slug into the cutters without noticeable initial compression of the slug.

6.4 Motivating Gas and Talc Discharge Rate Measurements

In the proposed design of the dry agent disseminator a gas stored aboard the disseminator will be employed to move the powder from the center section of the unit out into the slip stream. As the compacted agent material is shaved off by the disaggregator cutters, it is mixed with gas and flows out through the discharge opening. The powder flow rate will be controlled by the rate at which compacted powder is fed into the rotating disaggregator. Even though the gas and discharge opening is not used to meter the agent material, the size of the opening, the rate of gas flow and the gas pressure within the cylinder must be adequate to insure that the material is carried out of the center section as it is disaggregated. Material must not accumulate in the center section. However, the space and weight allowed for gas storage is limited and, consequently, the gas must be used sparingly if the dissemination concept is to prove feasible. An objective of no more than 3 percent by weight of the agent material was established. Experiments have demonstrated that this condition can be achieved.

In the experiments being discussed here, air has been used to move the powder from the disaggregator section of the feeder through the discharge opening into the drum where it is collected and weighed. Eventually dry nitrogen will be used for this purpose. However, plant air is less expensive and more convenient to use than nitrogen and is quite adequate for the initial experiments. By the time the experimental work progresses to the

stage where it becomes necessary to use dry nitrogen, it is expected that test techniques will have been developed to the extent that gas wastage will be a minimum.

Much of the talc discharged in the two series of tests being reported on was expended while working on the torque problem and developing suitable operating procedures. However, six runs provided good powder and gas flow rate data and these results are summarized in Table 6.1. The two most significant accomplishments evidenced by the tabulated results are:

1) Powder flow rates of 30 lbs per min were achieved and exceeded.

2) The powder was discharged successfully with a gas quantity as low as 0.8 percent by weight of powder.

These favorable powder and gas flows were obtained with suitably low gas pressures within the feeder.

The diameter of the discharge opening was 0.375 inches on Runs A-3 and A-4 and 0.500 inches on the others. On Run A-4 the conditions were such that the talc did not discharge as fast as it was being fed through the disaggregator. As a consequence the center section filled with talc and the feeder jammed. When the discharge opening was increased to 0.500 inches in Run A-5 it was possible to feed talc at a higher rate (35 lbs per min compared to 28 lbs per min) while using a lower air pressure in the feeder (21 cm Hg compared to 36 cm Hg) than was required with the 0.375-inch opening. The limiting conditions resulting in jamming were not obtained with the 0.500-inch opening during these tests.

For the "A" series of runs the air pressure in the feeder is only 2 or 3 cm Hg below the supply pressure set by the regulator, whereas in the "B" runs the feeder pressure is from 6 to 25 cm Hg below the supply pressure. This difference in the two series of runs is explained by the presence of a flow restrictor between the regulator and the feeder on runs B-4, B-5 and B-6. This restrictor is used to provide a control over the amount of air entering the feeder. Without the restrictor the air flow is dependent upon the amount of powder being discharged. The powder tends to choke off the air.

Table 6.1 Test Results Using Compacted Talc in Experimental Feeder

Run No.	Talc Flow lbs/min	Air Flow lbs/min	Air-Talc Ratio	Air Pressure, cm. Hg. Supply	Air Pressure, cm. Hg. Feeder	Discharge Diam., Inches
A-3	28.0	0.425	0.015	38	36	0.375
A-4	30.3	0.359	0.012	32	29	0.375
A-5	35.0	0.296	0.008	23	21	0.500
B-4	27.5	0.221	0.008	20	14	0.500
B-5	34.0	0.418	0.012	44.5	19	0.500
B-6	34.0	0.403	0.012	41	22	0.500

Notes:

1. Average density of compacted talc in feeder was 0.44 gm per cc in the series "A" runs and 0.46 gm per cc in the series "B" runs.
2. On Run A-4 the center section filled up with talc because it was not discharging fast enough.

The curves in Figures 6.5 and 6.6 are presented to show the uniformity of powder flow observed during the tests. With the exception of test Run B-6, the time was recorded at 10 lb intervals as the powder accumulated in the collection drum. Five-pound intervals were used on Run B-6. The points have very little scatter from the straight line which was drawn through the points for the purpose of determining the flow rates for the various runs.

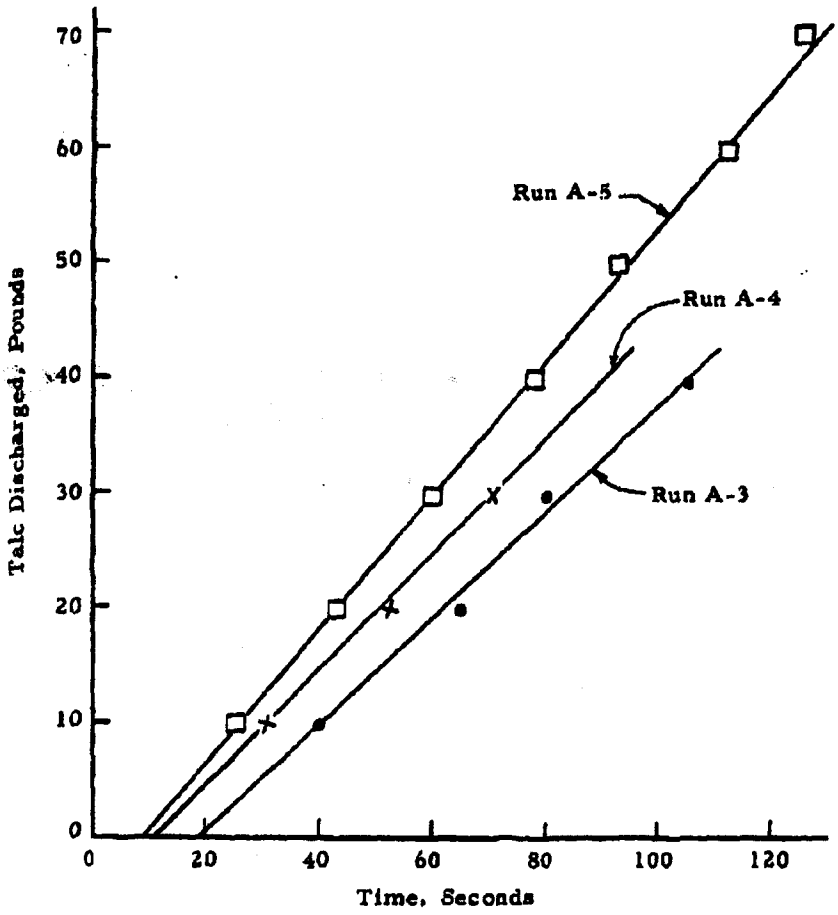

Figure 6.5 Discharge Rate Curves for Series "A" Tests using Talc in the Experimental Dry Agent Feeder

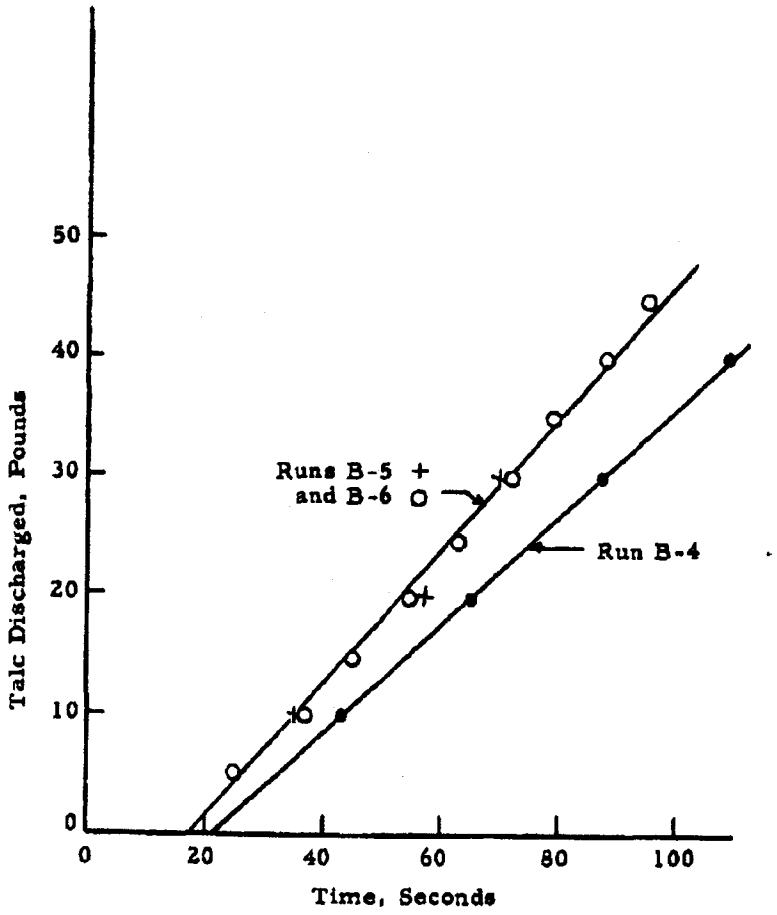

Figure 6.6 Discharge Rate Curves for Series "B" Tests using Talc in the Experimental Dry Agent Feeder

7. APPARATUS FOR DISSEMINATION EXPERIMENTS AT FORT DETRICK

During this reporting period, the wind tunnel apparatus and dissemination test fixture were completed in preparation for shipment to Fort Detrick. The dissemination test fixture was used at General Mills, Inc. in a series of experiments in the wind tunnel in our laboratories. This unit and the experimental work with it is discussed in Section 6 of this report. The wind tunnel design and fabrication were completed, incorporating the features outlined in our Sixth Quarterly Progress Report[9]. The main components included:

1) A nozzle and test section

2) A stilling chamber

3) A heat exchanger

4) Three air-storage tanks

5) Five oil-free, two-stage reciprocating air compressors

The installation of this equipment in the Fort Detrick facility and the dissemination experiments conducted with this apparatus will be covered in the next quarterly progress report.

8. DESIGN STUDIES ON A DRY-AGENT DISSEMINATION SYSTEM

During this reporting period, considerable progress was made on design studies covering the dry-agent dissemination system.

The initial concept of this external aircraft store was set forth in our Fifth Quarterly Progress Report[8]. The main features of this disseminator concept are: 1) an aerodynamically-shaped outer store structure with 2) a cylindrically-shaped inner agent container which holds two compacted slugs of dry agent; 3) a ram-air turbine which furnishes power to 4) a rotary actuator which drives 5) a piston feeding system, and 6) a rotating disaggregator which removes powder from the advancing slugs and utilizes, for conveying purposes, compressed gas from 7) a self-contained gas storage vessel.

In our Sixth Quarterly Progress Report[10], we reported the results of preliminary experimental work on a laboratory model of the center section of the disseminator which includes the piston feeding system and rotating disaggregator. Additional experimental evaluation of this laboratory model is discussed in Section 6 of this report. This feeding concept has been very successful in providing a uniform powder feed rate, as outlined in the above mentioned discussions.

We have also given attention to several of the other principal components of the airborne dry-agent disseminator and have established some of the characteristics of these as discussed below.

8.1 The External Configuration of the Store

As a result of studies of store shapes, we recommended two alternatives to Fort Detrick. One of these was the Douglas store configuration which was used for the liquid-agent disseminator fabricated under this contract, and the other was a smaller store (21.12 inches in diameter by 180 inches in length) which was originally used for a 150-gallon fuel tank on the Grumman

F9F-6, F9F-6P, F9F-7, F9F-8, and F9F-8B aircraft. After review of this question of the size of the store, including discussions with representatives of the Air Force and Navy, the Fort Detrick staff asked us to proceed with the design on the basis of the smaller store. This decision was influenced by several considerations including target size and compatibility of the store with operational and obsolescent aircraft.

As currently envisioned, it will be possible to provide a cylindrical agent container in the center section of this store which will have a diameter of 16.5 inches and a length of approximately 80 inches. With compacted dry agent, the payload will be approximately 350 pounds.

8.2 The Rotary Actuator

The feeding mechanism in this disseminator concept must be driven at relatively low rotational speeds. It is also desirable that several speeds be available, thereby providing a selection of the agent dissemination rate. A preliminary design study has been conducted on this rotary actuator because it is important to establish the feasibility of providing a suitably compact and lightweight drive unit before detailed design of the store is initiated.

The principal requirements which were used as a basis for this preliminary design study are listed below:

1) Output Speeds – 8, 12, 16, 24 and 32 rpm in either direction.

2) Output Torque – 2,500 inch-pounds in either direction at the above speeds.

3) Maximum Allowable Overhung Shaft Load – 1,500 pounds.

4) Maximum Allowable Inward Thrust Load on Shaft – 2,000 pounds.

5) Maximum Allowable Outward Thrust Load on Shaft – 2,000 pounds.

6) Duty Cycle - Continuous for periods up to 1/2-hour.

7) Life - 200 hours.

8) Operating Temperature - +160°F to -65°F.

9) Operating Altitude - Sea level to 15,000 feet.

10) Acceleration - 10 g's in any direction.

11) Vibration - 5 to 500 cps at 0.036-inch double amplitude or ±10 g whichever is the lower value.

12) Input Electrical Characteristics - 400 cycle, 200 volt, 3 phase, AC.

13) Connectors - Water-tight connector at cable entrance to actuator housing.

The actuator unit for this application will consist of an AC aircraft motor, a variable speed-reducing assembly and a fixed speed-reducing assembly. The motor will be a 4-pole motor, which has a nominal speed of 12,000 rpm at 400 cycles. The use of a relatively high-speed motor makes the actuator more compact and reduces the weight. The analysis shows that the motor will have a rating of approximately 2 horsepower. The variable speed-reducing assembly will be designed so that the motor pinion gear can be meshed with any one of five idler gears by rotating a supporting sleeve. The fixed speed-reducing assembly consists of a three-stage planetary gear package having an overall reduction ratio of 433.5 to 1.

A comprehensive analysis of the gear performance has been made which shows that the required life of 200 hours is feasible under the conditions of this design. The physical dimensions of the actuator unit, as currently envisioned, are an overall length of approximately 24 inches and a maximum diameter of approximately 8 inches. Depending on the final selection of the motor, the physical shape will vary somewhat. A preliminary weight analysis has been made which indicates that the complete actuator unit should weigh approximately 65 pounds, including the electrical motor.

8.3 The Power Generator

Based on the above analysis, it is anticipated that the motor power input requirement will be approximately 2 kilowatts. The ram-air turbine (General Motors, Allison Division) used on the liquid disseminator has a rating of 4.5 kva. Since this unit has adequate power and is relatively small and lightweight, we plant to incorporate it into the dry-agent disseminator design.

8.4 Gas Storage Vessel and Flow Regulating System

Experimental investigations using the laboratory model of the feeding system have shown that successful operation can be achieved using talc powder, when the ratio of air flow to power flow (on a mass basis) is approximately 0.01 to 0.02. In our preliminary studies of the pressure-vessel requirements in this airborne dissemination system, we have set the air (or nitrogen) storage requirement at 3 percent of the maximum payload (350 pounds) or 10.5 pounds of gas.

Since volume should be minimized, we have based our calculations on a storage pressure of 3000 psi. At this pressure, the required quantity of air will occupy a volume of approximately 0.7 ft^3, which is definitely compatible with the space available in the store. It appears that the most satisfactory shape will be a conical center section with (essentially) hemispherical ends.

With respect to materials, tanks of this type are available in glass fiber, steel and other alloys. Due to the major importance of safety in a system of the type under consideration here, we recommend the use of a steel tank. It is believed that inspection of glass-fiber reinforced plastic pressure vessels is not as well developed as procedures for steel tanks. The preliminary estimate for the weight of a suitable steel tank is 40 pounds. Two manufacturers of these tanks are Tavco and Kidde.

Initial studies of the flow-regulating system indicate that the most suitable technique for providing several levels of constant (but selectable) flow rate is to operate the system with a critical orifice in the line to the disaggregating section and an adjustable pressure regulator upstream of this orifice. Experiments with the full-scale laboratory feeding model have confirmed this opinion. It has been found that this mode of operation is superior to methods where the flow is controlled in response to the pressure in the center section.

Additional work on the proper sequencing of control functions is planned in the future.

9. SYSTEMS STUDY

In our Sixth Quarterly Progress Report[11], we presented the results of computer studies of the problem of line-source dissemination of two solid agents LE and N. The variable decay-rate model was used to determine the agent flow rate (versus downwind travel) required to deliver a minimum of the ID_{50} dose to the area covered.

During this reporting period, the same type of computer analysis has been conducted for the agent UL-2. However, in this case, information as to the dependence of decay-rate on time was not available so that a fixed decay-rate assumption was necessary.

The equations of the model were programmed on the Bendix G-15 computer and the results are presented in Figures 9.1 and 9.2. The following values for the various paramcters were used:

1) Biological decay rate (constant): 4.5% min^{-1}.

2) Concentration - to-infective-dose ratio, c/ID_{50}: 1.36×10^{13} lb^{-1}.

3) Height of the aircraft, h: 200 feet.

4) Efficiency of dissemination, E: 20%.

5) Efficiency of particle retention, E_r: 33%.

6) Speed of the aircraft, v: 546 mph.

It will be noted from Figures 9.1 and 9.2 that, over the range of downwind distances investigated, the flow rates are well below the maximum delivery rate (30 to 60 lb/min) which is planned for the dry-agent disseminator. It may also be seen that the influence of weather conditions is important, although it is less pronounced than in the case of the agent N, discussed in Reference 11. This is traceable to the difference in decay rate, the agent N having a lower decay rate.

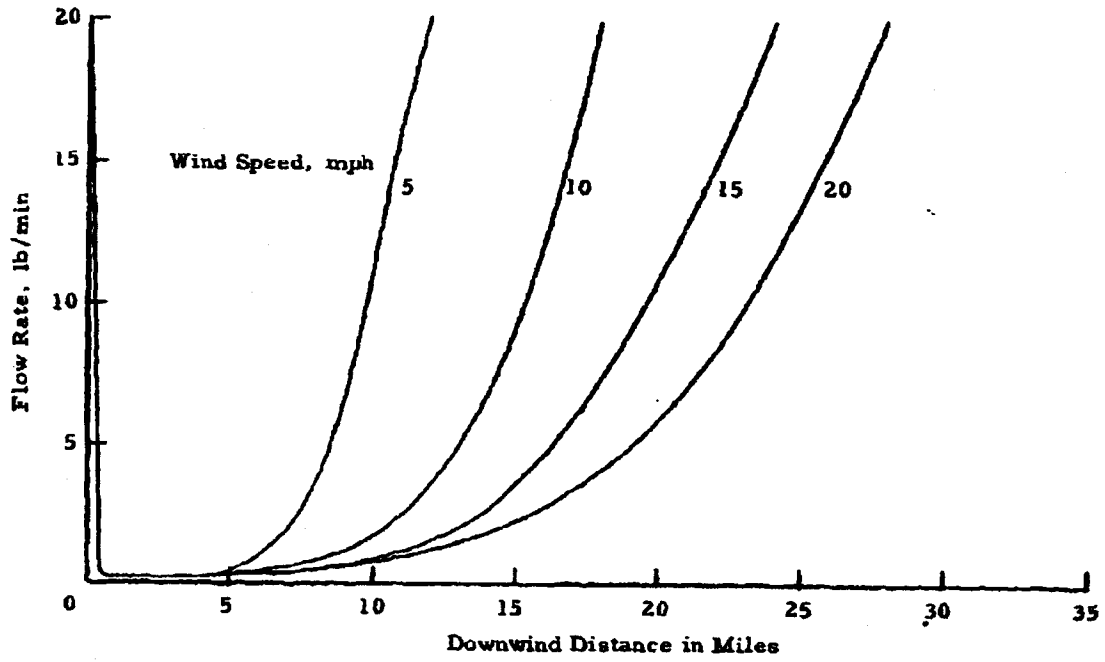

Figure 9.1 Flow Rate versus Downwind Distance for "Average" Weather Conditions – Agent UL-2

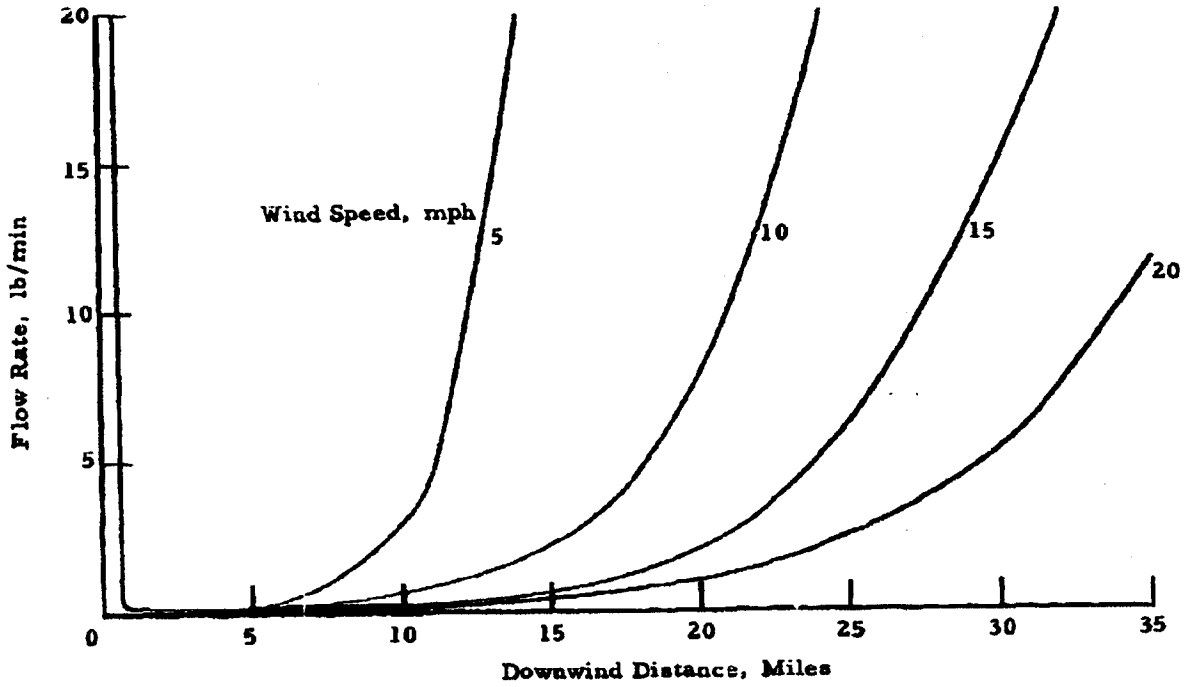

Figure 9.2 Flow Rate versus Downwind Distance for "Good" Weather Conditions – Agent UL-2

10. PROGRESS ON THE LIQUID DISSEMINATING STORE

Phase II of this contract includes the design and fabrication of a liquid BW agent disseminating store. The configuration and general characteristics of this unit are described in our Fifth Quarterly Progress Report[12]. Additional work toward completion of this task was covered in our Sixth Quarterly Progress Report[13] which outlined progress on design of the tank assembly, fluid handling system, electrical system and the boom assembly, and reported the status of the orders for purchased parts.

10.1 Work on Design and Fabrication

During this reporting period, work on this liquid agent disseminating store progressed so that the unit was completed to the point where successful laboratory-functional testing and demonstration was accomplished. Figure 10.1 is an external view of the disseminator, showing the ram-air turbine mounted on the nose of the unit.

One of the principal areas of work during this periond was on the detailed design, fabrication and testing of the fluid handling system. Figure 10.2 shows the plumbing assembly and Figure 10.3 is a view of the store with the aft section removed to show the completed installation.

Another important assembly is the boom and actuator system which is shown in Figure 10.4. The twin-boom assembly is mounted in the aft-end of the store. These booms contain the slit-type nozzles through which the agent is discharged into the slipstream. The actuator is an electrically driven unit which is capable of extending or retracting the booms.

During this reporting period, the electrical components were also procurred and (where necessary) specially fabricated and installed in the store.

The mechanical and electrical aspects of the liquid agent disseminating store are discussed in more detail in the section which follows.

Figure 10.1 External View of Liquid BW Agent Disseminator Showing Ram-Air Turbine Installation

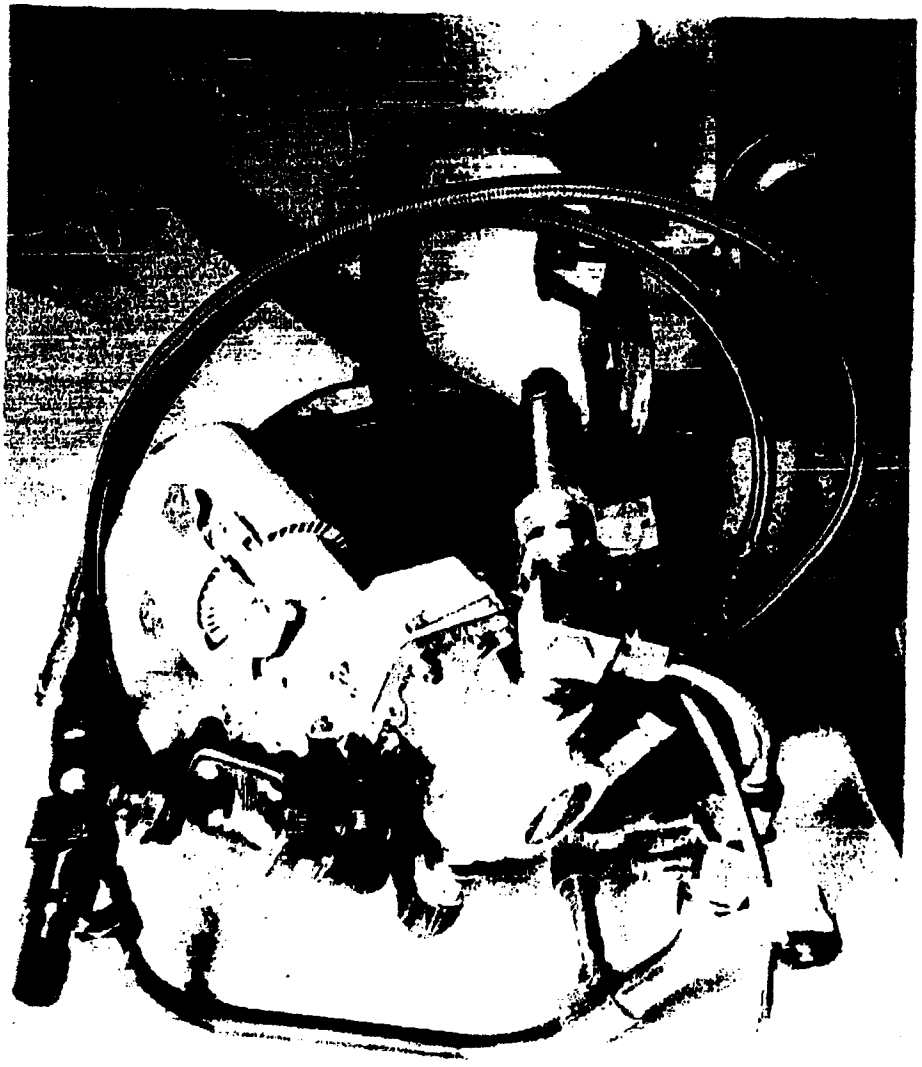

Figure 10.2 Fluid Handling System

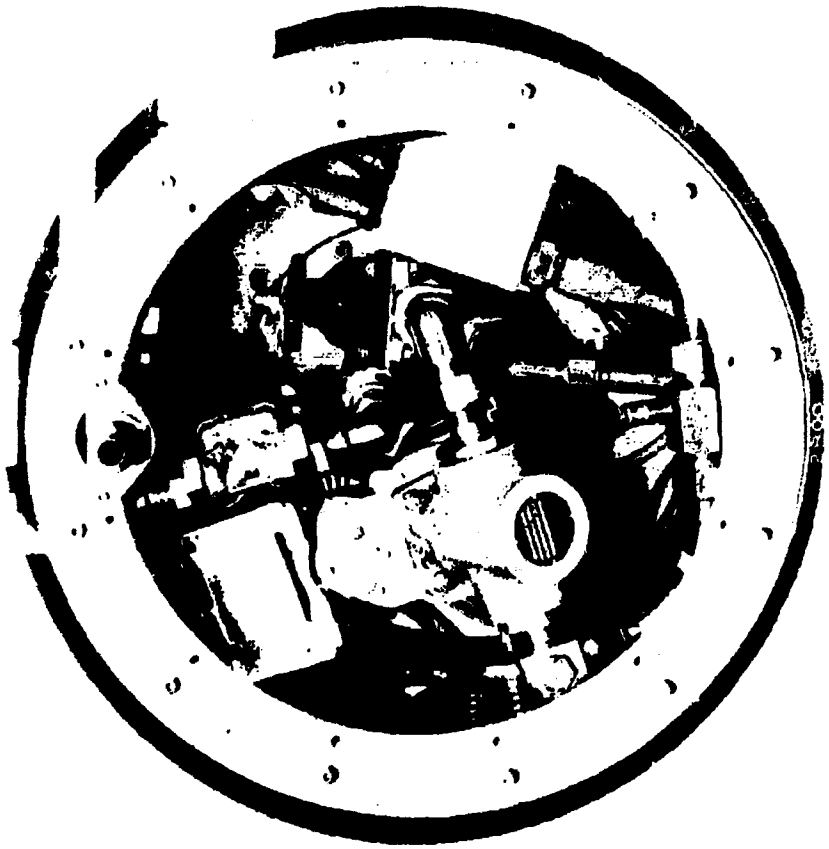

Figure 10.3 View of Liquid Disseminating Store with Aft Section Removed to Show Installation of Fluid Handling System

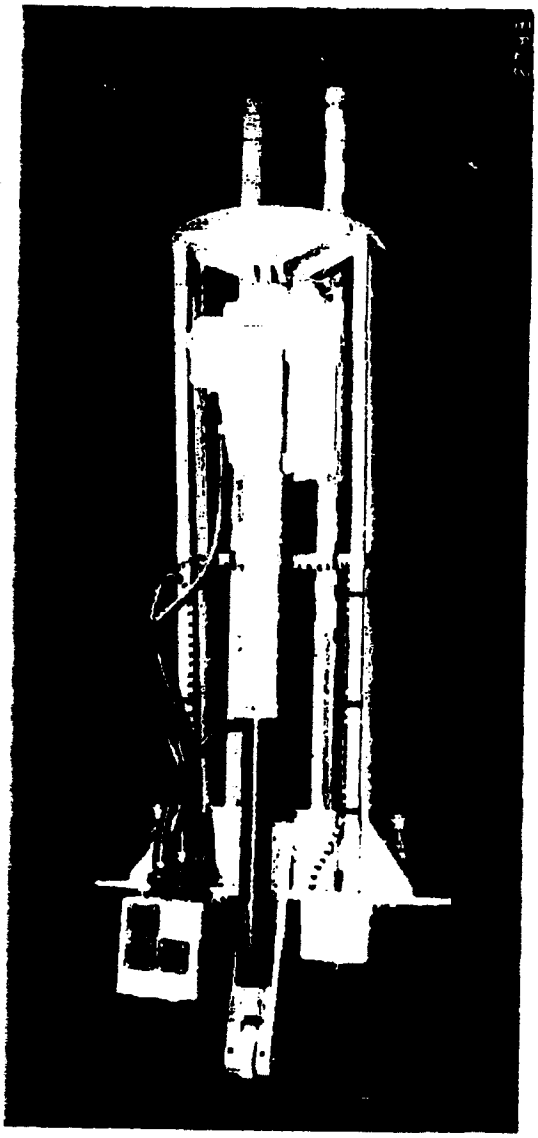

Figure 10.4 Boom and Actuator System

10.2 Disseminator Description and Information

The general characteristics of the disseminator are listed below:

Length: 227 inches
Maximum Diameter: 26.5 inches
Loaded Weight: 2075 pounds
Empty Weight: 575 pounds
Capacity: 180 gallons
Discharge Rate: 18.75 gallons per minute at 70 psig
Aerodynamic Configuration: Douglas store
Mounting Provisions: Standard lugs on 30-inch centers.

Details of the structure, the generator, the nose section contents, the plumbing assembly, the fluid handling system operation, the boom assembly and the actuator assembly are given in the paragraphs which follow.

10.2.1 Structure

The structure consists of three major separable sections: the nose, the center section and the tail section. In all of these sections, the skin is a major structural element for which the material is 6061-T6 aluminum. For the nose and tail sections the thickness of the aluminum is 0.071 inch and for the middle 3 feet of the center section it is 0.080 inch. At the separation stations between the three separable sections, rings are welded to the skin. These rings provide the flanges through which the sections are joined by bolts. Other structural rings extending around the inner circumference of the tank are used for supporting components within the tank. The joining and structural rings are also made out of 6061-T6 aluminum. All parts of the structure are of welded construction except for the door frames, the bulkheads and rings used for mounting components, and the wells in the tail of the tank into which the booms retract. These parts are riveted in place.

In more detail, the nose section which ends at the rear mounting surface of the air turbine generator has a spun aluminum skin, a forward mounting ring to which the air turbine generator is attached, a rear joining ring and an access door.

The center section consists of a skin, the front joining ring and bulkhead as one integral part, the inner tank mounting ring located toward the rear of the center section, the rear joining ring at the extreme rear of the tank, two access doors, and weld backup rings. The skin for the center section consists of three major sections welded together, one consisting originally of a flat aluminum sheet rolled into a cylindrical shape and welded along a longitudinal element and two made from flat aluminum sheet formed and welded into the frustrum of a cone. These two sections, having the shape of the frustrum of a cone, were then formed into the final complex shape by the use of pot dies. The term complex here is used to describe a surface in which none of the elements are straight lines. All the inertial loading and air loading applied to the tank is transmitted to the pylon of the transporting aircraft through a central structure. Major elements of the central structure are the strongback, the main support rings, and the attachment lugs that extend outward from the tank on the upper side. The strongback is an aluminum casting of 220-T4 aluminum extending approximately from lug to lug and being about 14 inches wide. The two main support rings are bolted to the strongback and extend around the inner circumference of the tank. Each ring is made in two pieces joined at the bottom of the tank by an expansion turnbuckle that is used to force the ring outward into tight contact with the tank. The material used for these rings is 4130 steel, heat-treated to a tensile strength of 170, 000 to 190, 000 pounds per square inch. The lugs are made of 4340 chrome, nickle, molybdenum steel, heat-treated to a tensile strength of 180, 000 to 200, 000 pounds per square inch. The skin and structure (exclusive of inner tank) have a weight of about 285 pounds.

The center section also contains the inner tank which is supported by being foamed-in-place and also being held by screws fastening it at the rear to the mounting ring riveted to the outer tank skin. In addition to serving as an insulation the foam joins the outer aluminum skin and the inner tank together into a laminated structure of great strength. Material for the inner tank is plastic-impregnated, filament-wound fiberglass built

up into walls of 1/10-inch thickness. This material was selected because of its resistance to corrosion and its light weight. The weight of the inner tank is 120 pounds.

The foamed-in-place insulation is a proprietary product called HITCO made by the H. I. Thompson Fiberglass Co. It has a density of 2 pounds per cubic foot, and a K value of 0.14 BTU per hour per square foot per degree Fahrenheit per inch of thickness. The compressive strength is 42 pounds per square inch at 160°F, and it will withstand 300°F. The thickness of the foam insulation is not uniform but varies from 1-3/8-inch to 1-5/8-inch. It was installed through holes drilled in the outer skin and these holes are filled with smoothing compound number 5-3000 called Organiceram made in Anaheim, California.

Immediately to the rear of the inner tank, but within the limits of the center section, is an insulated compartment about 12 inches long. This compartment is insulated with about 5/8-inch of foamed-in-placed insulation to protect the plumbing from freezing. A removable circular cover covers the rear opening to this compartment. The two doors providing access to this compartment are also insulated. Two pad-type heating elements thermostatically controlled supply 90 watts.

The uninsulated tail section consists of a spun aluminum skin, the forward joining ring, two actuator assembly mounting rings riveted to the skin and one access door. It also contains the boom wells into which the booms retract.

10.2.2 Generator

The generator is manufactured by the Allison Division of General Motors. It has the following characteristics:

1) Output 4.5 kva at 0.75 power factor

2) The current: 115/200 volt 400 cps 3 phase wye

3) Speed control is by a mechanical governor that adjusts the propeller blade pitch.

4) The speed range is from 11, 500 to 12, 900 rpm over a speed range 300/650 knots true air speed, at 500 ft altitude.

5) It uses a solid state voltage regulator separately packaged in a box about 4 x 4 x 3 inches.

6) Weight is 43 pounds.

7) It has a maximum drag of 100 pounds.

10. 2. 3 Nose Section Contents

Mounted on the forward end of the center section but actually located in the nose section are some electrical accessories and supports. The functions performed are: voltage regulation, switching for operation on ground power or generator power, and overload protection. The voltage regulator consists of solid state circuitry that regulates the voltage of the air turbine generator through regulation of the field excitation. This regulator is built by Allison. Three connectors are provided: one for connection to the power output of the generator, one for connection to the generator for voltage regulation, and one for connection to the ground power supply. The connector for connection to the ground power supply is very large in comparison to the size of the connector for connection to the generator output. The reason for its large size is that it must mate with the standard ground power supply socket. A circuit breaker is included for protection of the system and the power supplies. One relay is provided to automatically connect the active power supply to the system. In the normal position this relay connects the generator output to the disseminator circuits. When ground power is supplied, the relay acts automatically to disconnect the air turbine generator from the system and instead connect the ground power supply to the system. Also, whenever voltage is not being supplied by the ground power supply the contacts in the ground power supply connector are disconnected from the disseminator circuits. Another relay is used to control the supply of power

to the system in accordance with the position of a switch on the control panel located in the cockpit. All of the electrical components discussed so far (except for the air turbine generator) are mounted on a dishpan shaped mount attached to the forward end of the center section. The relays and circuit breakers are mounted inside of this mount and the voltage regulator is mounted on the outside as shown. The dust cap covers the circuit breaker reset button.

10.2.4 Plumbing Assembly

The plumbing assembly is located in the space of the aft insulated compartment. Much of the support for the plumbing assembly is provided by the inner tank cover which is made out of Type 304 stainless steel. This cover not only supports the plumbing assembly but also provides a seal for retaining the contents of the tank. A ridge on this cover fits into a groove of the inner filament-wound tank and the seal is provided by an "O" ring fitted into the groove. To the rear of the cover plate is the fluid control and plumbing assembly. The functions performed by the equipment here include filling, venting, pumping, pressure relief, by-pass and flow sensing. Filling and venting are accomplished through the two flexible tubes. The flexible tubing is Aero-Quip Type 666. It consists of a teflon inner tube, a woven stainless steel jacket, and a neoprene dip coat. The pump is a 1.5 horsepower unit (motor pump) made by Lear-Romec and it is a vane type having a capacity of 18.75 gallons per minute at a pump outlet pressure of 70 pounds per square inch gauge. The weight of the pump is 12.9 pounds. The pressure drop from pump outlet to far end of boom is 35 psi. Pressure drop along boom does not exceed 1/2 psi.

10.2.5 Fluid Handling System Operation

The primary function of the fluid handling system is to transfer under pressure the liquid from the store to the disseminating booms. To accomplish this task satisfactorily the fluid handling system must also provide

for controlling the flow of fluid, recirculating or mixing the fluid, filling the tank with fluid and provide adequate means to allow decontamination of the tank. Figure 10.5 shows a schematic of the plumbing system.

Following is a brief description of the function of the components in the system. As a starting point it is assumed that all three manual valves are in the full open positions as they would be for an airborne operation. The system will be in one of three states while airborne. They are: STATIC (pump shut off), RECIRCULATE, or DISSEMINATE. Sequence functions have been neglected.

In the STATIC mode solenoid valves 4, 5, and 6 are closed. The fluid is thus confined by check valve 8, solenoid valve 5 and check valve 7.

In the RECIRCULATE mode solenoid valve 4 is opened and the pump started. The fluid is thus drawn from the tank and pumped through the plumbing system back into the tank at a 18 gpm rate. Solenoid valve 5 remains closed thus preventing flow of fluid into the booms. Solenoid 6 remains closed thus backing up check valve 7 and preventing any loss of fluid through the vent line. Under normal conditions the relief valve also remains closed but if, due to some malfunction, the flow of fluid in the recirculate line is restricted with a consequent rise in pressure, the relief valve opens and allows fluid to flow into the tank through the vent line.

In the DISSEMINATE mode solenoid valve 4 remains closed while solenoid valves 5 and 6 are opened, the pump is started and fluid flows through solenoid valve 5 into the boom assembly and is disseminated. As the fluid flows out of the tank a negative pressure is created within the tank. Thus, since solenoid valve 6 is open the pressure differential causes check valve 7 to open allowing flow of air into the tank. The relief valve again is normally closed and functions only when the flow is restricted causing rises in fluid pressure beyond the preset relief pressure.

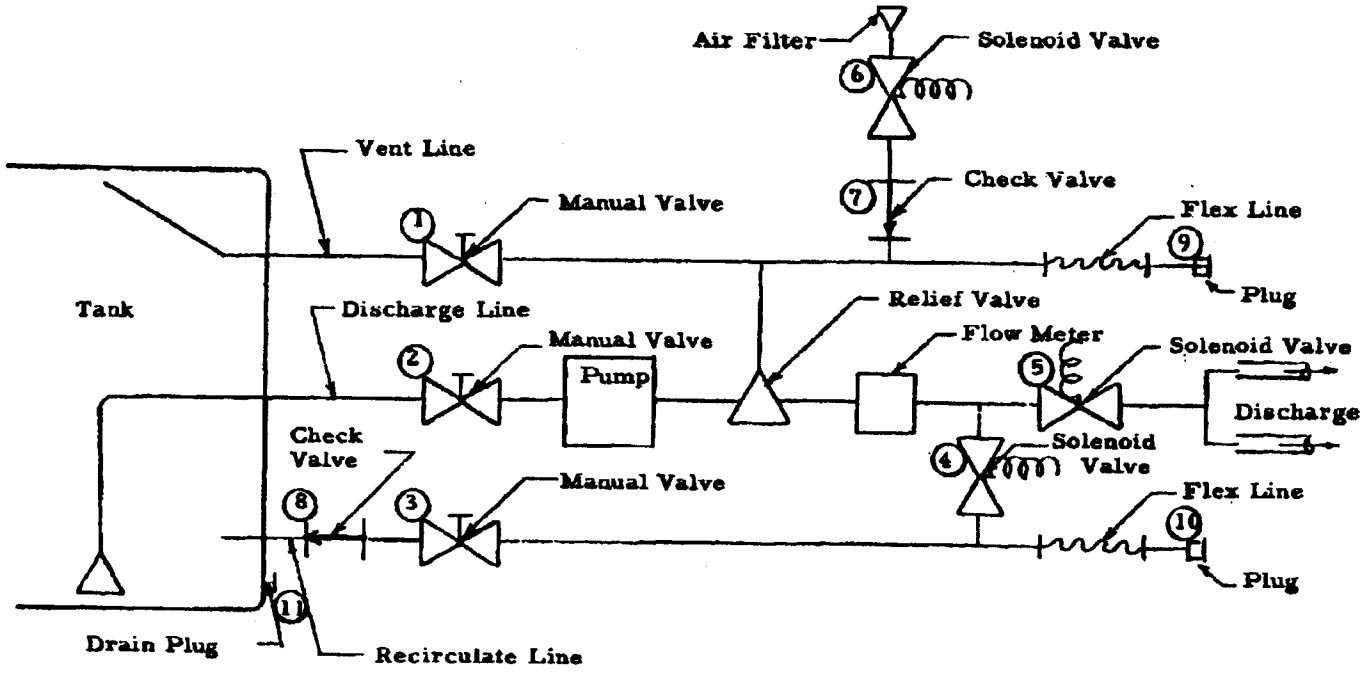

Figure 10.5 Plumbing Schematic

10.2.6 Boom Assembly

This is a welded assembly consisting of the two booms, their fairings, the shaft and the boom arm. The booms are made of 17-7 precipitation hardened stainless steel one-inch in diameter and 35 inches long. Each boom has two rows of orifices diametrically opposed and each row has 13 orifices. Each orifice is located in a flat spot milled on the boom. Knife edges used for cutting glass filament tape covers applied over the boom wells are welded to the booms. Fairings made of the same metal as the booms are welded to the booms to provide greater strength to resist bending caused by aerodynamic drag. The booms and the tubes transmitting the fluid to the boom shaft in the tail compartment are coated with Electrofilm. The Electrofilm consists of four layers: an insulating coating applied to the surface of the boom or other part to be heated, the conductive coating applied to the insulating surface, another insulating coating, and finally on the outside a white ceramic coating. 1140 watts are supplied to each boom. A thermostat located in the fairing of each boom controls the electric current supplied to the Electrofilm by on-off control. The boom shaft has machined journal surfaces at each end. Cams located on the boom arm actuate microswitches for making the indicator lights, on the cockpit control panel, tell whether the boom is extended or retracted. The aerodynamic drag is about 12 psi or about 750 pounds total for the two booms.

10.2.7 Actuator Assembly

The actuator (made by AiResearch) has a normal push-pull of 2400 pounds, (clutch slips at 3,000 pounds) weighs 15.6 pounds, extends the boom in approximately 20 seconds and retracts it in the same length of time. The actuator operates on three phase current. The boom actuator support structure consists of two mounting plates joined by a structure of round bars. The rear mounting plate and the bars are of type 304 stainless steel and they are welded into one assembly. The front plate is of aluminum and is

attached to the bars by means of screws. Plates welded to the bars near the front mounting plate are equipped with Oilite bronze bearings in which the boom shaft is free to turn.

10.3 Structural Testing

During this reporting period, structural tests were performed on the liquid agent disseminating store. These tests included a static structural test, slosh and vibration tests and ejection tests. All of the tests were successfully passed. The results of these tests are being analyzed further and are being used in preparing a structural report on the store. This testing program will be covered in detail in another report.

11. SUMMARY AND CONCLUSIONS

During this reporting period, important progress was made in many areas of the program, as summarized below in the order the topics appear in the body of this report.

To support the theoretical studies of powder mechanics, two types of experimental apparatus have been designed and fabricated. These are: 1) an improved device for measurement of the energy of compaction, and 2) a triaxial shear test device. Further study has been given to the shear strength data obtained with the direct-shear apparatus, with the result that the residual shear strength (after the compressive load has been removed) has been recognized as an important parameter. Additional data were obtained relative to the wall friction of powder against various surfaces, showing that the friction angles were in several cases substantially below the shear angle for the powder. The data from earlier compaction experiments have been re-examined and the equivalent elastic modulus has been determined (for three powders) as a function of specific volume. A new technique for measurement of bulk tensile strength of compressed powders has been developed and it appears that this property of the powder can be isolated without dependence on the geometry of the system. A mathematical analysis of the piston-cylinder friction test has been made which supports the belief that the compaction of a dry powder occurs under conditions of imminent shear (Section 2).

The design and fabrication of an aerophilometer, a light-scattering instrumented aerosol chamber was essentially completed during this period. To permit experiments on aerosol stability in this chamber, a bursting-diaphragm type powder-dispersing apparatus is being developed, as well as a filter sampling system for obtaining confirming data (Section 3).

The studies of the viability of Sm and Bg aerosols were continued. Measurements of the effect of heated airstreams were extended up to 200°C to provide data for calculation of the thermal-death-time parameters.

Preliminary studies were undertaken to evaluate the effect which coating Sm with Cab-O-Sil has on the viability of the system, its culturing properties and the susceptibility to heated airstreams. No loss of viability was indicated when the Sm was stored under refrigeration for short periods under these conditions. In the elevated temperature experiments, the addition of the Cab-O-Sil did not exert any deleterious influence on the viability. Possible toxic effects of buna rubber (a sample of the liner in the liquid agent disseminator) on Sm were studied experimentally. The results indicate that the rubber did not exert a bactericidal effect and that its toxic principle was essentially bacteriostatic (Section 4).

The wind tunnel studies of dissemination and deagglomeration were continued. Attention was focused during this period on a study of small-scale agglomerates in the 1 to 20-micron range. An analysis revealed that previously reported estimates of deagglomeration efficiency are conservative, due to the probability of forming agglomerates during the filtration process. During this reporting period, a new high-flow-rate dissemination test fixture was developed, which employs a pneumatically driven piston feeding system which will give instantaneous mass flow rates of 30 to 40 pounds per minute when charged with approximately one gram of powder. Auxiliary apparatus for preparing the sample (in a manner which simulates the processes in the airborne dry-agent disseminator) has also been developed (Section 5).

The experimental work on metering and conveying finely-divided dry solids has been continued, using the full-scale laboratory model feeding system. Measurements of the air flow required in the pneumatic conveying system and the torque and power required to drive the machine have been made. Also, the general operation of the machine has been observed, with very successful performance being achieved (Section 6).

The design and fabrication of the wind tunnel and associated apparatus was completed in preparation for installation in the Fort Detrick Test Sphere Facility (Section 7).

Design studies were made, dealing with several important aspects of the new dry-agent airborne disseminator. Recommendations on the overall size and configuration were submitted to Fort Detrick and these features were established. A detailed analysis of the rotary actuator required to drive the internal mechanism was made. The characteristics of the gas storage and flow regulating system were studied (Section 8).

The computer studies on line-source dissemination were extended to include the agent UL-2. The flow rates required under different weather conditions were determined (Section 9).

Work on design and fabrication of the airborne liquid agent disseminator progressed very well during this period. The unit was completed to the point where it was successfully functionally tested in the laboratory. This unit was (at a later period) also successfully flight-tested at the Naval Air Test Station at Patuxent River, Maryland (Section 10).

12. REFERENCES

1) General Mills, Inc. Electronics Div. Report no. 2249. Dissemination of solid and liquid BW agents (U), by G. R. Whitnah et al. Contract DA-18-064-CML-2745. 5th Quart. Prog. Report (Nov. 30, 1961). Confidential.

2) ----. Report no. 2200. Dissemination of solid and liquid BW agents (U), by G. R. Whitnah et al. Contract DA-18-064-CML-2745. 3rd Quart. Prog. Report (May 15, 1961). Confidential. (AD 323, 598).

3) ----. Reports no. 2112 and 2148. Fundamental studies of the dispersibility of powdered materials, by J. H. Nash et al. Contract DA-18-108-405-CML-824. 1st and 2nd Quart. Prog. Reports (Sept. 26, 1960 and Dec. 31, 1960). (AD 243, 607 and AD 249, 913).

4) ----. Report no. 2216. Dissemination of solid and liquid BW agents (U), by G. R. Whitnah et al. Contract DA-18-064-CML-2745. 4th Quart. Prog. Report (Aug. 10, 1961). Confidential. (AD 325, 247).

5) Wyss, O. Chemical factors affecting growth and death. In Bacterial physiology, ed. by C. H. Werkman and P. W. Wilson. N.Y., Academic Press, 1951. pp. 178-213.

6) General Mills, Inc. Electronics Div. Report no. 2264. Dissemination of solid and liquid BW agents (U), by G. R. Whitnah. Contract DA-18-064-CML-2745. 6th Quart. Prog. Report (Feb. 23, 1962). pp. 5-10 to 5-12. Confidential.

7) Ibid. pp. 6-1 to 6-11.

8) ----. Report no. 2249, op. cit., pp. 33-46.

9) ----. Report no. 2264, op. cit., pp. 7-1 to 7-4.

10) ----. Report no. 2264, op. cit., pp. 6-1 to 6-10.

11) Ibid. pp. 9-1 to 9-12.

12) ----. Report no. 2125. Dissemination of solid and liquid BW agents (U), by G. R. Whitnah et al. (Oct. 13, 1960). Contract DA-18-064-CML-2745. 1st Quart. Prog. Report (Oct. 13, 1960). pp. 59-68. Secret. (AD 324, 746).

13) ----. Report no. 2264, op. cit., pp. 8-1 to 8-5.